Immiscible WAG Injection:

A Core-Scale Investigation of Operational Parameters

Impacts

by

© Thuan Dang Quach

A Thesis submitted to the School of Graduate Studies

In partial fulfillment of the requirements for the degree of

Master of Engineering

Faculty of Engineering and Applied Science

Memorial University of Newfoundland

May 2020

St. John's
Newfoundland and Labrador

ABSTRACT

Water Alternating Gas (WAG) injection, commonly used in light to medium crude oil reservoirs, is a well-established technique for enhanced oil recovery combining the effects of two conventional oil recovery processes - water injection and gas injection. Immiscible water alternating gas (IWAG) injection is considered as an appropriate injection type dependent on economical and productive aspects. During the IWAG process, injected gas and oil are always in separate phases due to low-pressure maintenance, and it takes advantages in improving the stability displacement front in the macroscopic sweep as well as enhancing microscopic sweep in narrow pores. In order to check the optimum operational condition in which to apply IWAG injection at the field-scale, this injection process is usually tested as a core-flooding experiment, which is time-consuming and expensive. In this research, a model of core-scale IWAG injection is introduced with validation by Double Displacement Process (DDP) experimental data from previous research. Response Surface Methodology (RSM) with CCD design is used to investigate the impact of five operational parameters on the volume of oil recovery. Particle Swarm Optimization (PSO) is employed to determine the optimum combination of operational parameters to achieve the highest oil recovery factor for each operation scenario. The results indicate that all the main operational parameters, including timing, ratio, flow rate, slug size, and sequence, are significant for the response surface model. The PSO models reach good convergent results, with the volume of oil recovery for each case as 0.613, 0.650, and 0.666 pore volume. The performance of optimum IWAG injection is significantly better than only water-flooding or gas injection, with results approximately 5% higher than water-flooding, similar to double displacement process (DDP), and approximately 20% better than gas injection for the same operational conditions. These optimization tools

are recommended for further research of WAG injection, both the experimental and simulation processes.

ACKNOWLEDGMENTS

TABLE OF CONTENTS

LIST OF FIGURES

LIST OF TABLES

NOMENCLATURE

ANOVA	Analysis of Variance
BBD	Box-Behnken Design
BV	Bulk Volume
C1	cognitive learning coefficient (PSO)
C2	social learning coefficient (PSO)
CCD	Central Composite Design
DDP	Double Displacement Process
DOE	Design of Experiment
EOR	Enhanced Oil Recovery
GA	Genetic Algorithm
GOR	Gas-Oil Ratio
HCPV	Hydro-Carbon Pore Volume
IFT	Interfacial Tension
IOIP	Initial Oil in Place
IRF	Incremental Recovery Factor
IWAG	Immiscible Water Alternating Gas
K	Absolute Permeability
K_{rg}	Relative Permeability of Gas
K_{ro}	Relative Permeability of Oil
K_{rw}	Relative Permeability of Water
MBO	Million Barrels of oil

MDT	Modular Formation Dynamic Tester
NPV	Net Present Value
OD	Optimal Design
OWC	Oil Water Contact
PSO	Particle Swarm Optimization
PV	Pore Volume
RSM	Response Surface Methodology
RF	Recovery factor
S	Saturation
SA	Simulated Annealing
S_{or}	Residual Oil Saturation
S_{wi}	Initial Water Saturation
TVDss	True Vertical Depth
WAG	Water Alternating Gas
WF	Water-Flooding
t_{max}	total number of iterations
Vi	Velocity of particle i in the PSO formulation
μ	viscosity
ρ	density
φ	porosity
σ	interfacial tension
θ	contact angle
ω	inertia weight in the PSO formulation

Subscripts

c   refers to critical saturation

g   refers to gas phase

o   refers to oil phase

w   refers to water phase

CHAPTER 1. INTRODUCTION

1.1 Hibernia Field Introduction

This research is focused on the Hibernia field, which is located 315 kilometers southeast of St. John's, Newfoundland, Canada in 80 meters of water; it is one of the major developed oil fields offshore Newfoundland and Labrador [Lawrence et al., 2013]. The Hibernia field is extremely faulted combining various sand bars and fluvial channels, including two main reservoirs of Cretaceous age: the Hibernia reservoir at an average depth of 3700 meters and the Ben Nevis–Avalon (BNA) reservoir at a depth of 2400 meters. The first wildcat well was drilled in the Hibernia field in 1979 and more exploration wells were drilled in the next several years [Lawrence et al., 2013]. Most wells target an area of 200-meter thickness that has a high net to cross section of stacked, braided fluvial channels at the depth around 3700-3900 meters TVD. A few wells target the upper BNA shallow marine sand and estuarine reservoir at the depth roughly 2300 – 2500 meters TVD.

Fig. 1-1: Hibernia oil field location map [Richards et al., 2010]

According to Wang et al., the Hibernia field was developed with 27 oil production wells, 18 water injection wells, and six gas injection wells by the end of 2005. The cumulative oil production is almost 455 MBO by continuing applying all stages of exploration, expansion, and optimization on the field during this period [Wang et al., 2006].
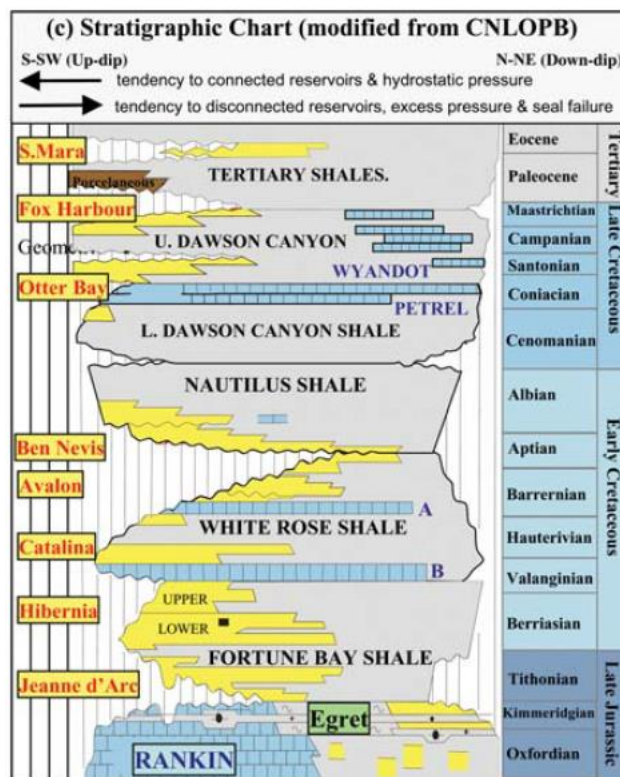
Fig. 1-2: Hibernia Field reservoirs stratigraphic column [Richards et al., 2010]

As can be seen from the stratigraphic column, there are two main reservoirs in the Hibernia field. Most field production comes from the deeper pool, which is a high-quality, productive sandstone reservoir and extremely connected. The Hibernia formation is a combination of inter-distributary channels and major fluvial channels.

Cores used for this research were obtained from the research of Wang et al., and all of them were collected from well B16-17 and distributed vertically with depth from 4039.83 m to 4041.13 m. This zone of the reservoir is characterized as a mature sandstone, very fine to very

coarse grained, moderate to well-sorted. Its reservoir properties are good to excellent with porosity varying from 15 to 22% and permeability ranging from 500 to 5000 mD. The physical condition of the cores is well representative for this area with porosity and permeability typical of the observed reservoir.

1.2 Oil Recovery Processes Overview

Generally, a reservoir goes through these typical phases, including primary, secondary, and enhanced oil recovery (EOR) during the producing life [Nadeson, 2001]. The lengths of these stages are based on different particularly reservoirs will vary to optimize both productive as well as economic aspects.

Primary recovery is the recovery process that depends mostly on the natural forces of the reservoir for the displacement of oil to be produced. These natural energies are solution gas drive, gas-cap drive, water influx, fluid/rock expansion, and gravity drainage. In real cases, all or a few natural forces are combined during the primary stage [Lake, 1989]. The primary process will be over when the reservoir pressure is decrease or the production volume drops due to weak natural forces; then the recovery process will move to the secondary stage.

Secondary recovery employs the injection of water or gas into the reservoir to maintain or improve the natural energies inside to keep a high rate of oil production. The impact of gas injection could be used as gas-cap expansion and/or to sweep immiscible oil to the production well. However, it has been proven in real cases that water-flooding is more effective in comparison with gas injection as secondary recovery due to better volumetric sweep efficiency and economic convenience [Green and Willhite, 1998].
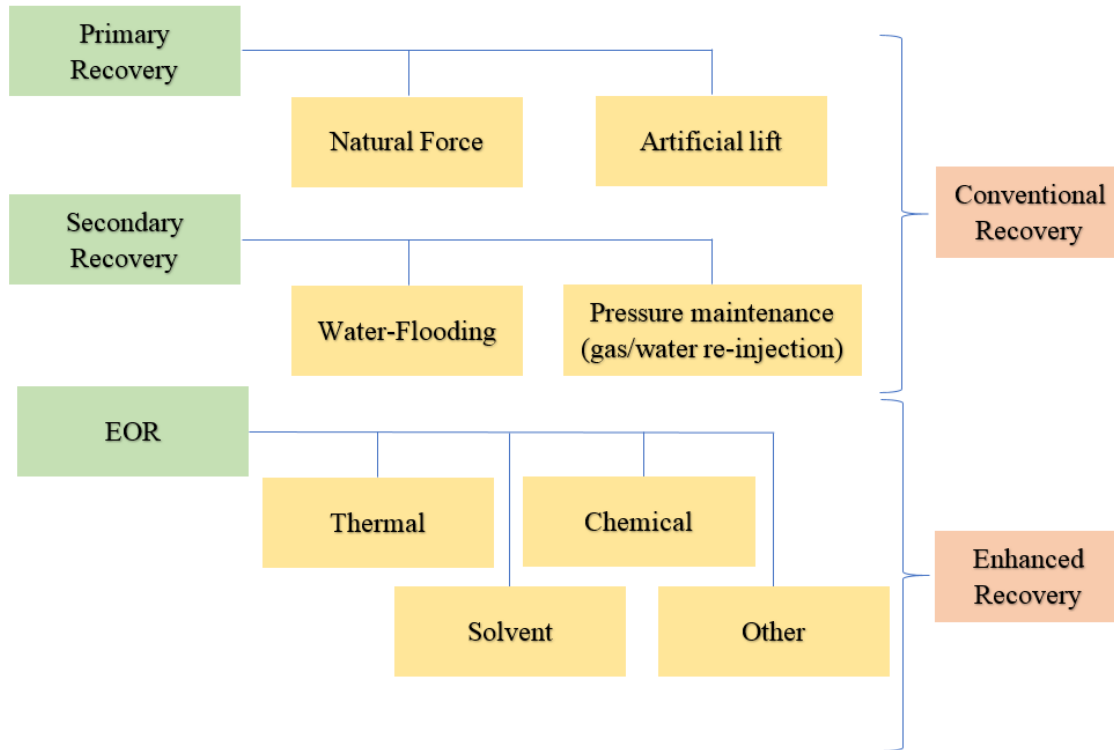
Fig. 1-3: The classification of reservoir oil recovery [Lake, 1989]

After the primary and secondary recovery processes, in many cases, a vast residual oil volume remains in the reservoir, then EOR could be applied to recover more oil. EOR is applied after the secondary stage, typically using special fluids such as gas, chemicals, and thermal energy to displace additional oil [Sohrabi et al., 2001]. Thermal EOR is defined as injecting steam or hot water into the reservoir to improve the displacement efficiency as well as to reduce the viscosity of reservoir fluids to be recoverable, the thermal energy of the process is maintained by combusting reservoir oil [Lake, 1989]. Thermal EOR shows a remarkable advantage in thin reservoirs or heavy oil reservoirs [Hassan et al., 2018]. Chemical EOR is employed to improve the interaction between injected fluids and reservoir rock/oil to make a favorable environment for oil recoveries such as lowering interfacial tension (IFT), reducing oil viscosity, changing wettability or oil swelling. Typically, chemicals have been studied to for

EOR application, including alkalines, surfactants, polymers, and combinations of them [Sheng, 2011]. However, chemical EOR has proven itself as a technique that requires significant financial resources for field application. The double displacement process (DPP) is an EOR method that takes advantage of gravity drainage by injecting immiscible gas to create gas cap expansion after water-flooding [Fassihi and Gillham,1993].

Water alternating gas (WAG) was proposed as an optimum EOR technique that could satisfy both technical and economic aspects of tertiary recovery due to the advantage of combining increased sweep efficiency by gas injection and controlling mobility ratio as well as stabilizing the front by water injection [Righi et al., 2004].

WAG injection has been applied in many fields with remarkably positive results since the first field test in 1957 [Christensen et al., 1998]. WAG injection involves three-phase flow (gas, water, and oil) to decrease residual oil saturation and it is much more complicated to estimate its efficiency compared to just water or gas injection [Zhang et al., 2006]. Determination of the saturation path in the three-phase system is also much more complicated than the two-phase model because of the different hysteresis effect [Righi et al., 2004]. Therefore, core-flooding experiments are often employed to clearly understand any aspects relating to the WAG injection process before applying to field case studies.

1.3 Optimization Theory Background

The meaning of optimization can be defined as a process that seeks the optimum values of variables that lead to the optimal result through a condition function. From that statement, identifying the objects and the input parameter would affect the characteristic from design. The number of input variables makes a huge impact on the optimization problem exponentially, therefore, keeping the number of input parameters as low as possible would

19

simplify the optimization process. The relationship between optimization problems and input parameters can be either an experimental or numerical process [Cavazzuti, 2013].

With m input parameters υ_i, i = 1,…, m and n ≤ m input variable x_j, j = 1, …, n then the Euclidean geometrical spaces of the input parameters and the input variable are R^m and R^n respectively.

Considering p as output parameters w_k, k = 1, …, p and the objective function y; g(x) and f(x) are the function defining the output parameters and the objective function respectively; X is the design space for domain, we have

$g(x): X \subseteq R^n => W \subseteq R^p \qquad w_k = g_k(x), k = 1, …, p$

$$(1.1)$$

$f(x): X \subset R^n => Y \subset R \qquad y = f(x, w) = f(x, g(x)) = f(x)$

The optimization process aims to optimize f (x), x ∈ X ⊆ R^n. This procedure acquires iteration by the algorithm to get the solution x*

$X* \in \{x^{(1)}, …, x^{(t)}\}: y(x*) = \text{optimum } y(x^{(r)}), r = 1, …, t$ (1.2)

The classification of the optimization technique related to experiment and simulation is divided into two main areas: the design of experiments (DOE) and computational optimization algorithms [Cavazzuti, 2013]. Details of these categories of optimization problems will be reviewed in detail in Chapter 2.

1.4 Research Objectives

This study focuses on optimizing the efficiency of the oil recovery process of core-scale immiscible WAG (IWAG) injection by determining the most significant WAG operational parameters for core-flooding experiments with the intent of reducing the number of experiments required. First, a core-scale model is built using Schlumberger Eclipse and is

validated using experimental results of the double displacement process (DDP). A comparison is also made between the recovery performance of DDP and IWAG injection for the simulation model. The optimization methods are presented and investigated using simulation at the core scale through different techniques, DOE and Particle Swarm Optimization (PSO). The objective of the optimization process is to maximize the volume of incremental oil recovery by IWAG injection for the composite core simulation by investigating WAG operational parameters. Furthermore, the impact and correlation between the operational parameters on the incremental oil recovery factor is also estimated. The variables of IWAG injection are optimized, including six main parameters: water and gas flow rates, timing, cycle ratio, slug size, total injection, and sequence/order of injection process. The results of the optimization techniques are analyzed and compared, then used as the input data for the core-flooding experiment in the future.

1.5 Thesis Outline

The thesis consists of five chapters:

Chapter 1: Introduces the background of the Hibernia field as well as composite core geology properties used for the simulation. A brief introduction to EOR techniques, especially for double displacement process and WAG injection, is presented generally. Optimization methodology is described as a base for optimizing the problem. The objective of the thesis is defined to clarify the purpose of this research.

Chapter 2: Summarizes the main works that relate to the four main problems addressed in the thesis including a literature review of double displacement process (DPP), WAG injection, WAG operational parameters and optimization techniques with a screening of their application for oil and gas production.

Chapter 3: Presents the methodology and framework for core-scale simulations, both DPP and IWAG injection, as well as for optimization techniques, including response surface methodology (RSM) and particle swarm optimization (PSO).

 Chapter 4: Demonstrates the results and discussions of the simulation for two main case studies including a comparison of the performance between DDP and WAG injection; and optimization process with optimum operation parameters and the effect of the interaction between these parameters.

Chapter 5: Finally, the conclusion is summarized, and the recommendations are suggested to improve further research.

CHAPTER 2. LITERATURE REVIEW

In the first section of the literature review chapter, all aspects related to Water Alternating Gas (WAG) injection, including general description, operational mechanism, classification, and its worldwide applications are presented. The second section focuses on reviewing all works that investigate WAG operational parameters for the core-flooding experiments of immiscible WAG (IWAG) injection, detailed papers screening of core-scale IWAG injection are also included. The third section focuses on reviewing all studies that involve the double displacement process (DDP). In the last section, optimization techniques applied in the oil and gas industry are reviewed, especially Response Surface Methodology (RSM) and computational optimization methods, which have been employed for WAG injection applications.

2.1 Water Alternating Gas (WAG) Injection

2.2.1 WAG Description

Water injection is the most common technique for oil recovery. The volume of oil remaining in the reservoir after water-flooding is usually significant and could be reduced by applying gas injection in a later stage [Lake, 1989]. Due to the lower of interfacial tension (IFT) between gas/oil compared with water/oil interaction, the sweep efficiency by gas injection is technically better than water-flooding [Kulkarni and Rao, 2005]. Various types of gases have been used around the world for oil recovery processes, including hydrocarbon (HC), CO_2 (mostly in the U.S), LPG, propane, exhaust gas and N_2 [Christensen et al., 2001].

Water alternating gas (WAG) injection, commonly used in light to medium crude oil reservoirs is a well-developed technique for enhanced oil recovery. It combines the effects of two conventional oil recovery processes - water injection and gas injection [Green and

Willhite, 1998]. Parrish originally presented the procedure for this method in 1966; the research focused on investigating the mechanism of reducing gas mobility and improving the sweep efficiency for continuous gas injection in reservoirs [Minssieux and Duquerroix., 1994].

WAG injection is a cyclic method that alternates gas and water cycle injection and repeats the process several times depending on the operator plan (Figure 2.1). During the WAG injection process, a three-phase zone is created by water and gas injected from the same injection well. The most significant advantage of three-phase interaction is that it leads to a reduction in the mobility of the water and gas phases inside the pore system. Mobility control is especially important for gas injection due to its low viscosity, which usually causes gas fingering and early gas breakthrough then reduces the macroscopic (areal and vertical) sweep efficiency, due to less bypassing behavior [Zekri et al., 2011]. Therefore, only continuing gas injection could not make an economic remarkable additional oil recovery. However, alternating gas and water injection can significantly reduce the mobility of the gas phases due to gas trapping [Caudle and Dyes, 1958]. The presence of gas is usually considered as most non-wetting phase in the three-phase system can also push oil out of the larger pores to increase the oil connectivity, then the water phase will more easily to sweep oil out of the pore system.
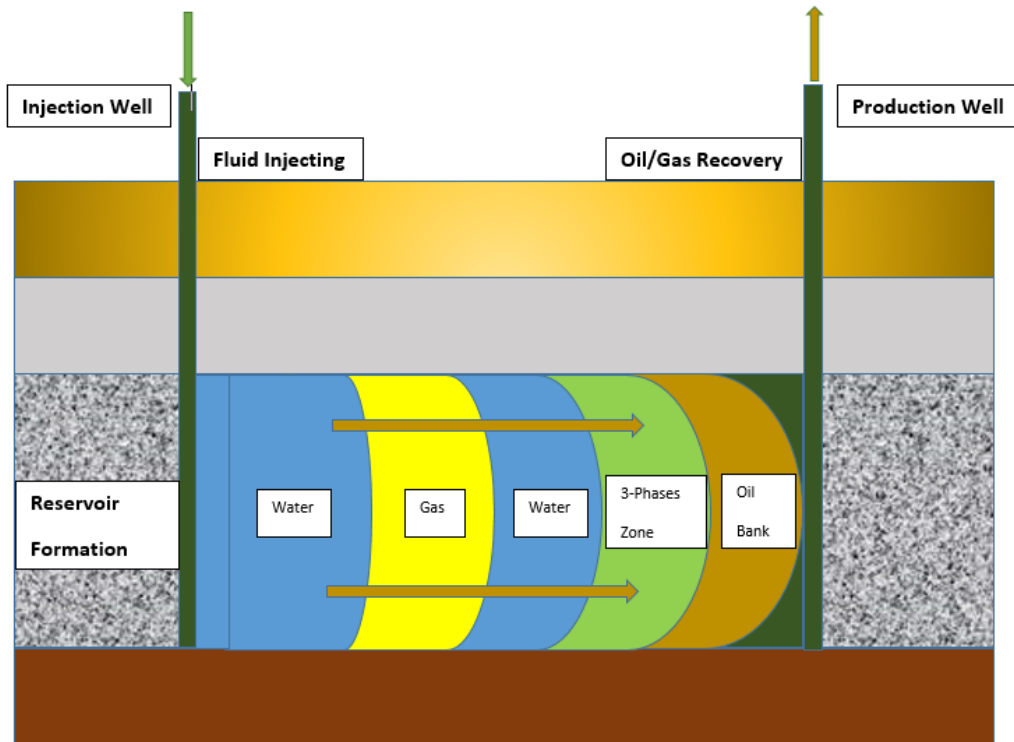
Fig. 2-1: Schematic of the WAG process [Tunio., 2011]

Despite the many advantages of WAG injection, several aspects should be considered before applying this method. The three-phase zone has a limited area because of gravity segregation, the gas phase tends to move to the upper zone while the water phase falls to the bottom. This effect makes a clear impact on the sweep efficiency for upper and lower layers of the reservoir [Choudhary et al., 2011]. Furthermore, despite the advantage of gas mobility reduction by alternating water injection cycle, switching to gas injection may lead to a decrease in water injectivity and a critical challenge in maintaining the injection pressure [Lien et al., 1998].

2.1.2 WAG Recovery Mechanism

The general mechanism of oil recovery by WAG injection could be described as an improvement of the combination of microscopic and macroscopic sweeps by injected fluids

to oil volume inside the pore space. The overall displacement efficiency of the WAG process can be generalized as the following equation:

$$E_{WAG} = E_{Micro} \cdot E_{Macro} \qquad (2.1)$$

where E_{WAG} is the total displacement efficiency (the volume of oil recovery by WAG injection divided by the amount of oil in place at the start of WAG injection). E_{Micro} is defined as the effectiveness of water and gas injection through physical and chemical properties between rocks and fluids on oil recovery. In contrast, E_{Macro} is considered as the effectiveness of water and gas floods through the physical space between the injected point and production point on oil recovery [Aurand, 2017].

Macroscopic sweep efficiency

Macroscopic sweep is usually divided into a horizontal sweep and vertical sweep. The horizontal sweep depends significantly on the mobility ratio. The mobility ratio is defined as the ratio of the mobility of displacing fluid on the mobility of the displaced fluid at the front contact [Fanchi., 2010]. When the mobility of the displacing fluid is higher than the displaced fluid, it will cause viscous fingering that leads to an early breakthrough. A mobility ratio of less than one is required or a good sweep efficiency. The vertical sweep refers to a vertical cross-section swept by an injected fluid due to the density difference of injected fluids. In reservoir, gas tends to move to the top while water prefers to move to the bottom. Therefore, maintaining the three-phase region extending as far as possible from the injection point will optimize the oil recovery process.

Other factors that also take part in the macroscopic sweep are listed as physical arrangements of injectors and producers in the field, reservoir heterogeneity, permeability, porosity, and fluid saturation [Slb.com., 2019].

Reservoir Heterogeneity makes a clear impact on water/gas displacement of WAG process. It affects the microscopic scale such as changing of pore connectivity, the sorting of grains, a variation of pore size and presence of impurities and on macroscopic scales such as the various distribution of stratification, formation thickness, layers communication or facies of reservoir [Satter and Iqbal, 2015].

Porosity is the volume of space in the reservoir and can be divided into absolute and effective porosity [Lyons and Plisga, 2011].

$$\text{Absolute porosity, \%} = \frac{Volume\ of\ all\ pores\ and\ voids\ in\ rock}{Bulk\ volume\ of\ rock} \times 100$$

$$(2.2)$$

$$\text{Effective porosity, \%} = \frac{Volume\ of\ interconnected\ pores\ in\ rock}{Bulk\ volume\ of\ rock} \times 100$$

The effective porosity is important to detect the general volume of reservoir fluid due to their interconnected properties, fluids placed in isolated pore will not contribute to the production. *Permeability* is a rock property that indicates how well fluid can be transported through the pore system and channels inside the reservoir in three-dimensions [Satter and Iqbal, 2015]. A high permeability presents for good productivity and better recovery efficiency of the reservoir. Absolute permeability is defined as the permeability of rock when saturated by one fluid, while effective permeability represents for the permeability of one fluid for a rock that fully saturated by another fluid.

Fluid saturation is defined as the ratio of the pore volume divided by the volume of a specific fluid. Hence the value of fluid saturation ranges between zero to 1. Generally, the total fluid saturation of the reservoir is the summary of gas, oil, and water saturation. Understanding saturation distribution with both end-point saturation and critical saturation of each phase while processing the injection is important for recovery efficiency [Kantzas et al., 2012].

Microscopic sweep efficiency

The microscopic sweep defines the efficiency of how the displacing fluids mobilize the residual oil once the interfacial contact occurs. Factors affecting the interaction between them include interfacial tension, wettability, capillary pressure, and relative permeability.

Interfacial tension (IFT) is the force that exists at the surface that separates two immiscible fluids such as oil/gas, gas/water or water/oil and is considered a prime property as phase boundaries [Lyklema, 2005].

Wettability is the ability of a solid surface to be in contact with a specific liquid rather than another one, it is determined by the balance between the interaction of liquid to surface and liquid to liquid [Moldoveanu and David, 2016]. For a water-wet reservoir, the residual oil after secondary water-flooding tends to remain in the larger pores far away from the rock surface, which prefers to attract water; an injected gas cycle would push the residual oil into smaller pores that helps to increase the oil injectivity, which improves oil recovery [Suicmez et al., 2006].

Capillary pressure (Pc) is defined as

$$P_c = \frac{2\sigma cos\theta}{R} \tag{2.3}$$

where P_c is the capillary pressure [dynes/cm^2], σ is the interfacial tension [dynes/cm], $cos\theta$ is the contact angle [degrees] and R is the radius of the pore [cm]. Capillary pressure in the reservoir defines the fluid distribution, hence affects the alternating of fluid saturation [McPhee et al., 2015].

Relative permeability of rock to aqueous phases (gas/oil/water) is defined as the ratio between the effective permeability of the given fluid and the absolute permeability of rock types when 100% saturated by that fluid [Satter and Iqbal, 2015]. The relative permeability depends on

the interfacial tension and is usually visualized as both a drainage curve and imbibition curve. In a water-wet system, the drainage curve is present the decreasing of wetting phase (water) saturation, and imbibition curve is illustrated as increasing of wetting phase (water) saturation.
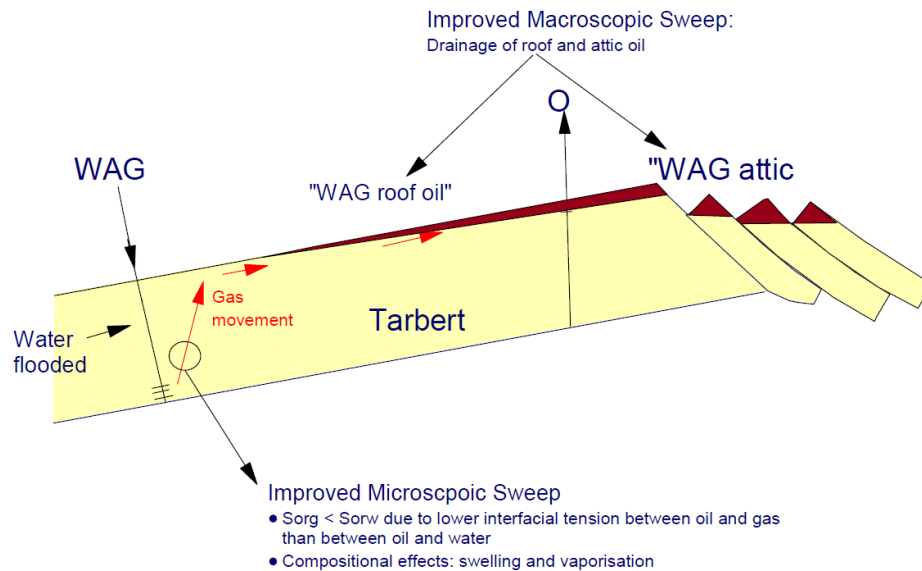
Fig. 2-2: Illustration of both microscopic sweep and macroscopic sweep improvement during gas injection in the WAG process [Crogh et al., 2002]

Optimizing WAG injection requires balancing the efficient volume of gas and water needed to be injected into the pore system. Too much injection water would lead to poor microscopic sweep efficiency, or a large volume of injected gas would reduce the stability in front and macroscopic sweep effect.

2.1.3 WAG Classification

The WAG injection process can be divided into various comprehensive classifications based on injection pressure and method of injection. The most typical WAG processes applied so far in oil reservoirs include miscible WAG (MWAG), immiscible WAG (IWAG), simultaneous WAG (SWAG) and hybrid WAG (HWAG) [Christensen et al., 1998; Awan et al., 2008; Darvishnezhad et al., 2010].

Miscible WAG Injection

Miscible WAG injection is defined as the process that maintains the injection pressure higher than the minimum miscibility pressure (MMP) to achieve a miscible flood process, which also makes the reservoir bubble point pressure increase [Al-Shuraiqi et al., 2003]. When the miscibility is developed when the gas cycle is injected, as gas displaces oil, it will create first contact or multi-contact miscibility with the reservoir oil [Skauge and Sorbie, 2014]. MWAG takes advantage of microscopic sweep by dissolving a gas slug into oil, which leads to reduced oil viscosity, making it easier to mobilize trapped oil. However, the miscible flood is also responsible for poor volumetric sweep efficiency at the front because of its low viscosity. Furthermore, injecting water cycle support increases the macroscopic sweep efficiency for MAWG [Fatemi et al., 2011]. Most miscible WAG projects are applied onshore and are performed on close well spacing, but there are few attempts to apply this process for offshore well spacing [Panda and Lenig, 2010; Kumar et al., 2017].

Immiscible WAG injection

When the gas cycle of WAG is injected to the reservoir with the injection pressure lower than MMP it cannot create miscibility with oil inside the pore system, this process is called immiscible WAG (IWAG). In the IWAG process, both displacement efficiency and sweep efficiency are increased by taking advantage of improved trapped gas saturation [Khanifar et al., 2015]. The main objectives when applying IWAG are to improve frontal stability through the 3-phase zone and to create oil film flow, which behaves as a pathway for oil movement in the presence of water and gas, after gas sweeping oil out of larger pores [Holtz, 2016]. IWAG has been applied in many lab-scale and field-scale projects for various types of oil and injected gas. It is reported to be a low-cost technique with good recovery efficiency [Afzali et al., 2018;

Christensen et al., 2001]. This research focuses on immiscible WAG injection by simulating the core-scale condition with gas used as synthetic gas, which does not create miscibility with oil, and minimum miscibility is not measured by applying a suitable injection pressure.

Simultaneous WAG injection

In simultaneous WAG injection, both water and gas cycles are injected at the same time into a portion of the reservoir [Ma et al., 1995]. This technique was proven to be a good option that improves mobility control more than conventional WAG, which leads to a higher oil recovery efficiency. It also reduces both capital and operating costs by combining water and gas injection lines [Shetty et al., 2014]. Two options can be used to describe SWAG process by verifying the combining point of the system. In the first option, water and gas for injection are combined at the surface and transfer through one wellbore, which was previously used for secondary recovery, this process is usually called SWAG. For the second option, slugs of water and gas are injected through a dual completion injector into the formation by taking advantage of the gravity segregation, water injection for the upper zone and gas injection for the lower zone. This process is referred to as Selective SWAG [Barnawi, 2008; Darvishnezhad et al., 2010].

Hybrid WAG injection

In hybrid WAG (HWAG) injection, the amount of water and gas slugs injected into the reservoir are varied, such as after injecting a large slug of gas into the reservoir followed by several small slugs of water and gas [Larsen and Skauge, 1999]. The main advantages of the HWAG process are better gas utilization, reduced chance of water blocking, improved injectivity and combining efficiently with continuous injection method at an earlier stage in comparison with conventional WAG [Bagrezaie et al., 2014].

2.2.4 WAG Worldwide Applications

Since the first WAG injection was applied for a sandstone reservoir of the North Pembina field in Alberta, Canada in 1956, various fields around the world, both offshore and onshore, have employed this method with a majority of them located in Canada, the U.S and the North Sea region claiming successful application [Christensen et al., 2001].

Christensen et al. reviewed the WAG injection process application of approximately 60 field cases, most of which were successful [Christensen et al., 2001]. Generally, the majority of WAG field applications have been reported in the U.S. However, the most recent application was from the North Sea area, and the recovery stage that WAG process was applied is also sooner than other areas, which often happens after secondary recovery. The increased recovery was reported to vary from 5% to 15% and could increase up to 20% for some specific cases such as the Rangely Weber and Slaughter Estate fields.

In 2001, the majority of WAG field applications were the miscible type (79%) in comparison with 18% of observed fields planned to be an immiscible injection. The overall average improved recovery of miscible type is also higher than immiscible type, 9.7%, and 6.4% respectively. A high-permeability reservoir is considered as the dominant rock model used to apply WAG injection and over half of the observed projects are sandstone reservoirs, the rest of them are divided into dolomite, limestone and carbonate rock groups. Only six out of 59 projects in this research are reported from the offshore environment with hydrocarbon gas used as injected gas; the rest were applied onshore.

WAG Projects Classification - Injection Types

WAG Projects Classification - Rock Types
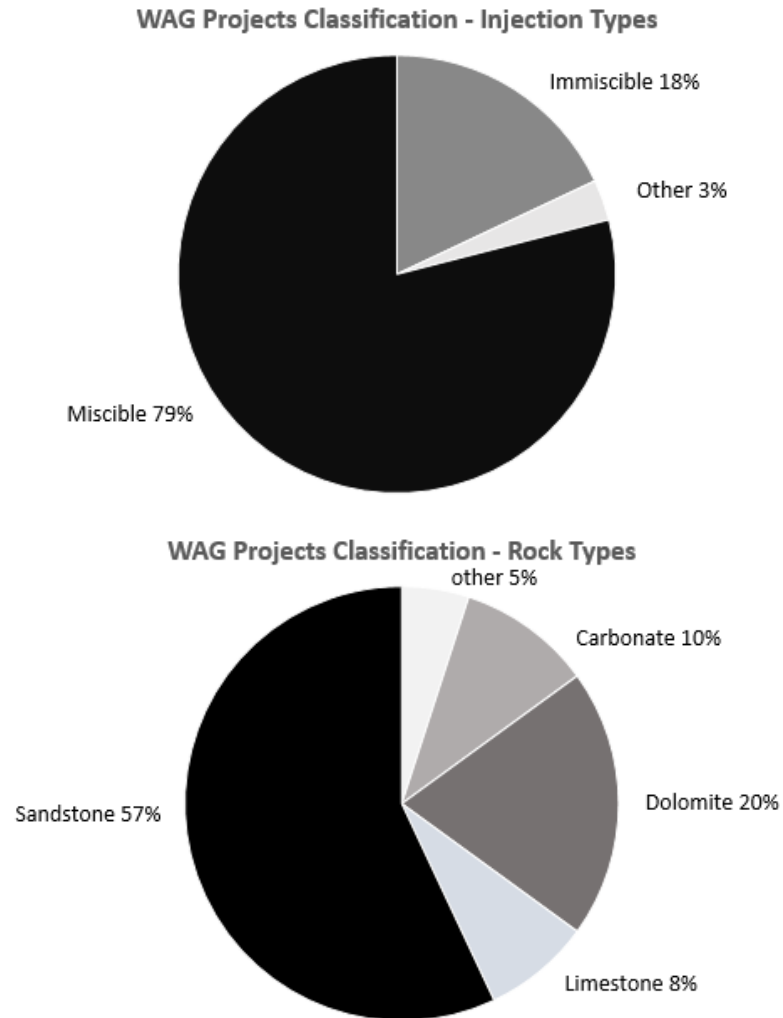
Fig. 2-3: WAG projects classification over 59 fields [Christensen et al., 2001]

The North Sea area is considered to have many favorable fields for the application of WAG injection, which is the most successful EOR technique employed. In 1980, Thistle was the first field to implement WAG injection and later performed in the 1990s [Teigland and Kleppe., 2006]. WAG injection applied in the North Sea is not the same as onshore field application. Onshore, a 5-spot injection pattern has been reported as the most successful for WAG injection; this however would be extremely expensive offshore. Therefore, wells have to be established based on geological consideration.

Awan et al. conducted a survey about EOR application in the North Sea and noted that most EOR field applications were WAG injection processes with a total of 19 projects; six were immiscible types, three were miscible WAG, two were FAWAG (foam assisted water alternating gas injection) and one was SWAG [Awan et al., 2008]. The main reason is because of the advantage of improving both macroscopic and microscopic sweep efficiency of WAG when adjusting the favorable mobility ratios. Most fields in the North Sea contain a lot of attic oil that is preferred to be exploited by gas injection rather than only water-flooding, which makes downdip WAG injection become an efficient application for these offshore fields [Crogh et al., 2002; Instefjord and Todnem, 2002; Lien et al., 1998]. Most projects that applied WAG recovery in the North Sea are focused on using HC gas as the injected gas due to its availability and affordable cost [Christensen et al., 2001]. Although a few of them are using CO_2 alternating with water for injection have proven to achieve greater efficiency in comparison with HC gas and water injection, CO_2 application will be not be an attractive approach because of the limited resource in this area.
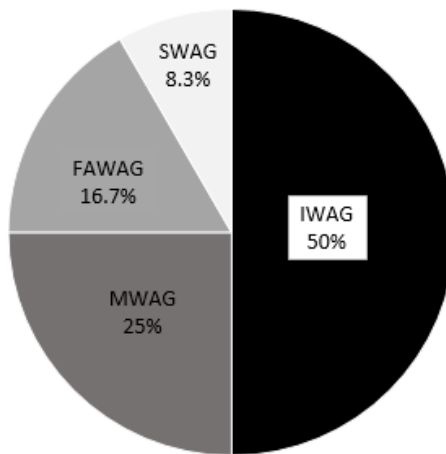
Fig. 2-4: WAG projects application in the North Sea [Awan et al., 2008]

2.2 Immiscible WAG Injection Overview

Immiscible water alternating gas (IWAG) injection is considered as an appropriate injection type depending on both economical and production aspects. During the IWAG process, injected gas and oil are always in separate phases due to low-pressure maintenance, and it improves the stability displacement front in the macroscopic sweep and enhances the microscopic sweep in narrow pores [Itriago et al., 2018]. IWAG uses the mechanism of three-phase flow (gas, water, and oil) to decrease residual oil saturation and it is much more complicated to estimate the efficiency than just oil or gas injection [Christensen et al., 2001]. Understanding the correlation of all the parameters related to this injection process, through core-flooding experiment, would lead to a successful reservoir simulation and enhance the recovery factor in field tests.

2.2.1 Critical Operational Parameters

Operational parameters used as input data for core-scale WAG process include the following main components: types of gas and water for the injection, time to start WAG process, WAG ratio, WAG slug size, WAG flow rate and the sequence in every cycle. Generally, based on the type of reservoir with different geological properties, as well as interaction properties between rock-fluid and fluid-fluid, suitable operational parameters should be optimized for each injection process. Many types of research have been done to investigate appropriate injection patterns for various types of reservoirs as well as the correlation between them on the oil recovery efficiency.

Gas injection

The gas used for the injection process has a significant effect on the oil recovery volume. Three typical classes used as injected solvent are non-hydrocarbons (CO_2 not included), CO_2, and hydrocarbons (HC).

Nitrogen is used in a few fields due to their economic prospects and resource availability [Christina et al., 1981]. Salehi et al. injected nitrogen, one of the gases typically used in both miscible and immiscible gas injection for an oil reservoir, at a constant flow rate for the tertiary recovery process known as Surfactant-Alternating-Gas (SAG) by varying the ratio between the volume of surfactant and N_2 [Salehi et al., 2014]. The best result of these tests is 87% than compared with WAG, water-flooding, and gas injection with the following ultimate recovery factors as 70%, 66%, and 50% OIIP respectively. Janssen et al. compared the effect of different N_2-WAG injection schemes on the efficiency of oil recovery [Janssen et al., 2018]. By changing the backpressure conditions and the sequences of the recovery process, the study concluded that immiscible N_2-WAG injection gives the highest oil recovery factor (60% OIIP) in comparison with water-flooding or N_2 continuous injection (approximately 50%) after 16 PV of injection for Bentheimer sandstone cores.

However, oil recovery with CO_2 appears to be better than using N_2. Ghafoori et al. [2012] experimentally investigated the performance of WAG injection and continuous gas injection (CGI) processes using nitrogen and CO_2 in a porous carbonate sample. The result showed that CO_2-WAG injection attained about 13% more oil recovery than nitrogen WAG. The same result was observed by Amadi et al. [2015] when oil recovery form CO_2-WAG is higher, about 8.5% than N_2-WAG.

Srivastava and Mahli presented a laboratory investigation about WAG injection for a mature light oil field. They used HC gas and CO_2 as injected gas and alternating WAG parameters to

achieve the optimum oil recovery [Srivastava and Mahli., 2012]. CO_2 gas with five cycles of WAG account for an incremental displacement efficiency about 40% of HCPV, which is significantly higher than around 20% of HCPV for 5-cycles HC-WAG.

Among the 60 WAG field applications reviewed by Christensen et al. [1998], 28 WAG injection cases employed CO_2 as the injected gas, which is popular to use for miscible injection due to easy solubility of CO_2. However, 24 offshore fields used hydrocarbon gases in dry or enriched form, despite the environmental benefits of using CO_2, simply because of the availability in the production site of HC gas for most offshore WAG projects. This study focuses on optimizing injection patterns for synthetic gas as the HC gas condition for the injection process to take advantage of the offshore recovery.
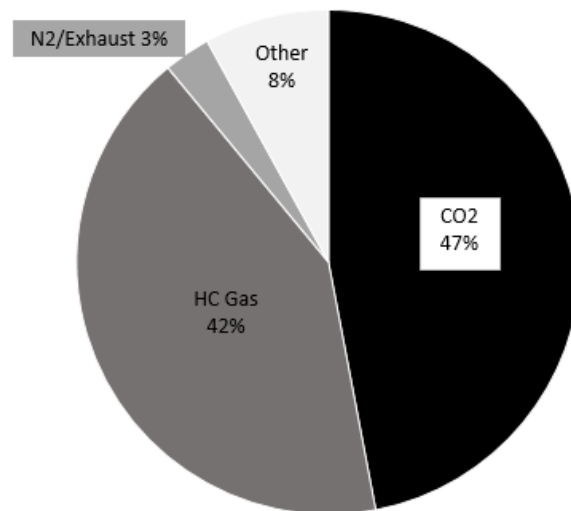
Fig. 2-5: Injection gas used in 59 WAG projects [Christensen et al., 2001]

Water injection

The brine used for the injection process of reservoir recovery has to be estimated for recent time because of the effect of salinity on oil recovery. Brine salinity affects enhanced oil

recovery process through many mechanisms inside the pore system such as ion exchange, mobility control, and wettability alteration [Ramanathan et al., 2015].

Jiang and Nuryaningsih investigated the effect of brine salinity on WAG injection by conducting a series of core-flooding experiments on Berea sandstone with two different oil samples [Jiang and Nuryaningsih, 2010]. A synthetic brine with NaCl salinity in the range of 1000 to 32,000 ppm, and a synthetic brine is containing 4000 ppm NaCl and 4000 ppm $CaCl_2$ were used to examine the recovery performance. They concluded that with the same miscible condition, the tertiary oil recovery will increase when increasing the salinity for both oil models due to the decreasing level of CO_2 solubility. They also indicated that secondary water-flooding would be more effective with low salinity brine compared with high salinity. This statement has been proven through experimental and simulation research [Zolfaghari et al., 2013; Dang et al., 2014; Ramanathan et al., 2015].
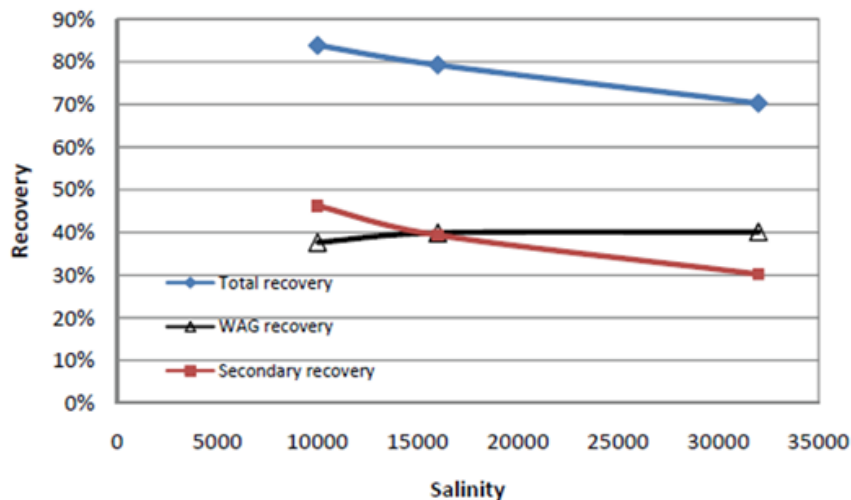
Fig. 2-6: The recovery of water flooding, WAG flooding, and total as a function of salinity [Jiang and Nuryaningsih., 2010]

Zolfaghari et al. [2013] ran a set of core-flooding tests for heavy oil with low and high salinity brine for CO_2-WAG injection; they concluded that low salinity brine combined with CO_2 in

WAG injection gave the optimum recovery for heavy oil, both as a secondary or tertiary process.

Dang et al. mentioned that the main mechanism contributing to the efficiency of low salinity brine injection is wettability alteration by moving to the water-wet condition [Dang et al., 2014]. Furthermore, brine salinity also affects the recovery process through core aging condition. Ramanathan et al. conducted six core-flooding tests on Grey Berea sandstone cores by immiscible WAG injection to estimate the impact of the aging condition as well as the correlation with brine salinity on oil recovery [Ramanathan et al., 2015]. The result indicates that low salinity brine is more effective for the water-flooding process, while high salinity seawater gives a better recovery for WAG injection. The salinity makes a significant impact on wettability after aging core that affects the recovery process later.
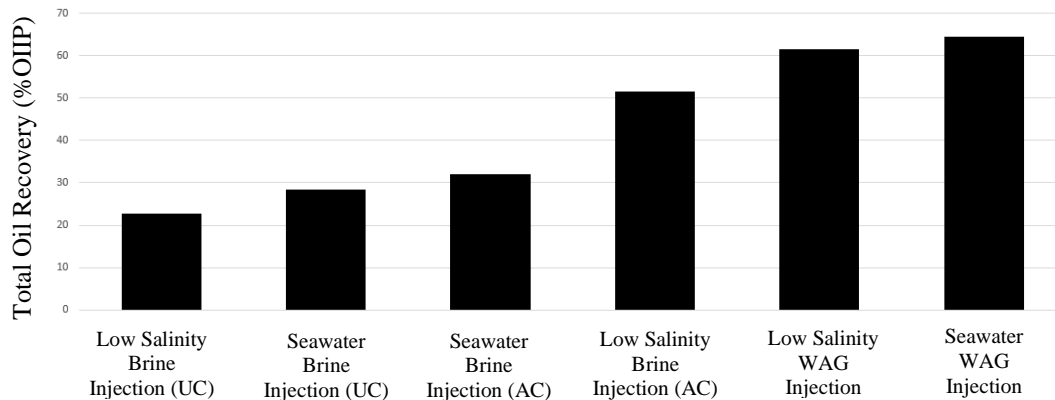
Fig. 2-7: Comparison of oil recovery between different processes on Grey sandstone [Ramanathan et al., 2015]

In this research, brine with a high salinity (102,435 ppm) [Wang et al., 2006] is used as injected water to simulate the core-scale IWAG process, which is similar to the experimental works of the double displacement test from the research of Wang et al.

WAG timing

Tanner [1992] proposed a process called "Denver Unit WAG" injection process; it is an optimum mechanism they suggest to recover oil from the world's largest CO_2 EOR project. Based on numerical models that match the historical recovery from CGI (continuous gas injection) and CO_2-WAG for this area, they suggest that the optimum operation parameters for this unit are 60%-80% pore volume CGI followed by WAG injection with ratio 1:1. This conclusion has raised a concern about the optimum time to start WAG injection after secondary recovery stage as water-flooding or gas injection.

Amin et al. [2012] presented results from a set of core-flood tests to compare the efficiency of miscible CGI and CO_2-WAG for a carbonate unit in the UAE. They also concluded that timing plays an important role in the injection process. Running WAG injection in the early stage as a secondary recovery would give a better oil recovery, an incremental over 12% remaining original oil in place (OOIP), than starting as a tertiary process after CO_2 flooding.

Jiang et al. [2012] pointed out the variation of 3-phase saturation after water-flooding can significantly affect the optimum timing to start WAG injection [Jiang et al., 2012]. Their experiments were set up for water-wet Berea sandstone cores under the miscible condition with injected fluids as synthetic brine and high purity CO_2, the results indicate that starting the injection process too early or too late would lead to a lower recovery factor. In a range from 0% to over 50% pore volume oil recovery after water-flooding, the most suitable timing to start WAG injection is around 30% PV oil recovery. In the middle of this range, due to the appropriate volume of oil left after water-flooding that allows to CO_2 easily contact then improve microscopic sweeping efficiency as well as enough volume of water to enhance the gas trapping mechanism.
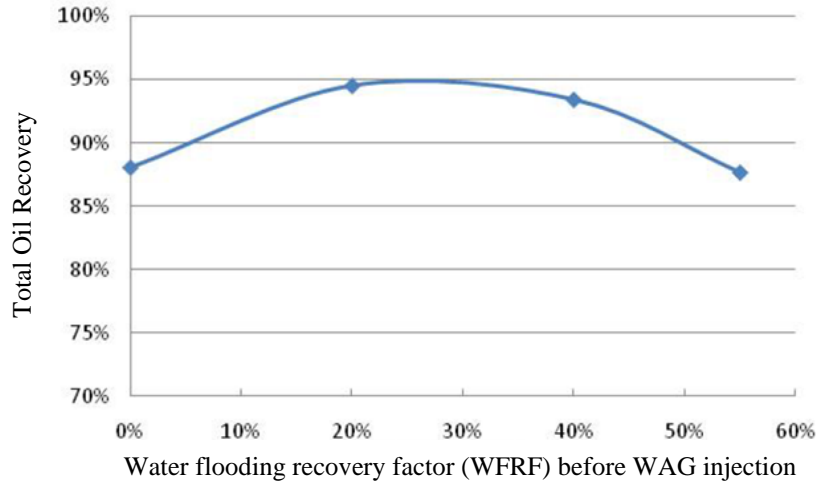
Fig. 2-8: WAG recovery efficiency at different starting points [Jiang et al., 2012]

In 2015, Batruny and Babadagli also verified a similar conclusion. Their experiments were conducted at ambient pressure and temperature on a pure silica sand pack with a porosity of approximately 37%. Heptane was used as injected gas for these experiments [Batruny and Babadagli, 2015]. To investigate the timing effect on WAG injection efficiency, three cores with different oil saturation after water-flooding were used to run tests including 20%, 35%, and 50% oil saturation. The highest oil saturation condition as a result also accounts for the biggest recovery factor, over 80% OOIP, almost double the recovery value of the 20% oil saturation option.
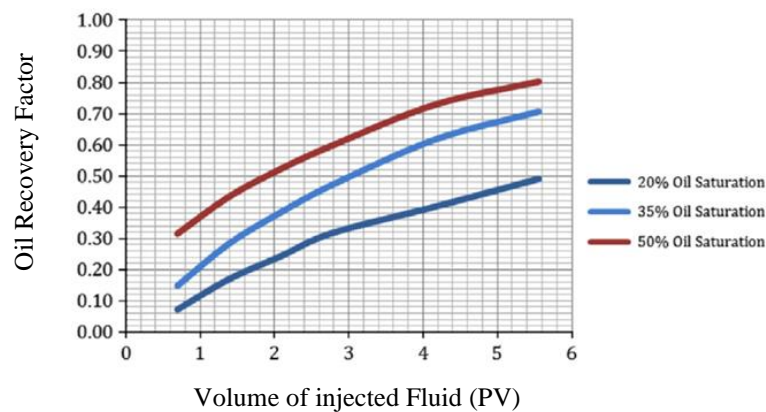
Fig. 2-9: Total fluid injection (PV) vs. recovery factor (% OOIP) at different stages of oil saturation [Batruny and Babadagli, 2015]

41

Hence, defining the right time to start WAG injection will make a clear impact on improving oil recovery efficiency.

WAG ratio

WAG ratio, defined as the volume of injected water divided by the volume of injected gas, could be considered as the most important operating parameter for planning the injection process. An optimum ratio must be not only get the highest oil recovery, but also control the most appropriate volume of solvent used for injection, which would improve the economic benefit [Juanes and Blunt, 2006].

Jackson et al. [1985] pointed out that the wettability has a significant impact on WAG ratio. They suggested the ratios 0:1 for water-wet bead pack and 1:1 for the oil-wet pack. Stern. [1991] also concluded similar results when investigating the mechanism of miscible oil recovery, after 16 core-flooding experiments for both water-wet and mixed-wet cores. He indicated that for water-wet rock, a high WAG ratio could lead to less oil recovery because the presence of water will reduce the contact between oil and solvent; for the mixed-wet system, the impact of WAG ratio is not significant on recovery efficiency, but he suggested the use of the ratio of 1:1 as the optimum number.

Zekri et al. [1992], after comparing three different ratios of 1:1, 2:1 and 1:2 from miscible WAG injection for sandstone composite core with oil-wet preferred, the optimum ratio also suggested 1:1 for the lowest residual oil saturation, only 12.38 %PV, after tertiary recovery process with CO_2 as injected solvent.
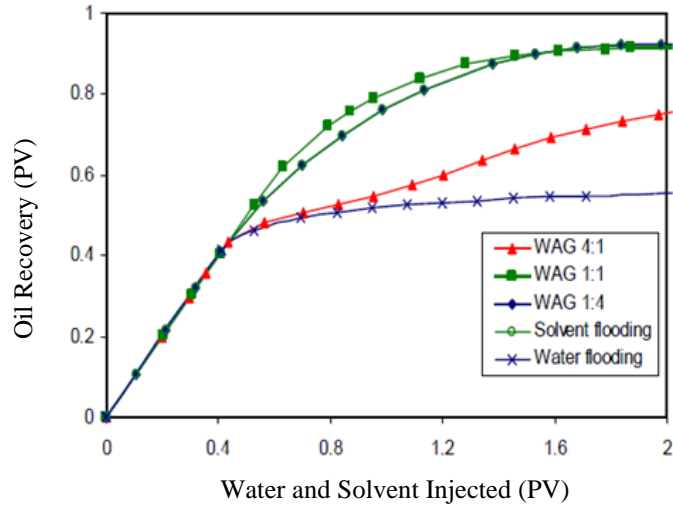
(a)
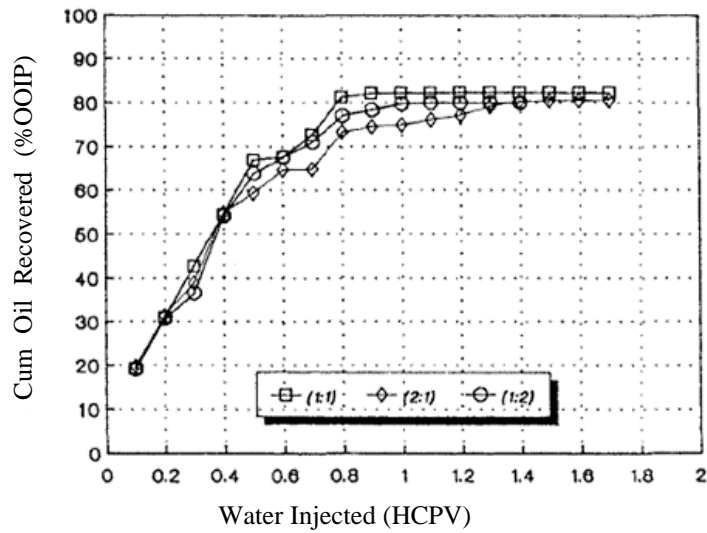
(b)

Fig. 2-10: Comparison between different WAG ratios for the water-wet system (a) [Al-Shuraiqi et al., 2003], and the oil-wet system (b) [Zekri et al.,1992]

Various researchers have focused on investigating the effect of WAG ratio for a water-wet system for both miscible and immiscible injection. In 2003, Al-Shuraiqi et al. compared three ratios of 4:1, 1:1 and 4:1 from WAG injection process for miscible displacement process on

Ballotini glass beads with ISOPAR V as oil, and paraffin as the injected solvent. The highest oil recovery was achieved with a ratio of 1:1, with the flow rate as 5 ccs/min [Al-Shuraiqi et al., 2003]. In 2004, Wu et al. simulated a 2-D model under miscible condition with injected solvent as combination of 85 % CO_2 and 15 % NGL, after comparing results from 5 different ratios, the highest oil recovery after injecting 1.5 PV was obtained with the 2:1 case, however, just slightly higher than the recovery factor of 1:1 case, approximately 1-2% [Wu et al., 2004]. In 2015, Kim et al. simulated miscible WAG injection in a 1-D model with dimensions of $50 \times 1 \times 1$ grids, the results were presented to compare the recovery efficiency of different operation parameters for the core-flooding model and suggested ratio of 1:2 as the optimum case, which had a recovery factor of 65%, slightly higher than the 1:1 case (62%) which showed a better efficiency in CO_2 consumption [Kim et al., 2015].

The WAG ratio around the point 1:1 is considered to be the best optimum parameter to improve the injection process for both field and laboratory operations with the advantages of balancing the solvent-oil contact efficiency as well as optimizing the volume of solvent injection [Christensen et al., 2001; Panda et al., 2009; Amin et al., 2012; Han et al., 2015; Batruny et al., 2015; Khanifar et al., 2015].

WAG slug size

Generally, WAG slug size is defined as the volume of injected gas, or the volume of injected water, for each cycle of WAG. Based on almost 60 observed WAG project operations, it was clear that the length of injected water and solvent processes are various for different reservoir properties [Christensen et al., 2001]. In 2004, Wu et al. varied the WAG cycle length (45, 75, 150, 300, and 600 days) for a total of 1.5 PV injected for his model simulation and the length

as 75 days gave the highest oil recovery factor, however it raised a concern that the optimum option should be chosen from a range of slug size [Wu et al., 2004].

Namani and Kleppe. [2011], from results of both sensitive black-oil and compositional miscible WAG models, concluded that the relationship between half-cycle slug size and the volume of recovered oil is significant, but not simple, to predict and a suitable option could be optimized for different models. The total length of the injection process also varies through different rock-fluid properties and fluid-fluid properties to acquire the optimum oil recovery. Torabi et al. [2012] pointed out that changing rock permeability would lead to significant time for total fluid injection to archive the optimum oil recovery factor. For these cases, they varied the permeability from 11.4 to 39.9 Darcy and the length of injection for each option also increased from 1.8 PV to 4.5PV through a set of core-flood experiments.
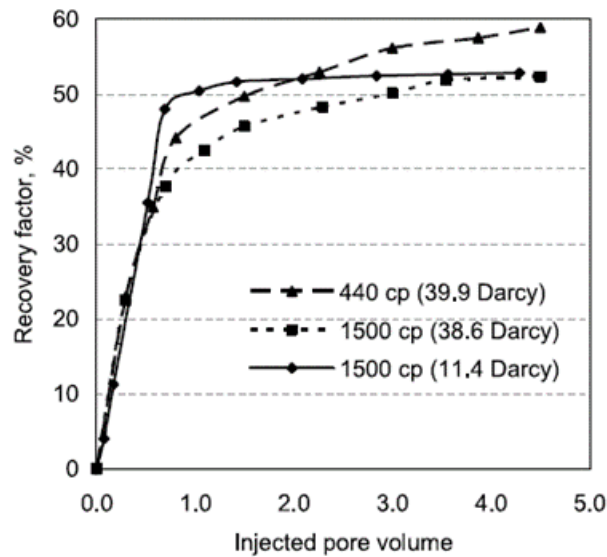
(a)
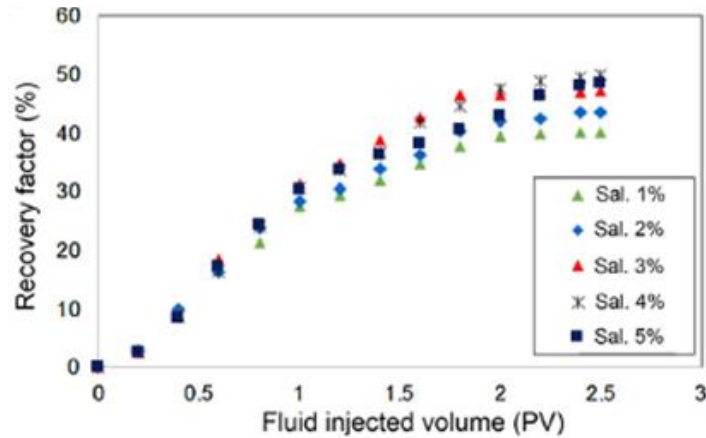
(b)

Fig. 2-11: Effect of injected fluid on oil recovery, (a) varying rock permeability [Torabi et al., 2012], and (b) varying brine salinity [Van et al., 2017]

By changing each cycle slug size, the interaction between the reservoir fluid and the injected fluid also changes, such as fluids mobility and contact time, which will result in the efficiency of the displacement process. Under the miscible condition, Nuryaningsih et al. [2010] conducted a set of core-flooding experiment on Berea sandstone core by changing half-cycles slug size from 0.05 to 0.75 PV with WAG ratio of 1:1. The results indicated that the option as 0.1PV is giving the highest oil recovery (almost 80% OOIP) after injecting 1.2PV in total, they pointed out that a high slug size would lead to a sooner gas breakthrough, while a significantly small size of slug would reduce the contact between oil and gas that make a negative impact on microscopic displacement efficiency.

Kim et al. [2015] made a similar conclusion after optimizing the parameters for a 1-D core model simulation; a suitable small slug was determined to be 0.04 PV from an investigated range between 0.01 and 0.3PV with a WAG ratio of 1:2. A bigger slug size may have a negative impact on oil recovery factor due to gravity segregation.

(a) (b)
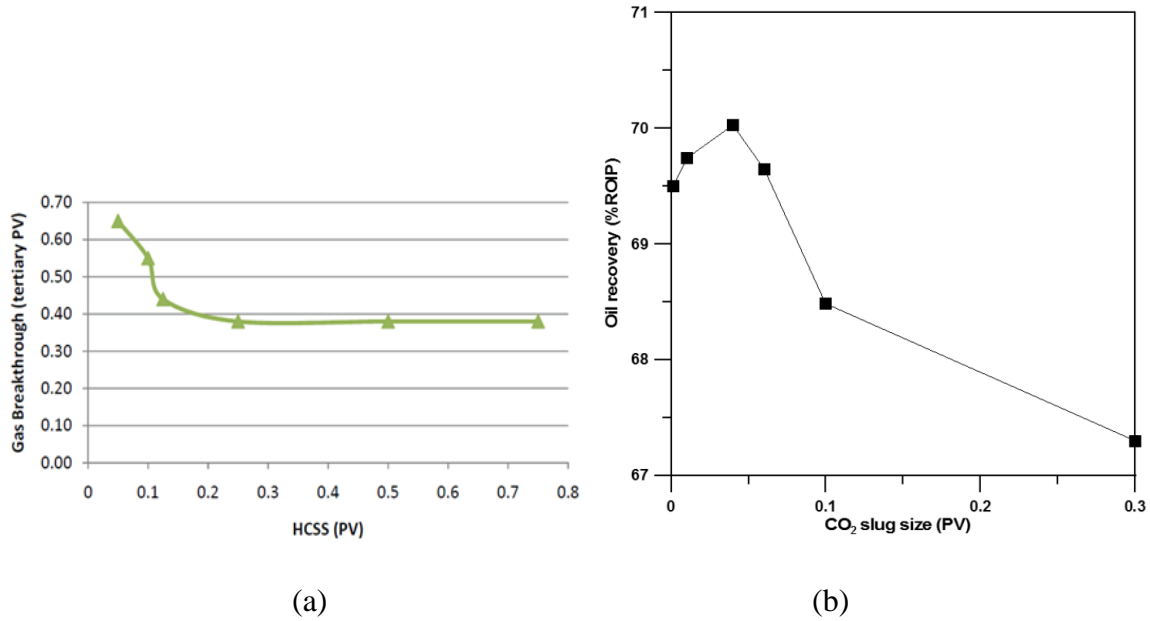
Fig. 2-12: (a) Gas breakthrough at different WAG half-cycle slug sizes (HCSS) [Nuryaningsih et al., 2010] and (b) Oil recovery per slug size [Kim et al., 2015]

Van et al. [2017] conducted a sensitive analysis regarding slug size and salinity effects by conducting a set of miscible WAG core-flood experiments and then applying a prediction method known as response surface models to optimize the suitable operation parameters. The range of slug size used for these experiments were from 0.2 to 0.6 PV with a fixed WAG ratio of 1:1. Salinity varied from 0.2 to 0.6 PV, and the final optimum result determined from the mathematical model was 0.455 PV with a salinity of 4.313% for a recovery factor around 51% residual oil volume after secondary water-flooding. It could be concluded that by varying the wettability condition of rock samples, water-wet [Han et al., 2015] or mixed-wet [Alkhazmi et al., 2017]. A suitable small slug size still gives a better oil recovery efficiency rather than a bigger one. Furthermore, they also pointed out that the recovery factor from WAG injection would not increase significantly after water breakthrough.

WAG flow rate

47

WAG flow rate is the operational parameter that impacts the length of the injection process as well as the relative permeability of each phase. In 1991, Stern, from a set of core-flood tests, indicated that there is a correlation between flow rate and maximum residual oil volume, namely that there is a limitation of flow rate that if higher the residual oil volume could be increased. There could be an optimum number of the range below limitation, this study also discussed that flow rate could affect capillary induce and viscous fingering, which results in the relative permeability. Al-Shuraiqi et al. [2003] used paraffin and water as injection fluids for both miscible and immiscible displacement tests, and varied the flow rate from one 1 cc/min and 5 cc/min. They found that there is a significant impact on the volume of oil recovered through total injected fluid volume, as well as water-cut status. The optimum flow rate of 3 cc/min was predicted through a simulation model to achieve the maximum oil recovery factor.

The flow rate proved to affect the viscous force, which has an impact on displacement efficiency [Namani and Kleppe., 2011]. Furthermore, for a different type of oil viscosity, flow rate also affects the total oil recovery factor. This phenomenon is related to viscous force efficiency [Torabi et al., 2012]. Batruny et al. [2015] found that flow rate as well as slug size had a significant impact on oil recovery efficiency. However, their research only compared the slug side effect for each case of injection rate and did not point out the correlation between them.

(a)	(b)
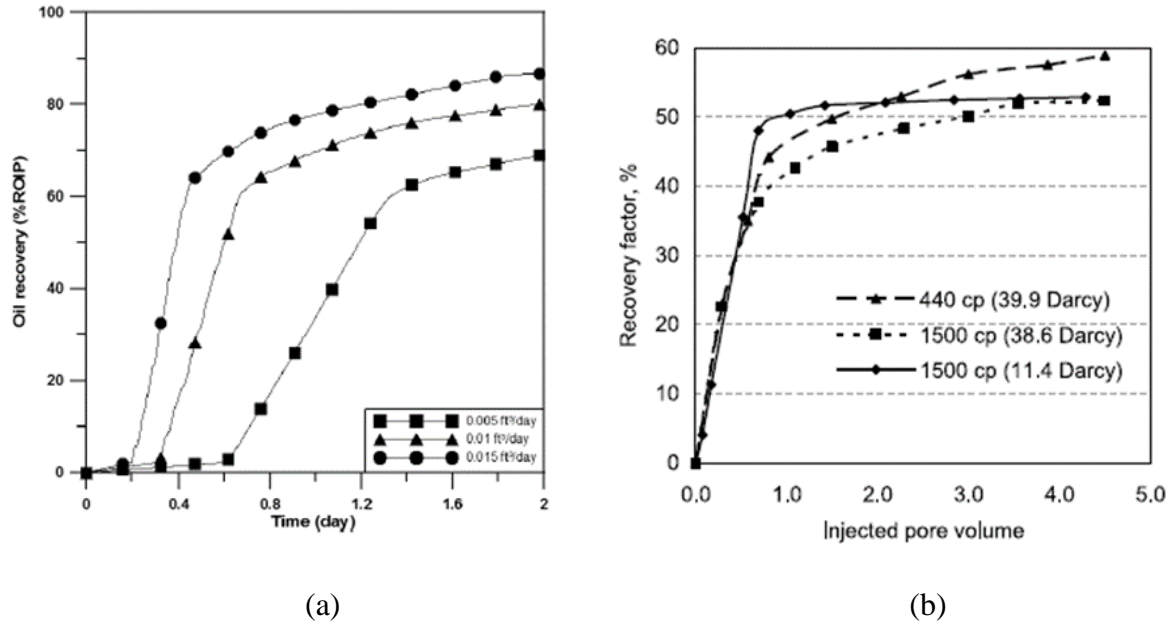
Fig. 2-13: Effect of flow rate on total oil recovery (a) [G. Kim et al., 2015] and the effect of flow rate on oil viscosity (b) [F. Torabi et al., 2012]

Kim et al. [2015] completed a simulation of the core model and reservoir model and discussed that WAG flow rate affects not only the total oil recovery volume but also the injected gas breakthrough time. In the range of injected rates investigated, the highest value ($0.015 \, ft^3/day$) resulted in the most efficient oil recovery.

Generally, it can be concluded that a suitable high flow rate can significantly improve the recovery factor in comparison with low value but does not lead to a critical bypassing level of injected fluid.

WAG Sequence

Injection sequence, i.e. starting first with a gas or water cycle, is a significant factor that would make a clear impact on the efficiency of the WAG injection process. Han et al. [2015] have investigated this factor through a series of nine core-flood tests for a tight oil formation, under the same operational parameters for WAG ratio, slug sizes, and flow rate, but changed the sequence of injection cycles to see how the RF would change. They concluded that when

49

running WAG injection as the secondary recovery stage, starting with water cycle first will give a better efficiency due to the higher volumetric sweep than gas cycles; these cases were compared even in different slug sizes. However, this research compares the effect happening as secondary recovery.
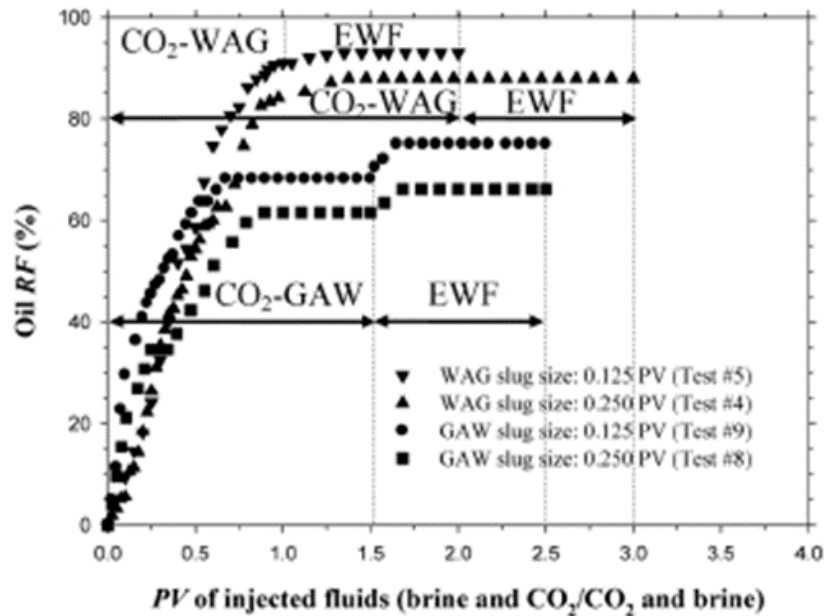
Fig. 2-14: Effect of injection sequence on oil recovery [Han et al., 2015]

Fatemi et al. [2015] investigated the effects of different IFT between oil and gas on the performance of immiscible WAG injection for a mixed-wet system. Their research clearly indicated that the oil recovery volume under different IFT schemes was dependent on the injection sequence. In the case of high IFT (2.7 mN/m), starting gas injection as the initial cycle gave a higher recovery, whereas for the case with low IFT (0.04 mN/m), starting with the water cycle first gave better results of oil recovery.

Batruny et al. [2015] also noted the significant effect of injection order on oil recovery. Their core-flooding experiment was performed under a miscible condition in a water-wet system. By changing the sequence of starting the injection process with heptane or water, the

conclusion for this case was made that starting by heptane, with a significant slug size, will give a better oil recovery result in comparison with starting with water, due to the higher efficiency of miscibility and sweep between the solvent and oil interaction inside the pore system.
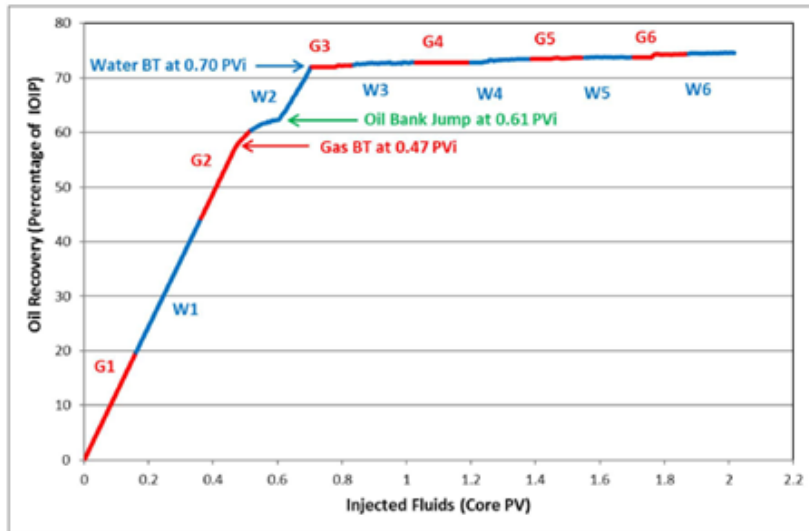
(a)
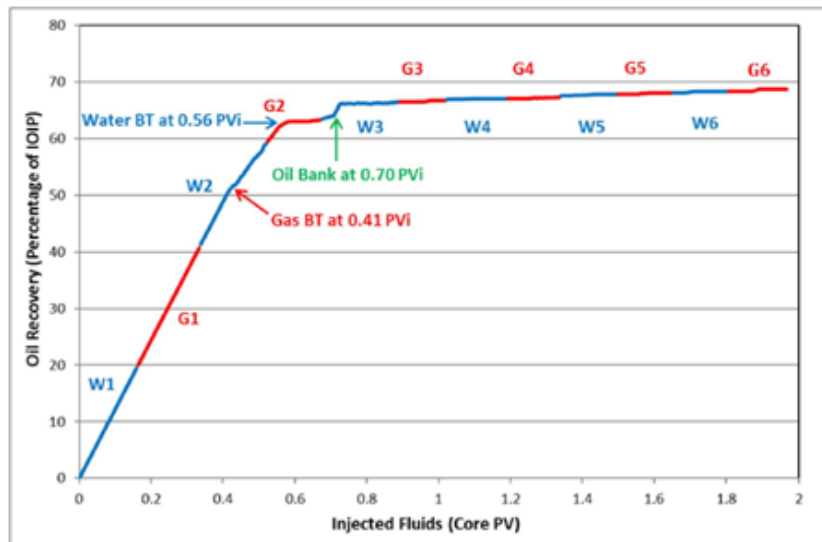
(b)

Fig. 2-15: Recovery for (a) GAW and (b) WAG injection [Alkhazmi et al., 2017]

Later for the case of immiscible WAG injection in a mixed-wet system, Alkhazmi et al., [2017] found that when comparing two processes as small slug size GAW and WAG injection, most oils were recovered after 2 cycles (0.8PV injection), and starting with a gas cycle would lead to a later gas and water breakthrough. Moreover, after 2PV injection, running gas cycles first would give better oil recovery results, around 75% IOIP compared to roughly 68% IOIP using the water cycle first.

Generally, it can be concluded that the sequence of cycle injection makes a clear impact on the efficiency of the WAG injection process.

2.2.2 Core-scale IWAG injection screening

In order to determine a suitable range of values for IWAG operational parameters as input data for the injection process as well as to generalize the efficiency of different core-scale IWAG injection schemes, a total of 18 projects [Table 2-1] were reviewed. Injection information that affects the oil recovery efficiency, such as type of injected fluid, reservoir wettability, time to start first WAG cycle, WAG slug size, ratio, flow rate and the sequence of each cycle, is tabulated. Generally, the WAG ratio equal to approximately 1:1 may result in a high oil recovery factor by balancing the sweeping effect of water and gas injections. The sequence of the injection process is significantly affected by when the WAG injection recovery started. WAG flow rate is usually simulated as the condition from the field production activity. WAG slug size usually ranges from 0.01 to 0.5 PV, and an appropriate small volume will improve the recovery process.

Core-Scale IWAG Injection Operational Parameters Screening													
Authors	Core Properties				Fluid Properties			WAG Timing	WAG Flow Rate	WAG Ratio	WAG Slug Size	WAG Sequence	Best Hydrocarbon Recovery Efficiency	Conclusions
	Type	Wettability	Porosity	Permeability	Reservoir Hydrocarbon	Injected Gas	Injected Water							
Cullick et al., 1993	Limestone core	Water-wet	11.3 - 26 %	0.3 - 10 mD	C3	C2 - nC4	Brine	Secondary stage	0.05 - 2 ft/Day	1:1	0.05 PV	Water first	Over 80 % IOIP after 1.2 PV injection	- WAG injection consumes less gas but more efficient than continuous gas injection. - Changing the injection rate does not make a clear impact on gas condensate recovery efficiency.
Nguyen et al., 1998	Silica Sand core	Water-wet	38 - 42 %	11 - 13 D	Crude Oil (Heavy)	CO2 - N2	Brine	Secondary stage	6 ft/Day	4:1	0.2 PV	Gas first	Over 50 % IOIP after 2.5 PV injection	- N2 affect the impurity of CO2 by decreasing the solubility and diffusivity. - More percentage of N2 in the gas mixture reduce the recovery efficiency.
Sohrabi et al., 2000	Micromodel	Water-wet	N/A	N/A	nC10	C1	Distilled Water	Tertiary stage	3 ft/Day	N/A	N/A	Gas first	Over 20 % ROIP after five cycles of injection	- Most oil recovery of WAG happened in the first two cycles. - Gas intends to occupy the oil-filled pore due to its lower IFT of gas/oil compared to gas/water.
Dong et al., 2002	Micromodel	Water-wet	N/A	N/A	Mixed Crude Oil	Air	Brine	Secondary stage	0.15 cc/Hr	2:1 3:1	0.3-0.4 PV	Water first	Over 50 % IOIP after 2.5 PV injection	- Injected gas tends to push the oil into the water channel when the residual oil saturation still high. - Trapped gas saturation increasing is the main recovery mechanism when Sor low. - More cycles of injection do not lead to a better recovery due to high water saturation and discontinuity of the oil phase.
Righi et al., 2004	Quartzose sandstone core	Water-wet	18%	25 - 300 mD	Live-Oil	Produced Gas	Brine	Tertiary stage	N/A	1:1	0.05 - 0.1 PV	Gas first	Over 20 % IOIP after 1.2 PV injection	-WAG produced a significant volume of oil as tertiary recovery. - A good matching between the core flooding experiment and simulation results.

Reference	Core	Wettability	Porosity	Permeability	Oil	Gas	Water	Stage	Rate	Ratio	Slug	Order	Recovery	Notes
Kulkarni and Rao, 2005	Berea sandstone core	Water-wet	N/A	N/A	n-Decane	CO2	Brine	Tertiary stage	60 cc/Hr	1:1	0.5 PV	Water first	Over 20 % IOIP after 2 PV injection	- The optimum process suggested by this experimental work is approximately 60%–80% pore volume CGI injection followed by 1:1 WAG; it is related to timing. - WAG floods show a significant dependence on brine composition.
Zhang et al., 2006	Sandstone core	Water-wet	N/A	N/A	Crude Oil (Heavy)	CO2 - N2 Flue gas	Brine Foam	Tertiary stage	20 cc/Hr	4:1	0.2 PV	Gas first	Over 5 % IOIP after 4 PV injection	- The efficiency of using flue gas is the same with pure CO2, which much better than being contaminated by N2. - Using foam instead of just brine will improve the recovery efficiency for heavy oil.
Zhang et al., 2010	Mixed silica sand core	Water-wet	N/A	N/A	Crude Oil (Heavy)	CO2	Brine	Tertiary stage	20 cc/Hr	1:1	0.5 PV	Gas first	Over 15 % IOIP after 4 PV injection	- Significant oil recovery was noticed by WAG injection to compare with only Polymer Injection. - The concentration of Polymer is important to improve the recovery efficiency of Polymer alternating gas Injection.
Ghafoori et al., 2012	Carbonate core	N/A	12.15%	0.36 mD	Live Oil nC10-nC4	CO2 - N2	Brine	Secondary stage	15 cc/Hr	1:1	0.05 - 0.25 PV	N/A	Over 80 % IOIP after 2 PV injection	- Slug size impact on oil recovery for N2-WAG injection after comparing different schemes. - The optimum time to start injection is 1:1 WAG followed after 0.5 PV of gas was injected.
Srivastava et al., 2012	Sandstone core	N/A	21.00%	323.23 mD	Live-Oil	CO2	Brine	Tertiary stage	10 - 20 cc/Hr	1:1	0.1 - 0.5 PV	Gas first	Over 12 % IOIP after 1 PV injection	- Slug size has a clear impact on the tertiary oil recovery by WAG. - Tapered WAG gives a general better oil recovery volume than a conventional WAG.
Jiang et al., 2012	Berea sandstone core	Water-wet	19.50%	125 - 130 mD	Crude Oil	CO2 - O2	Brine	Tertiary stage	18 cc/Hr	1:1	0.1 PV	Water first	Over 10 % IOIP after 2 PV injection	- The impurity of CO2 significantly impacts the efficiency of WAG recovery for both immiscible and miscible WAG.

Reference	Rock type	Wettability	Porosity	Permeability	Oil type	Gas	Water	Stage	Injection rate	WAG ratio	Slug size	Sequence	Recovery	Comments
Torabi et al., 2012	Sandstone core	N/A	36 - 38 %	12 - 43 D	Crude Oil (Heavy)	CO_2	Brine	Secondary stage	6 - 60 cc/Hr	1:1 2:1 1:2	N/A	N/A	Over 40 % IOIP after 4.5 PV injection	- WAG ratio has a clear impact on oil recovery; in this case, 1:1 is considered as the optimum value. - Base on the viscosity of the oil, a suitable WAG ratio should be suggested for an optimum oil recovery factor.
Zolfaghariet al., 2013	Sandstone core	Water-wet	29 - 31 %	330 - 340 mD	Crude Oil (Heavy)	CO_3	Brine	Secondary stage	18 cc/Hr	1:1	N/A	Water first	Over 80 % IOIP after 2 PV injection	- The low salinity brine tends to give a better oil recovery than the high one for both WAG injection and only water-flooding as secondary recovery stage.
Salehi et al., 2014	Silica Sand core	Water-wet	29%	350 mD	Crude Oil	N_2	Surfactant	Secondary stage	12 cc/Hr	1:1 3:1 1:3	0.15 PV	Surfactant first	Over 80 % IOIP after 1.2 PV injection	- The amount of oil recovery is highly sensitive to WAG ratio.
Fatemi et al., 2015	Clashach sandstone core	Mixed-wet	18.20%	65mD	n-Butane	CH_4	Brine	Secondary stage	25 cc/Hr	1:1	2.5 PV	Alternating	Over 70 % IOIP after 15 PV injection	- Ultimate oil recovery by CGI is less for the case of Mixed-wet than water-wet and RF of gas injection is lower than that obtained by water-flooding, also contrast with water-wet type. - The oil recovery is lower for extended gas injection performed at higher gas/oil IFT conditions. - For ultra-low IFT, WAG is better than GAW. - For high IFT, GAW is better than WAG. Hence, the sequence makes a clear impact on oil recovery efficiency.
Ahmadi et al., 2015	Sandstone core	Water-wet	13 -25 %	13.5 - 14 mD	Crude Oil (Heavy)	CO_2 HC gas N_2	Brine	Secondary stage	N/A	1:2	0.5 PV	Water first	Over 70 % IOIP after 1.5 PV injection	- Hot water is more effective than normal brine for WAG recovery. - Associated HC gas in compared with N_2 and CO_2 is better for improving oil recovery factor.
Khanifa et al., 2015	N/A	N/A	29 - 33 %	180 - 300 mD	Live-Oil	Mixed HC gas - CO_2	Brine Seawater	Tertiary stage	13 cc/Hr	1:1	0.2 PV	Gas first	Over 15 % IOIP after 4 PV injection	- WAG produced a significant volume of oil as tertiary recovery.

| Alkhazmi et al., 2017 | Clashach sandstone core | Mixed-wet | 18.20% | 65mD | n-Butane | CH4 | Brine | Tertiary stage | N/A | 1:1 | 0.15 - 2PV | Alternating | Over 70 % IOIP after 2 PV injection | - Highest performance of oil recovery was achieved by the injection of the first two cycles of small slug GAW (0.72/0.75 total IOIP) and small slug WAG (0.64/0.69 total IOIP).
 - Reducing the size of injected slugs can improve the performance of WAG.
 - Sequence significantly impact on oil recovery efficiency. |

Table 2-1: Screening of core-scale IWAG injection through 18 experimental projects

2.3 Double Displacement Process (DDP)

The Double displacement Process (DDP) is considered to be an effective oil recovery method that employs gas as the immiscible injection solvent and can be applied to oil reservoirs as a secondary recovery method after the natural water influx stage or as a tertiary recovery method after secondary water-flooding [Ren et al., 2004]. In 1988, the term of DDP was first introduced by Carlson in a study to investigate the performance of Hawkins field oil recovery under gas drive process [Carlson, 1988]. The results of this recovery process for this field project is remarkable, with a total oil recovery factor over 80%, much higher compared with water-flooding in which approximately 60% of the initial oil volume was recovered. Gases used for DDP vary with the popular types including hydrocarbon gas, flue gas, nitrogen and carbon dioxide [Merchant, 2010]; their worldwide applications are recognized with an average total oil recovery factor over 75% [Kulkarni and Rao, 2006]. When implementing DDP for field projects, gas is injected from the top part of the reservoir, and oil is produced from the bottom part.
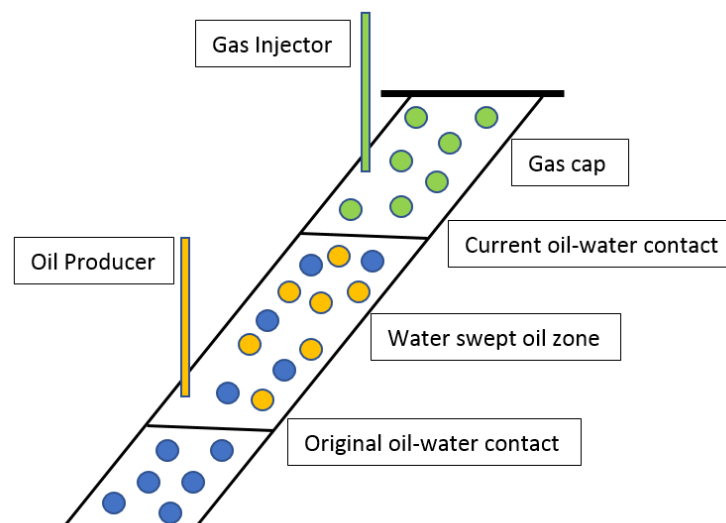
Fig 2-16: Double displacement process [Satitkanikul and Athichanagorn, 2013]

The main recovery mechanisms of DDP are gravity drainage and mobilization of residual oil from water-flooding by the displacement effect of gas cap expanding by the injection [Carlson, 1988]. Water-flooding is also uses gravity drainage to recover oil, but due to a smaller disparity in water-oil density than in gas-oil density gravity drainage is less effective for water-flooding than for gas injection. Double displacement processes, including gas-oil displacement, which is usually called the first drainage process, and oil-water displacement as a second drainage process to push the oil-water contact to the original position [Oren et al., 1992]. The benefit of double displacement processes, DDP, is improving the sweep efficiency then displace better for the gas-oil system to the water-oil system [Langenberg et al., 1995]. Various studies investigate DDP, fboth experimentally and through simulation.

Fassihi and Gillham. [1993] introduced the first project that employed air as the injected gas for DDP in the West Hackberry field. Air was chosen for this project because of its economic benefit, it was much cheaper than using nitrogen or CO_2 and was easy to mobilize the reservoir oil under high pressure and temperature condition. Based on the simulation results, they concluded that the gravity effect is considered as the main mechanism for the DDP recovery process in this field. Furthermore, the interaction between gas and oil phase is also significant to the recovery process by the effect of phase behavior and composition of fluids.

Oren and Pinczewski. [1992, 1994] continued the previous study about the effect of wettability and spreading on the recovery performance of DDP from water-wet system to oil-wet system by observing the recovery process in an experimental micromodel. Air was used as the injected gas, and ambient pressure and temperature were maintained for DDP. They observed that oil-wetting films in the oil-wet system were thicker and more productive than oil-spreading film observed in the water-wet system in the study of Oren et al. in 1992.

Another statement was also made that oil recovered from the oil-wet system is much higher than water-wet-system due to its positive spreading effect.

Ren and Bentsen. [2004] conducted pore-level experiments to investigate the main mechanisms of two gravity-assisted tertiary gas injection processes including DDP and second-contact water displacement (SCWD), an extended version of DDP with a second water-flooding. Nitrogen was used as the injected gas for both processes, with gas injected from the top of the cell, and water injected from the bottom of the cell to illustrate the same condition as the field operation. They confirmed that the oil firm is an important factor in the recovery process, and it depends strongly on the interfacial tension of the fluid system. Moreover, the length of SCWD is much shorter than DDP due to the effective second water-flooding and trapped gas effect.

Wang et al. [2006] investigated the properties of three-phase flow in DDP for an oil-wet composite core representative of the Hibernia reservoir. Synthetic gas and formation brine were used as injected fluids to set up the condition of the DDP test. The gravity effect was also noticed in simulating the core-flooding experiment by orienting the vertical direction of the core holder. After water-flooding, approximately 54% OOIP was recovered when the water-cut was at 90 percent. An additional approximately 13% OOIP was recovered after the first pore volume of gas injection and a total of around 33% OOIP was produced by the whole gas-flood at water-flooding residual oil. This result demonstrates that employing hydrocarbon gas for DDP is good not only for storage purposes, but also to produce a significant additional oil recovery after water-flooding.

To investigate the effectiveness of DDP application for a sandstone formation, Al-sumaiti and Kazemi [2012] proposed experimental and numerical simulation of DDP for a tight fractured

reservoir that has a wettability range from mixed-wet to oil-wet condition. The procedure of this research included examining the DDP tests for experimental fracture core, simulating the experimental by computational software and upscaling the experimental results to field-scale data. The experimental results from the DDP test indicated that all cores recognized a total oil recovery of all injection process is higher than 80% with the volume of oil recovered by gas-flood equal to the amount from water-flooding. The classical implicit pressure explicit saturation method created a good matching between the simulation model and experimental data. However, due to the complex structure of the fractured reservoir, scaling up the experimental data to field-scale could be challenging.

Satitkanitkul and Athichanagorn. [2013] presented an optimization procedure for DDP of a numerical reservoir model. Four important parameters were listed to be optimized, including the length of water injection, fluids injection rate, and well pattern. The results indicated that a high produced water leads to a better oil recovery factor. Furthermore, a high rate of fluid injection gave a higher amount of recovered oil; however, too high a rate will yield an excess of the formation fracture system. Finally, a horizontal production well is more effective than a vertical one.

In this research, the fluid information and cores used for the DDP test in the study of Wang et al. are employed to simulate the numerical composite core-scale model for further investigation of IWAG injection as well as validating with the experimental data from this study.

2.4 Oil and Gas Production Optimization

The main objective of oil production optimization is to investigate the most appropriate operational scheme to acquire the maximum volume of oil recovery from the reservoir but

still maintain a good balance for the operation and economic constraints. The optimization application was introduced for use in the oil and gas industry and developed through the time for many aspects. In the middle of the 1960s, research presented a simplified optimization method for the drilling of a gas reservoir to optimize the number of wells, the length of the drilling period and timing to start the drilling stages, for both technical and economic considerations [Goldfracht et al., 1966]. Later, a constrained optimization technique was employed to achieve the optimum operational parameters, such as production well rate and gas-lift rate, to increase production rate and decrease the operational expense [Wang et al., 2002].

Various optimization programming techniques have been applied to optimize oil and gas exploitation. The following information will generally categorize optimization methods and present the literature with respect to their application in the oil and gas industry.

2.4.1 Response Surface Methodology (RSM)

The Design of Experiments (DOE) is not just considered as an optimization technique, it is an effective tool to determine the relationship between cause and effect. Beginning in early 1920, Sir Ronald A. Fisher became the pioneer to lay the foundation for this technique originally focused on agriculture purposes [Fisher, 1958]. Three fundamental principles were introduced through his research for shaping the experiment design, including randomization, replication, and blocking. He also systematically presented general ideas about the design of experimental investigation, including the factorial design concept and the analysis of variance. *Randomization* is defined as a well understood probabilistic scheme to assign the treatment for units. A set of objects for the experiment are chosen randomly in both orders and subsets to achieve a well-designed experiment. Randomization methods can be achieved either

61

through physical or numerical ways [Gary, 2010]. *Replication* is the level of repeating experiment runs with the same factor settings in randomized runs and employed in the purpose of checking variability and constraining the experimental system. *Blocking* is explained as a categorical variable that is used to reduce the bias and errors variation for the designed experiment. Runs happening inside different blocks also need to be randomized [Anderson and Whitcomb, 2016]. *A factorial* design is a designed experiment in which all the combinations of the factor levels are concerned. As the number of factors or the level of each factor increases, the number of runs required for the design experiment increases significantly, then fractional factorial design or other advanced designed techniques should be considered to reduce the time for experimentation [Montgomery, 2017]. Analysis of variance (ANOVA) is used to examine if mean values of the populations are equal for the designed model. It also estimates the level of importance for each factor, as well as their interactions by comparing the response variable means with the producer's risk (alpha) [Gary, 2010].

Later in the 1930s, the industrial statistical design began, and the next development was classified as *response surface methodology (RSM)* [Box and Wilson, 1951]. This technique was widely used in the chemical and process industries by taking advantage of optimizing the related factors such as time of process, pressure, temperature, flow rate, etc. In the 1950s, an upgraded designed experiment technique was introduced by Kiefer and Wolfowitz known as *optimal design*. This approach is based on selecting a design that fits a specific objective through optimum criteria. However, at the time, this approach was not suitable for spreading use because of the lack of computation application for its advanced algorithms [Kiefer and Wolfowitz, 1959]. Later in the 1980s, Genichi Taguchi promoted a newly designed experiment termed as *robust parameter design* [Taguchi, 1986; Taguchi, 1987; Taguchi et al.,

2000]. In this design, the response has a fixed mean that will be optimized while minimizing the variation. The purpose of the design is improving the relationship between signal factor and response. Taguchi design is built on a mixed level through fractional factorial design and orthogonal designs. Its application is well recognized in automotive and aerospace manufacturers.

A well-designed DOE model collects the design space of sample to maximize useful output information while minimizing the amount of input data and lowering the number of runs. Time-consuming for experiments, as well as the numerical simulation, is reasonable reducing as useful effort. Therefore, choosing an appropriate sample size for experiment runs must be optimized to maintain the accuracy of the designed model. DOE follows various interpolation or approximation techniques such as linear, nonlinear, polynomial, stochastic, etc. that employ response surface methodology (RSM) techniques in different ways. Whenever an appropriate response surface of the objects is created through variables, the general optimization process of this design will be achieved accurately. The most significant advantage of RSM is reducing the duration of sample runs in comparison with conventional factorial design by reducing the number of runs. However, the optimization from response surface is always approximate due to the limitation of confidence level. The RSM technique is improved by distributing the input samples over the designed space [Cavazzuti, 2012].

Response surface methodology (RSM) is defined as a collection of mathematical and statistical methods that help to understand and optimize the response better through several variables [Deyhimi et al., 2006]. The purpose of this technique is to focus on investigating the relationship function with is unknown between input variables and the related response. When starting the RSM process, the first stage is establishing a suitable rough relationship between

response y and independent variables (x_i). A simple low-order polynomial is used to model the linear function of independent variables (x_i), which is called the first-order model as described below:

$$y = \beta_0 + \beta_1 x_1 + \beta_2 x_2 + \cdots + \beta_i x_i + \epsilon \qquad (2.4)$$

The first-order model can describe the response surface reasonably when the estimated region is a small portion and separated from the curved region such as maxima, minima, ridge, and saddle [Gary, 2010]. Hence, an improved model made by the steepest ascent method is suggested to solve this issue, which would make the response surface more advanced by including curvature [Weihs et al., 2006]; this model is called the second-order model

$$y = \beta_0 + \sum_{i=1}^{k} \beta_i x_i + \sum_{i=1}^{k} \beta_{ii} x_i^2 + \sum_{i<j} \sum \beta_{ij} x_i x_j + \epsilon \qquad (2.5)$$

where: $\sum_{i=1}^{k} \beta_i x_i$ called the linear terms; $\sum_{i<j} \sum \beta_{ij} x_i x_j$ called the interaction terms and $\sum_{i<j} \sum \beta_{ij} x_i x_j$ called the quadratic terms. *The second-order model* can describe the response surface as a quadratic surface which includes various shapes that significantly improves the accuracy of the designed model. The second-order surface possibly points out the stationary point, which is defined as either maximum or minimum points from a specific combination of designed variables in all directions of the modeled surface. If in the searching surface, it contains both the maximum point in some directions and the minimum point in other directions, the stationary point is called the saddle point. The model also could have no stationary point; then it is called a ridge surface [Gary, 2010].

The designs of the second-order surface can be classified with specific characteristics as the following methods below, including conventional designs such as central composite designs (CCD) and Box-Behnken designs (BBD) or unconventional design such as optimal designs.

2.4.1.1 Central Composite Designs (CCD)

CCD is the most popular design used to fit the second-order model [Carley et al., 2004]. Generally, CCD consists of factorial points, axial or start points and center points; it usually divided into five levels for each variable including low axial, low factorial, center, high factorial, and high axial [Anderson and Whitcomb, 2016].
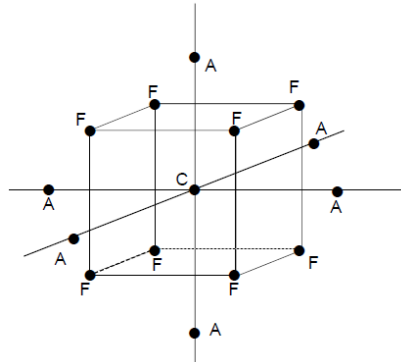
Fig. 2-17: Central composite design (CCD) in three dimensions with factorial points (F), axial points (A), and center point (C) [Anderson and Whitcomb, 2016]

First, factorial points are presented for fitting the first-order model, then adding axial points, and center points are used to incorporate the quadratic term into the designed model. Two important factors affect the efficiency of CCD design, including the distance (α), form axial points to the center point and the number of the center point. Good CCD design means that the response surface should be rotatable, it happens when all points (axial and factorial) should be the same distance from the designed center and placed on a sphere [Box and Hunter, 1957], these properties are appropriate when the design will provide an equal estimation for predicted response in all directions. The rotatability will be decided by choosing the suitable distance (α), for a spherical region the best choice of α is equal to $(2^k)^{\frac{1}{4}}$ with k is the number of variables. There are various types of CCD model that are based on the limitation of the searching range.
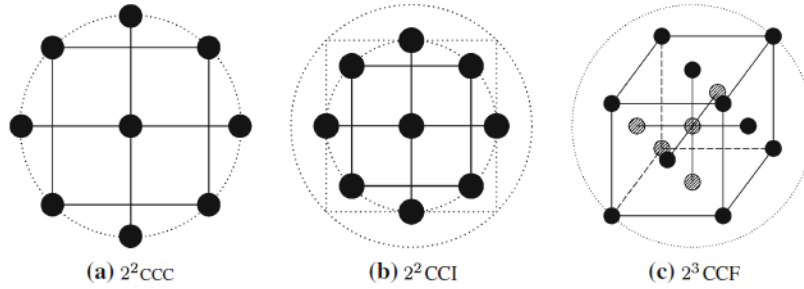
Fig. 2-18: Central composite design classification for the model of two-variables (a, b) and three-variables (c) [Cavazzuti, 2012]

The number of center point bases on the level of power for analysis is symbolized for the variability of the predicted response. For an experiment, this number should be placed in the range from three to five for a powerful analysis [Montgomery, 2017]. However, in the simulation model, the number of center-point can be equal to 1 due to no replication of runs.

2.4.1.2 Box-Behnken Designs (BBD)

BBD is built from the combination of two-level factorials with incomplete block design to become an incomplete three-level factorial designed model [Montgomery, 2017]. This model is introduced to maintain the size of the sample when increasing the number of variables [Box and Behnken, 1960]. In BBD, the block of two-levels factorial samples is repeated and changes through different variable combinations whereas the variable that is not contained in that block keeps the same mean value. This design could be either rotatable or near-rotatable depending on the distance of predicted response variance with the designed center point [Cavazzuti, 2012]. BBD proved itself as an economical design because it requires fewer design points than CCD. However, this design contains a clear limitation for applying to orthogonal blocking in comparison with CCD due to lack of embedded factorial design. Therefore, it is not suitable to be applied for sequential designs [Minitab, 2019].
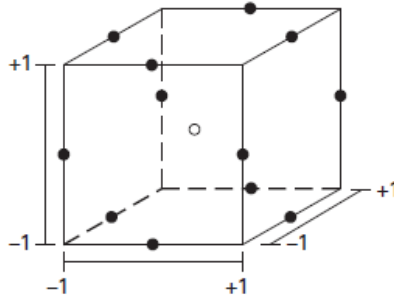
Fig. 2-19: Box-Behnken design (BBD) for three variables [Anderson and Whitcomb, 2016]

2.4.1.3 Optimal Designs (OD)

These designs are used as an upgraded design of RSM when the standard response surface methods as CCD or BBD are not capable of illustrating the experiment region in a higher order than second-order design [Anderson and Whitcomb, 2016]. Optimal design is used due to its special properties. Firstly, if the design variables are sensitive in the examined range of complex constraint must be established for the experimental system, the optimal design should be used to optimize the response [Montgomery, 2017]. Secondly, for some atypical experiments, the conventional model cannot deal with the high number of parameters or a high number of variable levels. Therefore, the nonstandard model as the optimal design is suggested to optimize the response surface; it seems like an adjustable model of the full factorial design with high levels of each variable [Cavazzuti, 2012]. Another advantage of optimal design is that if the experimenter can anticipate a good structure of the response surface by using optimal design, it could reduce the number of runs used significantly and could save time [Montgomery, 2017]. The most popular optimal model used is I-optimal; this model focus on minimizing the normalized average or integrated prediction variance [Cavazzuti, 2012]. Other optimal design models used for different specific purposes include D-optimal design, which aims to minimize joint confidence region volume on the vector of the regression coefficient. A-optimal design is used for minimizing the sum of variances of

the regression coefficients. G-optimal design focusing on minimization of maximum scaled prediction variance through the design space. V-optimal design, which is used to minimize the average prediction variance over observed points [Montgomery, 2017]. However, optimal design is not recommended unless the design model relates to a complex constraints model. Generally, the conventional response surface models are good enough to illustrate the optimum response [Anderson and Whitcomb, 2016].

2.4.1.4 Response Surface Methodology (RSM) Applications

Response surface methodology is used widely for optimizing processes in the oil and gas industry and have proven to be an effective model to optimize simulation process [Hood and Welch, 1993; Carson and Maria, 1997; Neddermeijer et al., 2000].

In 1999, Narayanan et al. used the RSM model to optimize one particular property, pseudo-relative permeability (used for geological model upscaling) due to its reasonable price in comparison with the fine grid simulation model. BBD was employed to present the quadratic and linear effect between the response of five factors including facies ratio, shale resistivity, cement permeability, angle of dip, and water injection rate. The result from response surface indicated that the shale resistivity and facies ratio make the most significant impact on pseudo-relative permeability variation. All other parameters also made an impact on response curvature with a confidence level at 95%.

Averbuch et al. [2005] employed RSM as an effective tool to design the response surface for the critical time of hydrate formation as a function of flow characteristics, including the gas-oil ratio, the water cut, the total liquid flow rate, the temperature and pressure at the manifold, and the heat exchange coefficient (U value) for a deep offshore field development. A total of 45 runs was employed based on the CCD design for six parameters, leading to a conclusion

that the critical time is strongly dependent on the U value with a good predicted quadratic response surface. Li and Friedmann. [2005] also used RSM for another deep-water field development in Africa. An upgraded model of RSM, named the amplitude-phase factor, was presented to design the response surface for oil rate and water cut from the relationship between eight parameters (including porosity, permeability and viscosity of multiplier) in addition to conventional RSM models such as regression and thin-plate spline. These response designs were applied at three levels of the total volume of water injection for a reservoir model with dimension as $78 \times 59 \times 116$ grid blocks. The results pointed out that the amplitude-phase model gave the best R^2, which is the coefficient between the predicted and actual response, for all cases in which the value are all higher than 0.95. The conventional regression model resulted in a good R^2 value for the case with 0.1 PV of water injection.

Mollaei et al. [2011] built up a general isothermal EOR forecasting tool to perform simultaneous WAG process for reservoir simulation model by CMG through components as material balance, segregation flow, and fractional flux. The input data used for this RSM model included WAG ratio, injection pressure, reservoir heterogeneity, and geostatistical dimensionless correlation length. The response surfaces covered three different aspects, including solvent front factor, oil bank front factor, and final average oil saturation. They concluded that the RSM model is good for modeling the WAG process through these observed parameters by fitting well with simulation results and reservoir heterogeneity is the most significant impact factor for the WAG process. Ghahri et al. [2011] optimized the clean-up process efficiency of injected fracture fluid for a hydraulic fractured well using the RSM technique with 16 parameters related to the pressure drawdown, capillary pressure, permeability and porosity of injected fluids, the matrix and the fractures. The response surface

focused on illustrating the predicted value of gas production loss through two injected fractured volume values. Both two-level full factorial design and three-level CCD and BBD were employed to establish the response surface by running an ECLIPSE simulation model. The result is clear that the more the production process continues, the impacts of input parameters increase based on RSM. For one-year of production, full factorial design and CCD suggest a better clean up efficiency than BBD model. Khosravi et al. [2011] applied RSM design for a fracture simulation model to examine the impacts of related reservoir parameters for the recovery process. The ultimate oil recovery factor from the natural depletion stage was investigated through a sensitive Monte-Carlo analysis model later based on the predicted response surface of RSM. After a sensitivity screening on different RSM techniques, BBD was employed to design the response surface by 49 runs from the combination of input parameters such as matrix block size, effective fracture permeability, matrix permeability, aquifer size, water relative permeability, and oil relative permeability. The predicted response was good, with R^2 values higher than 0.95, and pointed out the aquifer size has the most significant impact on oil recovery, and ultimate oil recovery factor can be up to 23%.

Ghaderi et al. [2012] used the optimal design of RSM to optimize the WAG process for a tight formation compositional simulation. A wide range of parameters related to the WAG process, including well pattern, well completion, fracture spacing, fracture half-length, average reservoir pressure, water-cut, WAG slug size, and WAG ratio, were selected to design the response for oil recovery factor, CO2 sequestration and NPV aspects. The results indicated that for different objects, there would be differences in predicted response surfaces as well as variables impact orders. To maximize the oil recovery factor, WAG ratio is the most

significant parameter, whereas the well completion method is the most significant in order to determine the NPV efficiency.

RSM method also proved itself as an effective tool to optimize core-scale WAG injection. Khezrnejad et al. [2014] employed RSM to optimize the oil recovery factor for the nanoparticle WAG process through three input parameters, including the salt concentration of brine, type of nanoparticles, and WAG ratio. From the ANOVA table and predicted response surface, he concluded that the salt concentration of brine is the most significant parameter, and silica nanoparticle is more effective than the alumina type. Van and Chon [2017] investigated the effect of brine salinity and WAG slug size on the oil recovery factor of a miscible WAG process by establishing the RSM model. For different volumes of fluid injection, range values of salinity and slug size were chosen to design the response surface. They found that this quadratic design model was suitable to present the relationship between observed parameters with oil recovery factor, with R^2 values generally higher than 0.95.

2.4.2 Computational Optimization Algorithms

Computational optimization algorithms are classified into various types based on different principles. Generally, the classification can be divided into deterministic optimization and stochastic optimization. The following literature will verify their definition and application for each type.

Deterministic Optimization

Deterministic optimization is defined as an optimization technique that relates to mathematical programming. By depending on a linear mathematical formulation that does not include the random variable, the result of deterministic will be clear and replicable for different runs. This algorithm focuses on searching the local optimum point of the response

variable from a set of feasible samples chosen based on specific criteria [Cavazzuti, 2012]. These criteria can be classified as two main types, including unconstrained optimization and constrained optimization.

Unconstrained optimization is employed when there is no significant influence of constraints on the designed model and usually focuses on the minimization of the response [Rao, 2009]. These algorithms, which are based on the approximate genetic objective function, start the optimization process from point x_1 and generate a line set of sequence point x_n until the design space is converging to the solution. The minimum response from unconstrained optimization should be qualified two conditions, including the first-order necessary condition and the second-order condition [Guler, 2010]. Furthermore, the order of convergence of these algorithms demonstrates that the level of iterates converge of the solution.

Constrained optimization is when the algorithms have input parameters that are constrained; these algorithms are described as following

$$\text{Optimizing} \quad f(x) \qquad\qquad x \in \mathbb{R}^k$$

$$\text{Subject to} \quad c_i(x) = 0 \qquad i \in E \tag{2.6}$$

$$c_i(x) \geq 0 \qquad i \in I$$

where $f(x)$ is the objective function, $c_i(x)$ are the constraint functions, E is the set of equality constraints, and I is the set of inequality constraints [Rao, 2009]. The group of points that satisfy the constrained optimization problem are called feasible points and the vectors of moving points of the optimization process are called feasible direction. The response solutions of the algorithms can be linear equations, nonlinear equation, or a mixture of them based on their complex constrained problem [Abidi et al., 2016].

Stochastic Optimization

Stochastic optimization techniques focus on solving the optimization situations involving probabilistic or stochastic variables [Rao, 2009]. These random variables could come from nature or any random sources and could be used to handle both linear and non-linear programming problems [Chen and Lee, 2011]. These algorithms can be classified as simulated annealing, genetic algorithms, particle swarm optimization, and Monte-Carlo methods.

2.4.2.1 Genetic Algorithm (GA)

In the 1960s, Genetic algorithms (GA) were proposed by J. Holland as an innovative evolutionary algorithm based on biological evolution [Holland, 1975]. Their development was continued by Holland and his students during the next decade [Goldberg, 1989]. The original goal of this technique was to establish a natural adaption algorithm for a computer system, and the significant innovation of these algorithms was the combination of crossover, inversion, and mutation. It begins with two individual groups defined as the parent group and the offspring group, where the offspring is a mutated version of the parent. Various individual populations and crossover are not incorporated until a later stage. The selection of offspring from parents is an important process of the GA method [Mitchell, 1998]. The GA method has many advantages in the application of combinatorial optimization problems. This technique can be applied for both continuous and discrete variables, being suitable for dealing with a high number of input parameters, and especially providing a group of optimal solutions, not just a single option. However, GA requires a significant number of function evaluations based on generation and individual; therefore, it can be unpredictable for the first starting point.

2.4.2.2 Simulated Annealing (SA)

In 1983, Kirkpatrick proposed a probabilistic technique, based on the Metropolis-Hasting algorithm, called simulated annealing to find a global optimum through several local minima

[Kirkpatrick et al., 1983]. This algorithm is known as SA due to its initial application to achieve the optimum case for annealing the solid in a heat bath by managing the heating and cooling processes through temperature variable. The annealing process will start at the maximum temperature, then, the solid will cool down while maintaining the thermal equilibrium [Bertsimas, 1993]. SA could be considered as an algorithm that attempts to continue the transformation from the current configuration to one of its neighbors; this process is described as a chain of trial when the result of each trial is dependent on the previous outcome [Aarts, 1987]. SA optimization is a completely random run over the design space and is more effective in a discrete searching space. For each optimization process, the input variables are usually random in a constraint range; therefore, it is a time-saving process. However, the optimum case is considered not as a local optimum but a global one [Cavazzuti, 2012].

2.4.2.3 Particle Swarm Optimization (PSO)

Particle swarm optimization (PSO) is a well-known, population-based stochastic optimization method that was originally introduced by Dr. Eberhart and Dr. Kennedy. [1995]. This random optimization search algorithm was inspired by observing and simulating the social behavior of birds, bees, or fish schooling. PSO methods are considered as a computational optimization technique that is quite similar to GA. Their systems both come up with a random solution of population and acheive the optimum case by updating generation. However, without evolution factors such as crossover or mutation, PSO is instead flying the particles in the searching space following the current optimum particle to get to the final optimum point. This increases robustness of the algorithm. This mechanism is based on bird flocking scenarios, when iteration the bird inter-communication to find the optimum location for food by following the

bird which is closest to the food point [Eberhart and Kennedy, 1995]. The original model of PSO focused on building models that were well represented for the unpredictable choreography of a flock of birds. A vector represents each particle of the swarm through the multidimensional searching space. This vector will decide the following steps for particle movement and is called the velocity vector. The PSO algorithm is generally an update process of particle velocity to get to the optimum global point by iterating many times until the minimum error of performance index is achieved, proving itself as an efficient optimization tool [Pampara et al., 2005]. Eberhart and Kennedy [1997] introduced an upgraded discrete binary model for PSO. The value of each particle varies from zero to one value, and the velocity vector is represented as the probability of a particle equal to one. Later, Shi and Eberhart [1998] presented an update from the conventional PSO model by introducing a new factor called inertia weight to illustrate the previous velocities of particles.

Generally, the PSO algorithm is a process that compares each particle with the nearest one to imitate which is better, then finally gets to the global optimal even if it is the nonlinear relationship, or problem environments are multidimensional [Abdelhalim and Habib, 2009]. The relationship between the current particle position $(x_i^{(n)})$ and the next position $(x_i^{(n+1)})$ is described as

$$x_i^{(n+1)} = x_i^{(n)} + v_i^{(n+1)} \tag{2.7}$$

where v_i is the velocity vector of the individual i. The velocity information could also be presented as the function below to update for the current particle

$$v_i^{(n+1)} = \omega \, v_i^{(n)} + C_1 r_1 \, (\bar{x}_i - x_i^{(n)}) + C_2 r_2 \, (\tilde{x} - x_i^{(n)}) \tag{2.8}$$

where: $v_i^{(n+1)}$ is the particle velocity; ω is the inertia weight; C_1, C_2 are learning factors; r_1, r_2 are independent uniform random numbers; $\bar{x}_i$ is the best local solution; and $\tilde{x}$ is the best global solution [Haupt and Ellen, 2004].

The inertia weight (ω) is defined:

$$\omega = \omega_{max} - \frac{(\omega_{max} - \omega_{min})^t}{t_{max}} \qquad (2.9)$$

where ω_{max} is the maximum magnitude of the inertia weight, ω_{min} is the minimum magnitude of the inertia weight, t is the current iteration and t_{max} is the total number of iterations.
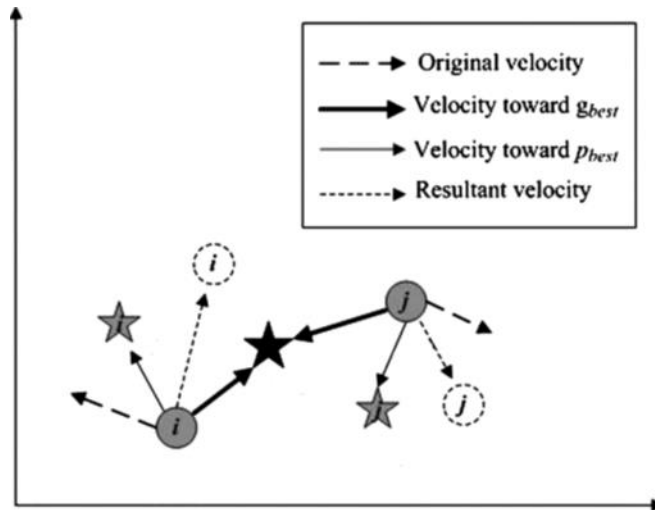
Fig. 2-20: Basic velocity update mechanism in PSO [Kiranyaz et al., 2014]

Although PSO has proven itself as a good global optimization method for any multidimensional problems, PSO still has the drawback of the risk of being trapped at the local optimum and not being able to improve anymore and guaranteeing further convergence. An improvement could be made by an improved local minimizer PSO model [Aote et al., 2013].

2.4.2.4 Monte Carlo Methods

In 1940, Monte Carlo simulation was first applied in the process of nuclear weapons development in Los Alamos [Kalos and Whitlock, 2009]. Simplistically, Monte Carlo methods are a group of stochastic algorithms that focus on analyzing the specific personalities of the object by repeating random sampling for different paths [Raychaudhuri, 2008]. The algorithms calculate different output options by repeating input data picks from observed variables suitable for statistical distribution and employing that to build the forecast response models. Then, the forecast model is able to define and analyze any optimum aspects based on the probability and value relationship. Monte Carlo simulation is widely used for purposes such as risk analysis, risk quantification, and prediction analysis [Mun, 2006]. There are three main evolutional mechanisms to describe the system models, including discrete-time models, continuous-time models, and discrete-event models [Brandimarte, 2014]. The biggest challenge when applying Monte Carlo simulation is picking a suitable statistical distribution for sampling values from input variables. With a suitable statistical distribution chosen, the Monte Carlo method is well recognized as an effective mathematic tool for forecasting optimization in the oil and gas industry [Murtha, 1994; Murtha, 2006].

2.4.2.5 Computational Optimization Algorithms Applications

The application of computational optimization algorithms has been widely recognized as an effective tool for forecasting in oil and gas exploration and production industries. Generally, GA techniques primarily used for the purpose of matching the simulation model with production history and improving the economic aspect of the production process. In 1999, GA was proposed as an evolutionary programming technique to forecast oil production by matching historical production with a simulation model of petrophysical rock properties, such

as permeability and porosity. Ten simulation runs for two different production strategies were conducted to give an uncertainty estimate prediction [Soleng, 1999]. Later, the advantage of GA for global optimization was also employed to characterize a hydrocarbon reservoir by matching the historical production data (such as bottom hole pressure, oil production rate, and water injection rate) with the reservoir simulation model based on geological and structural properties [Romero et al., 2000]. In 2015, Xu et al. adjusted crossover and mutation rates to modify the GA method to match the simulation data with experimental results for vapor extraction (VAPEX) heavy oil recovery process. The result of that fitting process were good with the obtained errors lower than 1% [Xu et al., 2015]. For economical production efficiency, in 1998, Harding et al. used GA to optimize the total net present value (NPV) for the reservoir production model. Constraint models were built under productivity and sequencing condition to focus on optimizing the input parameters, including the starting points of production and production rates [Harding et al., 1998]. Similarly, Sarich used GA as an effective tool to optimize investment decision-makers for oil and gas production. The economic indicators such as NPV and rate of return (ROR) were optimized based on managing the operation status of oil and gas production wells [Sarich, 2001].

SA applications are recognized in seismic interpretation optimization. In 1991, a framework of employing SA to implement seismic inversion was introduced, based on their particular genetic algorithms structure, it was possible to invert the seismic field data. The result clearly indicated that a subsurface model can be built from hundreds of input parameters of the SA model [Pedersen et al., 1991]. Later, Abdassah et al. optimized the inter-well reservoir characterization by applying the SA technique for seismic data processing. The object function was strongly built on the relationship between acoustic impedance data and porosity

data [Abdassah et al., 1996]. In 2005, SA was used to optimize the seismic shear-wave splitting analysis to correctly estimate the lateral and vertical variation of fracture properties based on the analysis of the input data as the time lag between S-waves and natural direction of S-wave [Dariu et al., 2005]. Another advantage of SA for inverted seismic data was proposed in 2008; Huang and Chou used SA to minimize the distance of hyperbola points in the hierarchical system by optimizing the parameter vector from the number of patterns and number of points in an image [Huang and Chou, 2008]. In 2011, three new different SA technique,s including normal SA, fast SA, and very fast SA, were proposed to detect the parameters of the hyperbolic patterns on seismic data gathering, the results also capering to each other [Huang and Hsieh, 2011].

The Monte Carlo method is mostly applied for optimization cases such as reserve estimation and production forecasting [Murtha, 2006]. In 1973, Evers and Jennings pointed out the importance of Monte Carlo simulation for field economic evaluation and suggested the calculation steps of two different probability distribution models of Monte Carlo simulation to present the profit of a gas field [Evers and Jennings, 1973]. Murtha also confirms the advantage of Monte Carlo simulation for modeling the economic key parameters for oil and gas production, such as net present value (NPV) and return of investment (ROI) [Murtha, 1997; Murtha 2006]. In 1994, Murtha introduced an essential procedure for incorporating historical production data into a Monte Carlo simulation to present effective statistical distribution models to predict the field reserve. Later, Gilman et al. employed Monte Carlo simulation to estimate the future production from the input parameters such as gas-oil ratio (GOR) and production rate [Gilman et al., 1998]. Komlosi et al. [2009] also built predicted reserved model and technical reserved model by probability distribution function of the Monte

Carlo simulation base on the geotechnical properties and production conditions. The results pointed out the importance of choosing input data smoothly for a highly accurate prediction. The PSO technique has a wide range of applications for oil and gas production optimization and has only been recognized recently. Onwunalu and Durlofsky [2009] introduced the PSO algorithm to optimize the well type and well location for a full reservoir simulation model for the first time. They also employed GA as a comparison technique. A detailed explanation was made with respect to PSO algorithms operational mechanism with iteration. The objective of this optimization process is NPV and the input parameters for this stochastic optimization procedure included all expenses related to good operation. After comparing the performance of PSO and GA, they concluded that as PSO gets to the optimum global point with fewer steps than GA, then it will be more efficient than GA for more complex variables. The swarm side and number of iterations of the optimization model should be flexible for different complexity levels. Assareh et al. [2010] also used both PSO and GA optimization techniques to estimate the demand of oil in Iran based on the input data as the volumes of oil consumption, imported oil, and exporting oil. After comparing four different scenarios, they concluded that the linear-PSO model outperformed other cases with the lowest relative average error rate.

Mohammed et al. [2011] proposed the multi-objective PSO procedure for history matching of a complex reservoir simulation model. The objectives functions included water and oil production rate based on the input parameters such as fault geophysical properties. The conclusions suggested that this multi-objective model led to the optimum result faster than the conventional single object approach and proved itself well-fitting with the reservoir model.

Awontunde. [2012] introduced the local-global PSO algorithm to estimate flow properties such as decomposition wavelets from permeability distribution to optimize reservoir performance. The optimization procedure went from a local search to global search, and the results indicated that by separating the two stages the model could predict a good fit for the optimum residual value with conditioning permeability distribution. Later, Zendehboudi et al. [2012] presented a feed-forward artificial neural network (ANN) optimized by PSO method to estimate a good value represented for Condensate-to-Gas ratio, which is extremely important for production preparing stage. Both PVT experiment and literature data were employed as input variables to build the PSO-ANN model, including temperature, dew-point pressure, and molecular weight. The result is clear that with a significantly high value of R^2 from the statistical analysis, this model is beyond the efficiency of the conventional ANN model.

In 2013, the PSO algorithm was proposed by Fortini et al. to analyze seismic velocity interpretation to reduce time-consumsumption and focus on multi-dimensionality optimization for both 2D and 3D velocity models. As a result, both cases with different described input parameters, PSO is creates a simulation curve that fits both the 2D and 3D velocity curves.

Wang and Qiu. [2013] employed PSO algorithms, including three different models, to optimize the oil recovery factor for a large, heavy oil reservoir. All the algorithms were compared based on the performance of convergence behavior and optimum results. The conventional one, Canonical model, got the best oil recovery factor, but all of them were significantly higher than the base case suggested.

Jesmani and Bellout. [2015] proposed PSO algorithms to develop the constraint computational optimization model for good placement in developing planning. Two producing cases were made to include the constraints of inter-well distance, well length, and well orientation. The objective of this optimized function is NPV based on the fixed economic parameters. The constraint handling methods used for these two cases included penalty function and decoder as a homomorphous mapping technique. A clear conclusion was made that the decoder technique is more efficient, incorporating different constraints of good placement. Further, there is no requirement for parameter tuning, and it is convenient to apply for both convex and non-convex feasible search space.

The application of PSO algorithms for WAG optimization has only recently garnered attention despite the applications of the reviewed computational optimization techniques have been recognized many times. In 2000, a genetic algorithm was introduced to optimize the production performance for a miscible WAG injection field. From the reservoir model, a production model was built to combine all the fundamental properties of the wellbore model and choke model with the objective of the GA optimization function is net present value. The constraints for this model were established, including pressure, material balance, and economic index properties. It concluded that GA is an effective method to optimize the production forecasting of WAG reservoir with stability and could handle different constraints [Yang et al., 2000]. Later in 2003, further research into the optimization of WAG injection performance for this field focused on employing both GA and SA techniques. The same economic aspect as the objective of the optimization process was used for the four production cases. The results indicated that the integrated model for production forecasting works well, and both GA and SA are effective and stable to optimize the control of the production-

injection operation systems [Yang and Gu, 2003]. In 2006, Esmaiel et al. introduced a response surface proxy model to optimize the economic perspective of the WAG process that applied well-smart technology. The optimization model was built based on the response surface methodology of the DOE, then upgraded the forecasted response by Monte Carlo simulation. The D-optimal design was used to determine the set of runs for five parameters, including WAG ratio, areal permeability multiplier, oil mobility, and the status of injection and production wells. The proxy model wasccapable of demonstrating the response surface simulation for oil recovery, NPV, and utility of the WAG process, and Monte Carlo simulation was proven to be adequate as a beneficial probability distribution function.

A WAG ratio equal to 1:1 is the best scenario for optimizing the response and the robust smart well technology with the optimum case which can improve the WAG process efficiency more than conventional wells [Esmaiel and Heeremans, 2006]. In 2010, an upgraded GA technique was proposed to optimize the production performance of miscible WAG injection in a a heterogeneous reservoir. The objective of the optimization was NPV based on the input parameters of injection rates, length of injection, and bottom hole pressure condition at producers. This upgraded hybrid GA method demonstrated a successful application to forecast production performance with a significant increase for oil recovery and NPV, 9.9% and 11.4 % respectively [Chen et al., 2010]. In 2016, Mohagheghian introduced the applications of GA and PSO methods to optimized WAG injection performance, for both productive and economic aspects, for a field-scale model simulation of a segment in the Norne field. The optimized WAG parameters included rates of fluids injection, bottom-hole pressures, WAG ratio, length of the injection process and the composition of injected gas. The results of this

research indicated a significant improvement in optimizing the NPV and oil recovery factor, over 13% for both cases [Mohagheghian, 2016].

Table 2-2: WAG Optimization techniques in literature

Authors	Optimization Objects	Optimization Methods	Optimization Variables	Research Observations
Yang et al., 2000	NPV	GA	Bottom hole pressure of producers and injection rates	- GA is an effective method to optimize the production forecasting of WAG reservoir with stability and well-handling different constraints.
Yang and Gu, 2003	NPV	GA and SA	Bottom hole pressure of producers and injection pressures	- The integrated model for the production forecasting works well, and both GA and SA are effective and stable to optimize the controlling of the production-injection operation systems.
Esmaiel and Heeremans, 2006	Oil recovery factor, NPV	DOE-RSM and Monte Carlo simulation	WAG ratio, Arial permeability multiplier, oil mobility, and the status of injection and production well	- The proxy model is well capable of demonstrating the response surface simulation for oil recovery, NPV, and utility of the WAG process. - WAG ratio equal to 1:1 is the best scenario for optimizing the response. - The robust smart wells technology with the optimum case can improve better the WAG process efficiency than conventional wells.
Chen et al., 2010	NPV	Upgraded GA	Injection rates, length of injection, and bottom hole pressure of producers	- This upgraded hybrid GA method demonstrated a successful application for the forecasting production performance with a significant increase for oil recovery and NPV, 9.9%, and 11.4 % respectively.
Mollaei et al. 2011	Residual oil saturation	DOE - RSM	WAG ratio, injection pressure, reservoir heterogeneity, and geostatistical dimensionless correlation length	- RSM model is capable to model the WAG process through these observed parameters by fitting well with simulation results. - Reservoir heterogeneity is the most significant impact

				factor for the WAG process.
Ghaderi et al., 2012	Oil recovery factor, CO_2 sequestration, and NPV	DOE - RSM	Well pattern, well completion, fracture spaces, fracture half-length, average reservoir pressure, water-cut, WAG slug size, and WAG ratio	- For different objects, there will be differences in predicted response surfaces as well as variables impact orders.
Khezrnejad et al., 2014	Oil recovery factor	DOE - RSM	The salt concentration of brine, type of nanoparticles, and WAG ratio	- ANOVA table indicates that the salt concentration of brine is the most significant parameter, and silica nanoparticle is more effective than the alumina type.
Mohagheghian, 2016	Oil recovery factor, NPV	PSO	Bottom hole pressure of producers, injection rates, WAG ratio, length of the injection process and the composition of injected gas	- Significant improvement in optimizing the NPV and oil recovery factor, over 13% for both cases.
Van and Chon, 2017	Oil recovery factor	DOE - RSM	Brine salinity and WAG slug size	- This quadratic design model is suitable to present the relationship between observed parameters with oil recovery factor with R^2 values are generally higher than 0.95.

In this research, both DOE-RSM and PSO techniques will be employed for optimization as well as to investigate the impact of a collection of WAG operational parameters to improve the oil recovery performance of a numerical, core-scale, core flooding model.

CHAPTER 3. METHODOLOGY

In this chapter, the first section presents all components that are related to building the numerical simulation models for the core-scale double displacement process (DDP) tests and immiscible Water Alternating Gas (IWAG) injection tests including rock properties, fluid properties, special core analysis (SCAL) properties and operational parameters with a detailed simulation model description. Later, workflows of optimization techniques, including response surface methodology (RSM) and particle swarm optimization (PSO), are presented step-by-step for their applications in this research to identify the significant operational parameters and the optimum combination for enhancing oil recovery efficiency of the immiscible WAG injection process.

3.1 Numerical Simulation Models

In this first part of the methodology section, a framework of building a numerical simulation model for composite core flooding is described. All the necessary components are discussed, including reservoir fluids properties; permeability, porosity, and fluids saturation distribution of the composite core. Generally, all the information in this section is referenced from the experimental data of the research in 2006 [Wang et al., 2006]. Schlumberger ECLIPSE software is employed to simulate the numerical composite core model, which is then used in the simulation of the DDP test, IWAG test, and optimization processes. The operational condition of all simulation tests is at a temperature of 210ºF, and pressure of 4500 psig, which is representative of the reservoir conditions.

3.1.1 Rock Properties

The cores used for this study were from the Hibernia exploration B16-17 well. First, ten horizontal core plugs were taken from the full core to test their properties, their dimensions

were approximately 3.8 cm in diameter and 5 cm in length [Wang et al., 2006]. Four of them were used for the centrifuge capillary pressure tests. Core plug #10 is used to illustrate the water-oil capillary pressure relationship and core plug #12 is used to present the gas-oil capillary pressure relationship. The other six core plugs, from depths ranging from 4039.83 m to 4041.13 m were combined to become a full, approximately 30-cm-long composite core. The total bulk volume (BV) of the composite core was approximately 349 cc. The average porosity and permeability of the composite core were 0.1789 fraction BV and 1919 mD, respectively, at 4000 psig net confining stress. The initial water saturation of the composite core is approximately 3% of PV by centrifuging the water-wet core, which was saturated by 100% brine and the grain density is approximately 2.65 g/cc [Wang et al., 2006].

Table 3-1: Horizontal core plugs properties [Wang et al., 2006]

	Composite Core						Capillary Pressure Curves	
Plug ID	A	B	C	D	E	F	10	12
Depth (m)	4041.09	4039.83	4040.96	4041.04	4041.13	4041.00	4039.71	4039.79
Permeability (mD)	1919						1705	1752
Porosity (% BV)	17.89						17.95	17.87

Fig. 3-1: The order of core plugs in composite core

3.1.2 Fluids Properties

The fluids used for this research are representative of Hibernia fluid properties. The brine used for conditioning cores and water-flooding is synthetic brine that has a salinity of approximately 102,435 ppm, similar to the formation water from MDT samples. At 4500 psig and 210 °F, the synthetic brine density is around 1.0793 g/cc, and the viscosity is about 0.411 cP. The gas used for injection and live oil recombination is a synthetic gas with density and viscosity of 0.2278 g/cc and 0.0293 cP, respectively. The oil used for conditioning the cores and all tests is a recombined live oil, which has a bubble point pressure around 4489 psig at 210°F and a stock tank oil gravity of 31.8 API.

Table 3-2: Composition of equilibrium oil phase by flash

Component	Mol %	Liquid Density (g/cc)
CO_2	0.79	0.817
C_1	53.92	0.299
C_2	6.11	0.356
C_3	4.50	0.507
$i\text{-}C_4$	0.07	0.563
$n\text{-}C_4$	2.45	0.584
$i\text{-}C_5$	0.23	0.624
$n\text{-}C_5$	1.24	0.631
C_6	1.65	0.685
C_7	2.51	0.722
C_8	3.59	0.745
C_9	1.97	0.764
C_{10}	1.95	0.778
C_{11+}	19.02	0.883

After tuning the recombined oil composition with Constant Composition Expansion (CCE) test data and the experimental bubble point pressure, a phases envelope diagram is presented as the following, with the estimated bubble point pressure around 4491 psig at 210 °F with the

solution gas-oil ratio (R_s) of about 174.5. This result is quite similar to the bubble point pressure (4489) of tested fluids used in previous research [Wang et al., 2006].
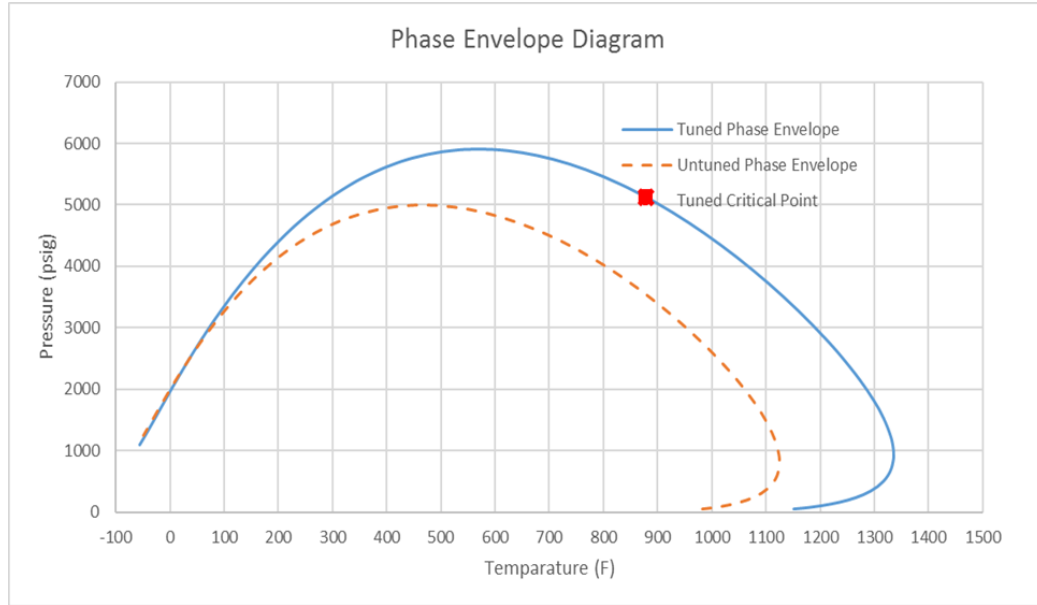
Fig. 3-2: Phase envelope diagram of recombined oil with Peng-Robinson EOS

3.1.3 SCAL Properties

The Corey function was used for fitting the two-phase relative permeability data obtained from the experimental data from the composite core flooding. The estimated saturations are accurate within 0.03 saturation units as the previous research done on this composite core [Maloney and Milligan, 2017]. The Corey functions for two-phase oil-water and gas-oil relative permeability are described as follows [Brooks and Corey, 1964]:

$$K_{ro} = K_{ro}^0 \left(\frac{S_o - S_{or}}{1 - S_{or} - S_{wc} - S_{gc}}\right)^{n_0}$$

$$K_{rw} = K_{rw}^0 \left(\frac{S_w - S_{wc}}{1 - S_{or} - S_{wc} - S_{gc}}\right)^{n_w} \tag{3.1}$$

$$K_{rg} = K_{rg}^0 \left(\frac{S_g - S_{gc}}{1 - S_{or} - S_{wc} - S_{gc}}\right)^{n_g}$$

where: K_{ro}, K_{rw}, K_{rg} are estimated relative permeability of oil, water, and gas; K_{ro}^0, K_{rw}^0 and K_{rg}^0 are the relative permeability of oil, water, and gas at the endpoint saturation; n_o, n_w, n_g are the exponents of relative permeability of oil, water, and gas. By using Microsoft Excel software to minimize the total errors between estimated relative permeability values and experimental relative permeability values, the optimum exponents are defined for this research as $n_{o-w} = 2.73$, $n_{o-g} = 3.8$, $n_w = 2.57$ and $n_g = 3.38$.

The experimental data from Wang et al. pointed out the residual oil saturation in the gas-displacing-oil process around 6.5 % of PV and the water-displacing-oil process yielded a residual oil saturation around 14.5 % of PV. The initial water saturation is approximately 0.03 for both displacing processes, and it is considered as the general initial water saturation for the composite core.
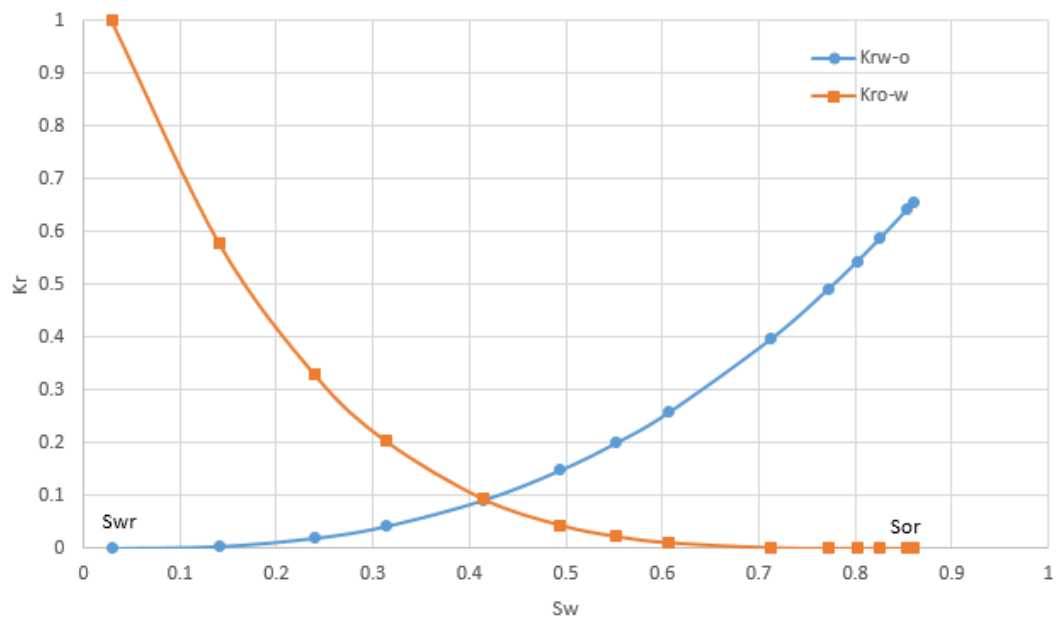
Fig. 3-3: Corey estimated water-oil relative permeability [Wang et al., 2006]

90
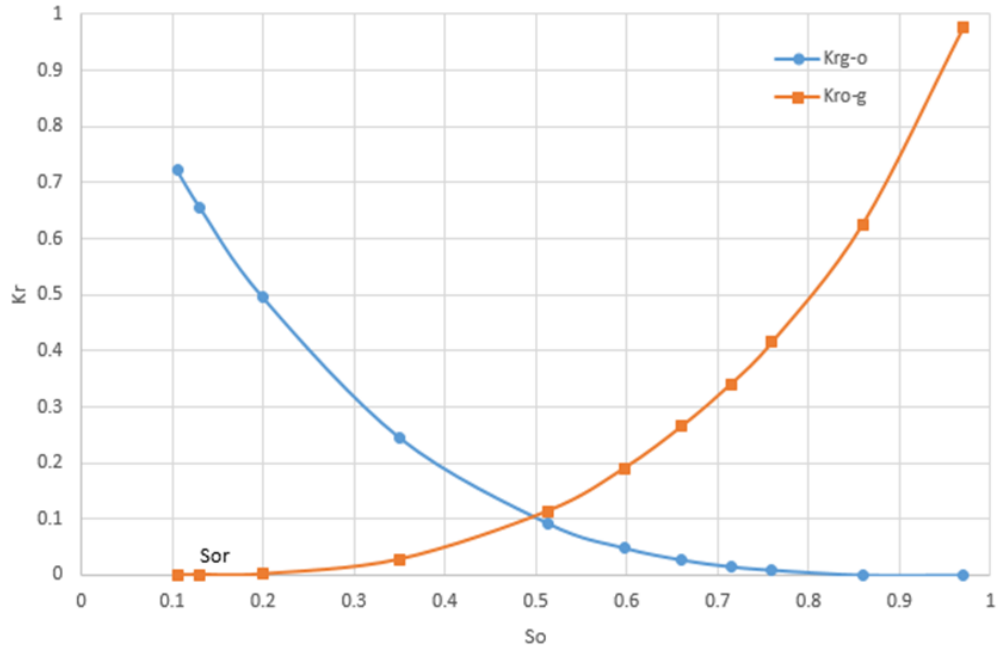
Fig. 3-4: Corey estimated gas-oil relative permeability [Wang et al., 2006]

Centrifuge tests were employed to investigate the capillary pressure relationship of water-oil on core plug 10 and gas-oil on core plug 12. At the residual oil saturation of the water-oil capillary pressure curve, the P_c value is around -2 atm, whereas at the residual oil saturation of the gas–oil capillary curve, the Pc value is nearly 7 atm.
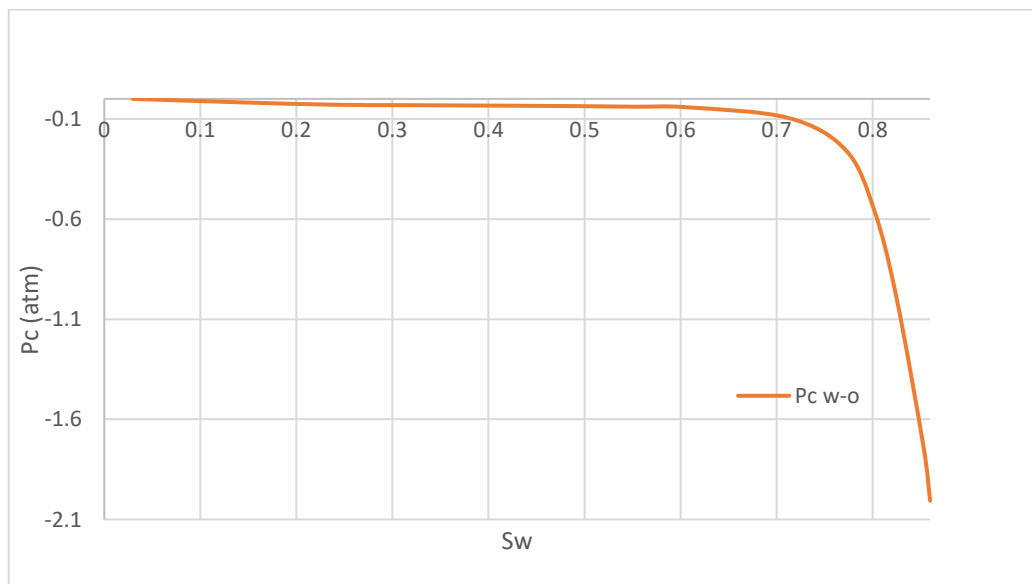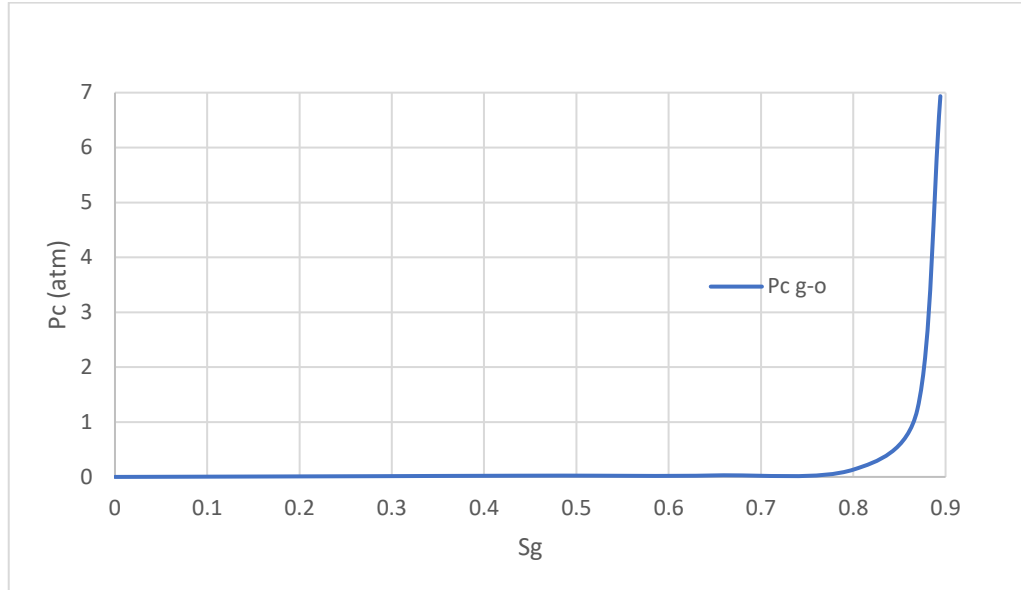
(b)

Fig. 3-5: Water-Oil and Gas-Oil capillary pressure curves from the centrifuge test on plug 10 (a) and plug 12 (b) [Wang et al., 2006]

3.1.4 Models Description

The following section describes the numerical composite models used for simulating the DDP test and the IWAG process. Both numerical models are made using Schlumberger ECLIPSE 100 software for black oil models. The structure below presents the main framework for the numerical simulation models:

• RUNSPEC Section: this is the first section of the ECLIPSE data file. It contains general information about grid properties such as title, unit, start date, used fluids, problem dimensions of wells and blocks. The simulations employed grid models with the dimension as $120 \times 2 \times 2$ grids. These grid models take advantage of counting the sweep efficiency for three dimensions of injected fluids in the composite core models. The unit used in the model

is LAB unit. The composite core models are placed in the vertical direction to simulate the experimental condition with consideration of the gravity effect.

- GRID Section: this section defines the properties of simulation grid and various rock properties such as porosity and permeability in each grid cell. These properties support the program to calculate the grid block pore volume, mid-point depths, and inter-block transmissibility. The Cartesian geometry was employed in this simulation model.

- PROPS Section: this section contains the information of pressure- and saturation-dependent properties of reservoir rocks and fluids information. The fluids properties used to input into these models are extracted from PVTsim software as sections, including DENSITY, PVTW, PVTO, and PVDG. The SCAL properties of models are filled by sections as SWFN, SGFN, and SOF3. The Hysteresis model applied for these models is the Killough model by considering their performance for drainage and imbibition processes in the previous studies [Kossack, 2000; Hamzei et al., 2011; Sharokhi et al., 2014].

- REGION Section: this section divides the computational grid model into regions for various purposes of calculation, including saturation functions, PVT properties, equilibration, fluids in place, inter-region flows, pressure maintenance.

- SOLUTION Section: this section focuses on using the sufficient input data to define the initial state, including pressure, saturation and composition of every grid block in the reservoir.

- SUMMARY Section: this section points out any variables that need to be written to summary files after each time step of the simulation. The time step of the model is set as the value equal to 100 to smoothly reading the output value.

- SCHEDULE Section: this section specifies the schemes of operation to be simulated, including the production and injection controls and constraints. The total of four injection wells are controlled by the constraint as reservoir volume rate (RESV) and four production wells are controlled by the constraint as bottom hole pressure (BHP). All operational parameters such as WAG ratio, WAG slug size, WAG flow rate, and WAG sequence are scheduled in this section sufficiently.

The detailed data files of numerical simulation model are listed in the appendix section of this thesis.

Double Displacement Process (DDP)

Based on the condition of the DDP experiment data from the research of Wang et al., the composite core was reconditioned by centrifuge after it went through two displacing processes to measure the water-oil and gas-oil relative permeability having the initial water saturation at 0.122 fraction PV, which is different from the original initial water saturation of the composite core at 0.03 fraction PV [Wang et al., 2006]. The numerical DDP model is simulated under the operational condition as an experiment with pressure equal to 4500 psig, temperature equal to 210°F, and the rate of injected fluids equal to 4 cc/min. At first, water was injected at the bottom of the composite core by four injected points covering all the bottom surface until the water-cut value of four production points at the topside got to 90%. Then, the gas injection process started at the injection points at the top of the core with a volume from 1 PV up to 2000 PV. The oil recovery factor was noted and compared with the experimental data to validate the integrity of the numerical simulation model. Finally, an additional optimum IWAG injection instead of gas injection after post water-flooding was tested to compare the efficiency between the two methods, DDP and IWAG.

Immiscible WAG (IWAG) injection

The numerical IWAG injection model is based on the original condition of the composite core with a pressure of 4500psig, temperature of 210°F, and the initial water saturation of composite core is 0.03 fraction PV. The slugs of water or gas are injected at the bottom of the core through four injected points which cover all core surface, and oil is produced at the top of core through four producing points. All the input operation parameters are optimized by the following techniques in the next sections to optimize the volume of oil recovery by IWAG process. The operational parameters of concern in this research include total injection (the total volume of fluids used for the injecting process); timing (the water saturation state when starting the WAG injection after water-flooding, counting from the starting point at the initial water saturation); ratio (the volume of water per volume of gas for each injecting cycle); flow rate (the injection rate of injected fluids); slug size (the volume of each injected slug for one cycle) and sequence (type of injected fluids start the injection cycle). Table 3-3 presents the range of operational parameters used to optimize the IWAG process for this research, based on the literature for core-scale IWAG injection in Table 2-1.
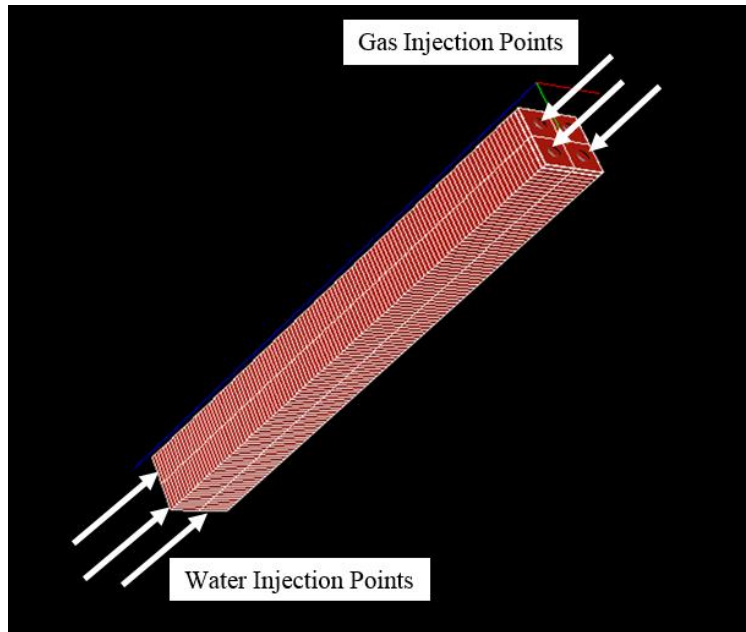
(a)
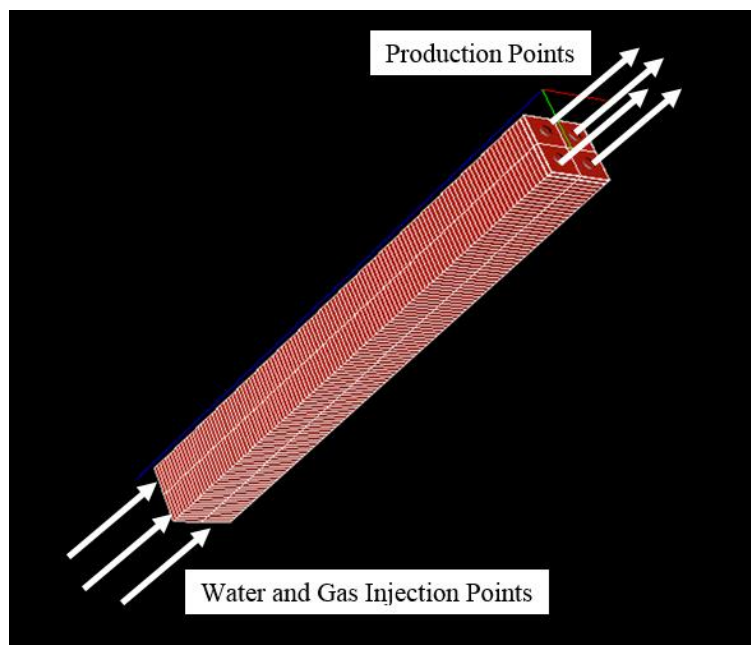
(b)

Fig. 3-6: (a) Composite core model for the DDP test with gas injected from the top and water injected from the bottom of the composite core, and (b) composite core model for IWAG with gas and water injected from the bottom of the composite core

Table 3-3: The range values of operational parameters for IWAG injection

Operational Parameters	Range of Value
1. Total Injection (PV)	0.8, 1.0 or 1.2
2. Timing (fraction PV)	0.03 – 0.40
3. Ratio	0.2 – 5.0
4. Flow rate (ft/d)	0.14 – 1.40 or 2 cc/h – 20 cc/h
5. Slug size (PV)	0.01 - 0.50
6 Sequence	Gas or Water

3.2 Response Surface Methodology (RSM)

RSM was employed to analyze the general idea of optimum operational parameters for IWAG core-flooding process, because it is saves time by only requiring a few runs and can illustrate the significant level of each parameter as well as their interactions. This research used Design-Expert version 11 software to apply the method of Central Composite Design (CCD) as an effective popular RSM model to optimize the objective function as the volume of oil recovery. The framework of response surface methodology is presented in Fig. 3-7.
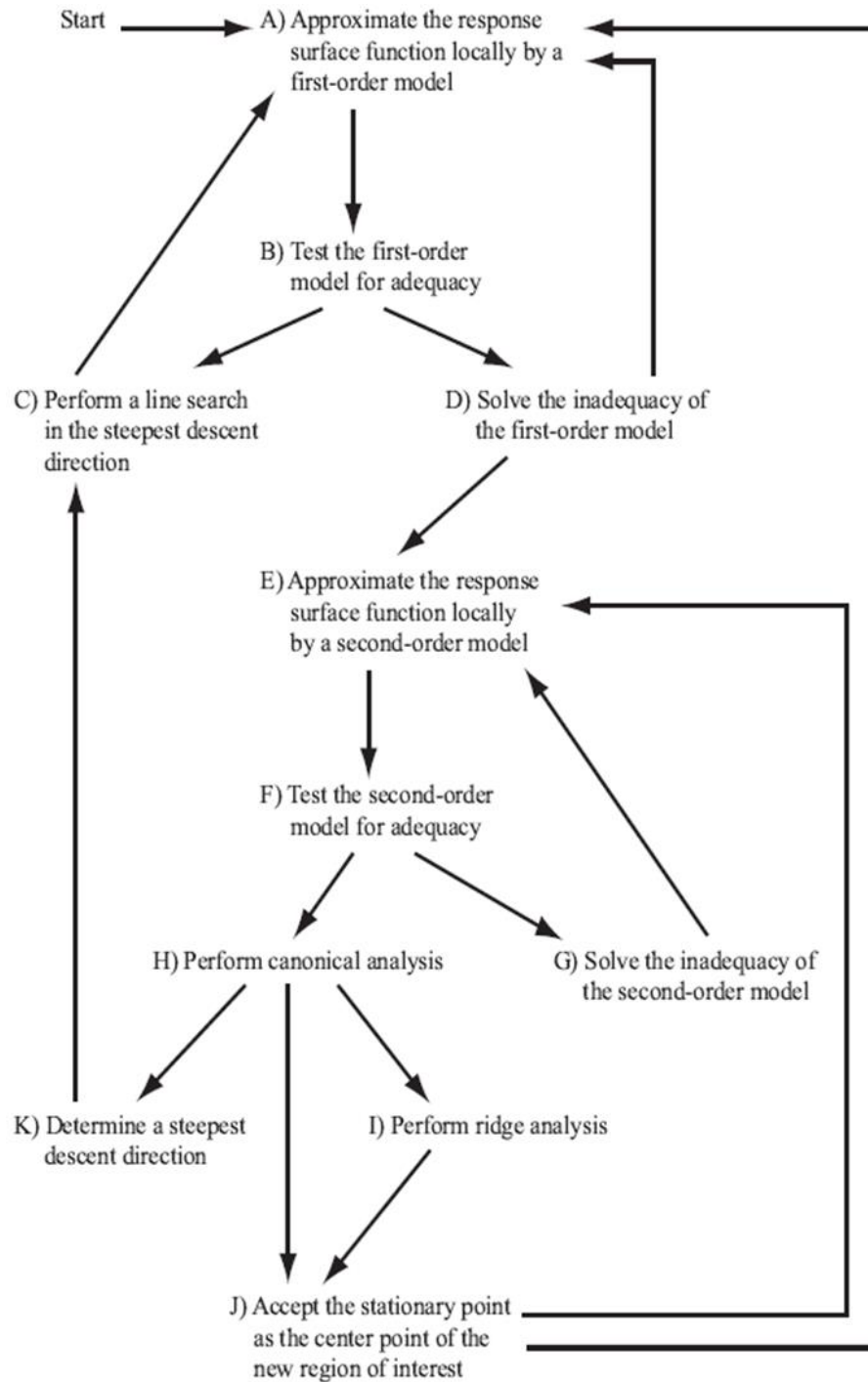
Fig. 3-7: Response Surface Methodology Workflow [Neddermeijer et al., 2000]

The CCI (Inscribed Central Composite) model of CCD was chosen as it fit the suitable range

of input parameters by dividing it into five levels. By fixing the case of total 1 PV of fluid is

injected, the other four numeric parameters and one category parameter are investigated. Table 3-4 presents the level of each parameter as input data. The α value is calculated to equal to 2 for a rotatable CCD model. The number of simulated runs to input into the CCD model is $2 \times (2^4 + 8 + 1) = 50$ with the number of the center point per block is equal to 1 due to the computer model needs no replication.

Table 3-4: The level of input parameters for CCD-RSM model

Optimized parameters	Level 1	Level 2	Level 3	Level 4	Level 5
A-Timing	0.030	0.123	0.215	0.308	0.400
B-Ratio	0.2	1.4	2.6	3.8	5.0
C-Flow Rate	2.0	6.5	11.0	15.5	20.0
D-Slug Size	0.010	0.133	0.255	0.378	0.500
E-Sequence	Gas or Water slug first				

3.3 Particle Swarm Optimization (PSO)

To enhance the accuracy of the optimization process for the core-scale IWAG injection numerical model, the PSO technique is employed as an optimum algorithm for that purpose due to its wide application in the oil and gas industry. The range of values of the operational parameters that need to be optimized are as shown in Table 3-3. MATLAB software was used to simulate the PSO process with the framework of PSO as presented below for the purpose of maximizing the objective function as the volume of oil recovery by IWAG process.
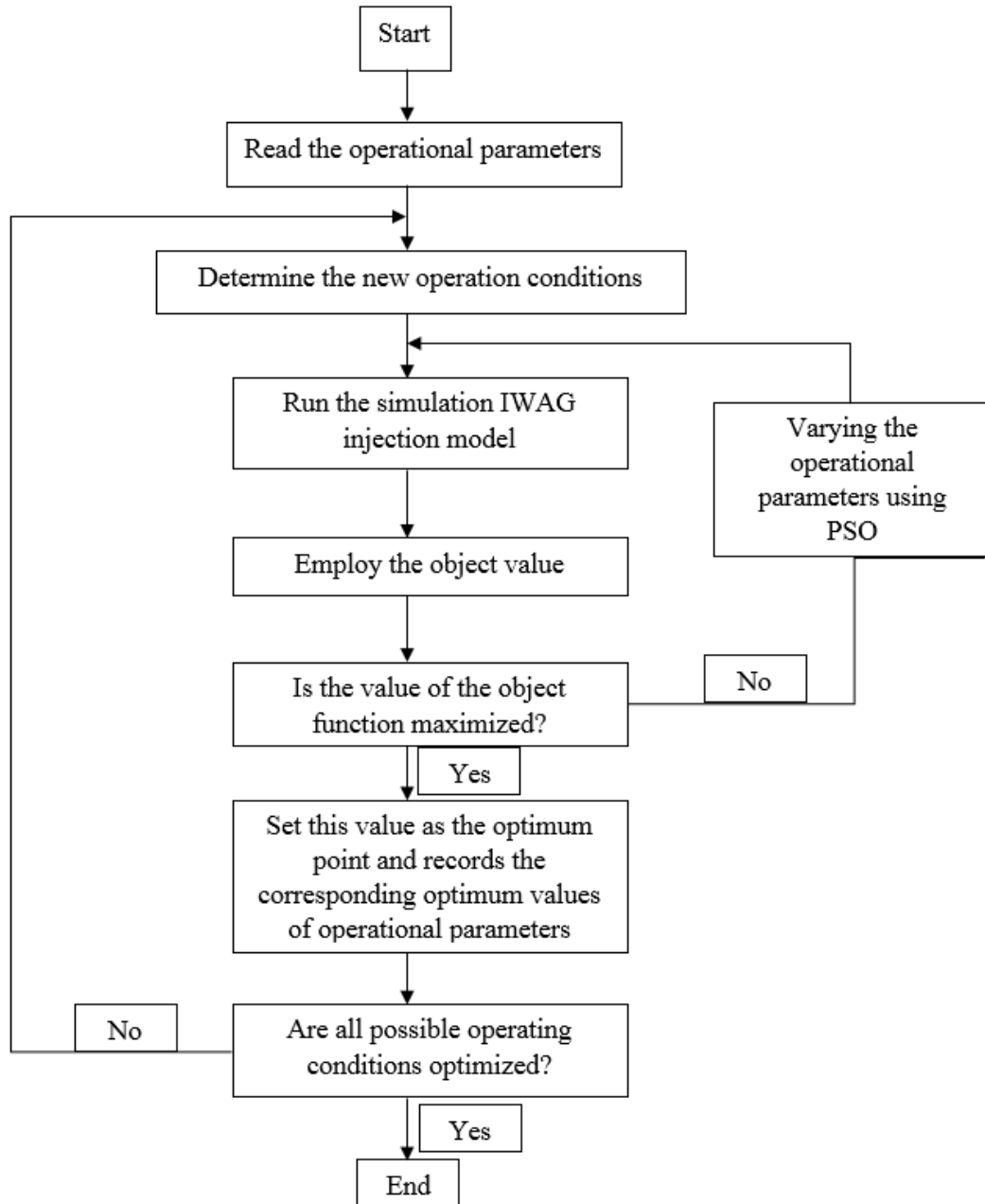
Fig. 3-8: Particle Swarm Optimization Workflow

One case of the PSO model was run to optimize the IWAG injection with a total of 1PV of

injected fluids to compare with the performance of 1 PV of gas injection in the DDP test. The

other three cases of PSO model were run to optimize the operational parameters for the IWAG

injection of the original composite core model. For each time implementing of PSO model, a

total of 2000 runs are required to reach the global optimum based on the reviewed literature, with the suggested number of particles equal to 50, and the suggested iteration equal to 40 [Mohamed et al., 2011; Mohagheghian, 2016]. The following parameters necessary for equations (2.8) and (2.9) were chosen from the literature that presented good convergence results [Cai et al., 2009; Bansal et al., 2011]. These parameters include $C_1 = 0.50$, $C_2 = 1.25$, $\omega_{max} = 0.9$ and $\omega_{min} = 0.4$.
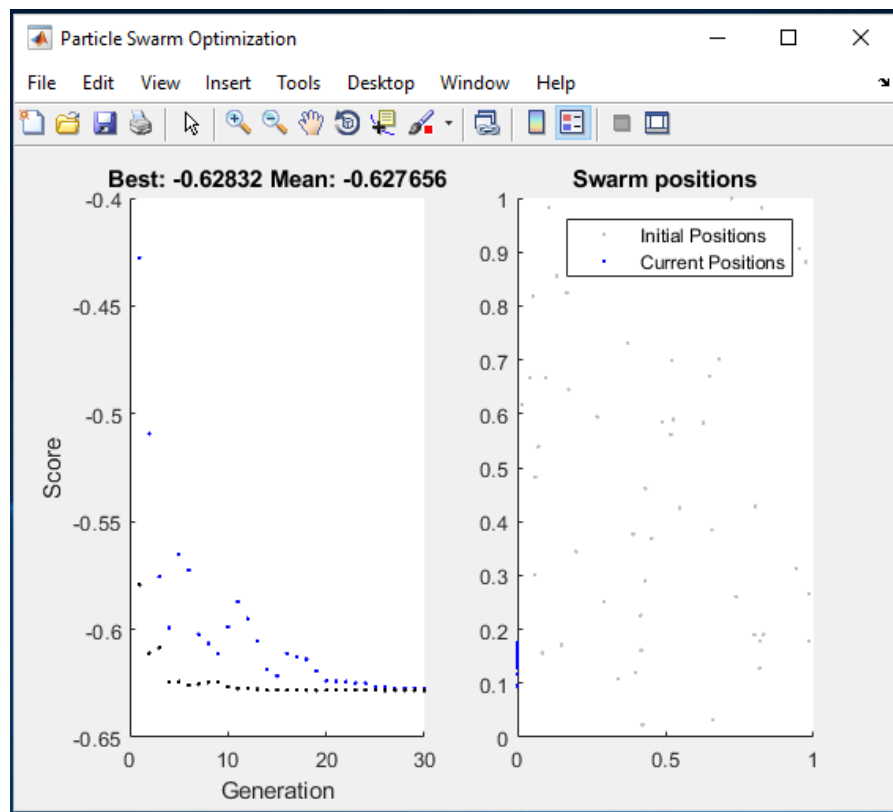
Fig. 3-9: The movement of particles by the PSO model in MATLAB

CHAPTER 4. RESULTS AND DISCUSSION

In the first section of this chapter, the numerical simulation model used for core-scale injection is validated by the experimental data of double displacement process (DDP) test from previous research (section 4.1). Once validated, the composite core simulation model was used to compare oil recovery efficiency between DDP and IWAG in section 4.2. Section 4.3 shows the simulation results obtained by applying response surface methodology (RSM) and particle swarm optimization (PSO) on the IWAG injection model to investigate the impact of operating parameters as well as the optimum combination of them. Finally, in section 4.4, the results of optimized IWAG injection applied after water cut level of post water-flooding led to 90% is presented with a significant improvement in oil recovery efficiency for the composite core model.
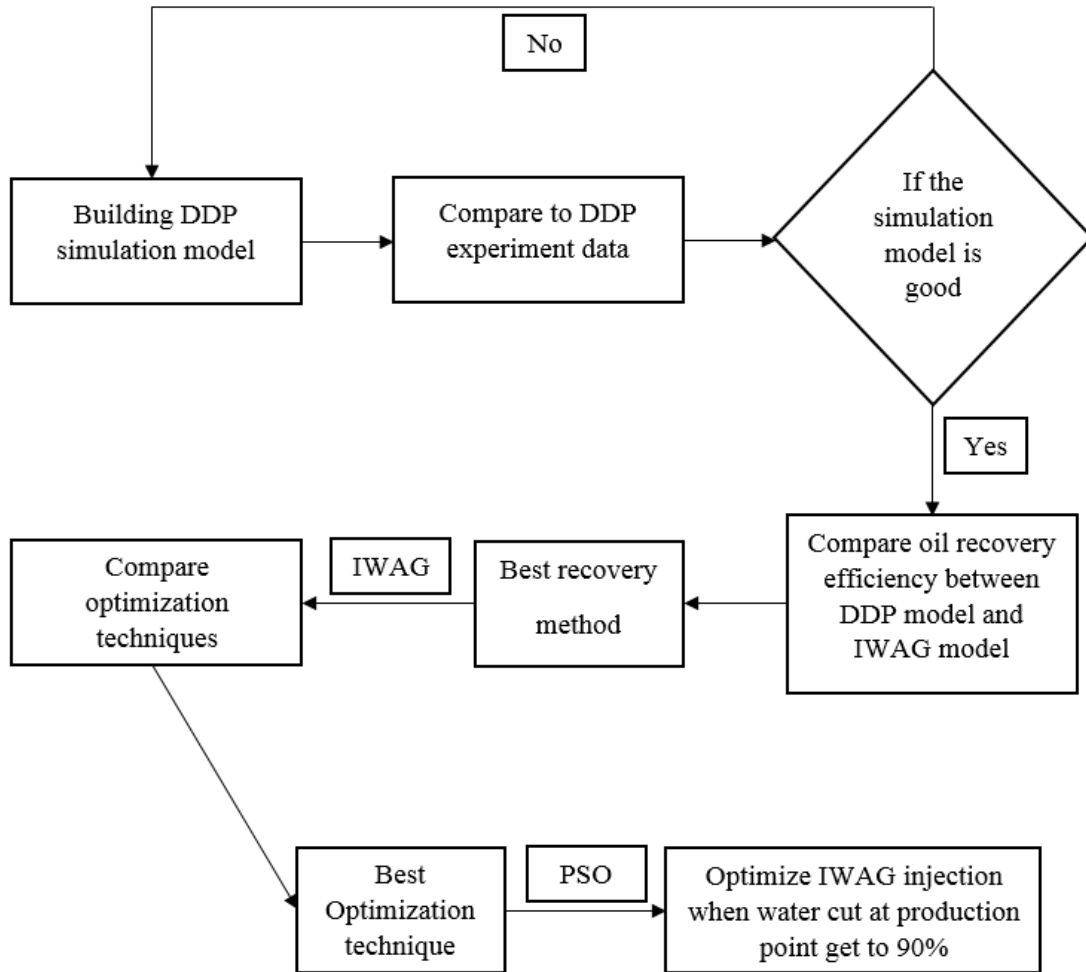
Fig. 4-1: Simulation implementation workflow

4.1 Composite Core Simulation Model Validation

Similar to the experimental DDP conducted by Wang et al., the simulation DDP process started at the initial water saturation $S_{wi} = 0.122$, with a post water-flooding injecting from the bottom of the composite core until the ratio of produced water and oil at the production points reached 9:1. The data from the DDP simulation indicated that a volume of 0.6 PV of water needs to be injected to get to 90% water cut level at the rate of 4 cc/min.
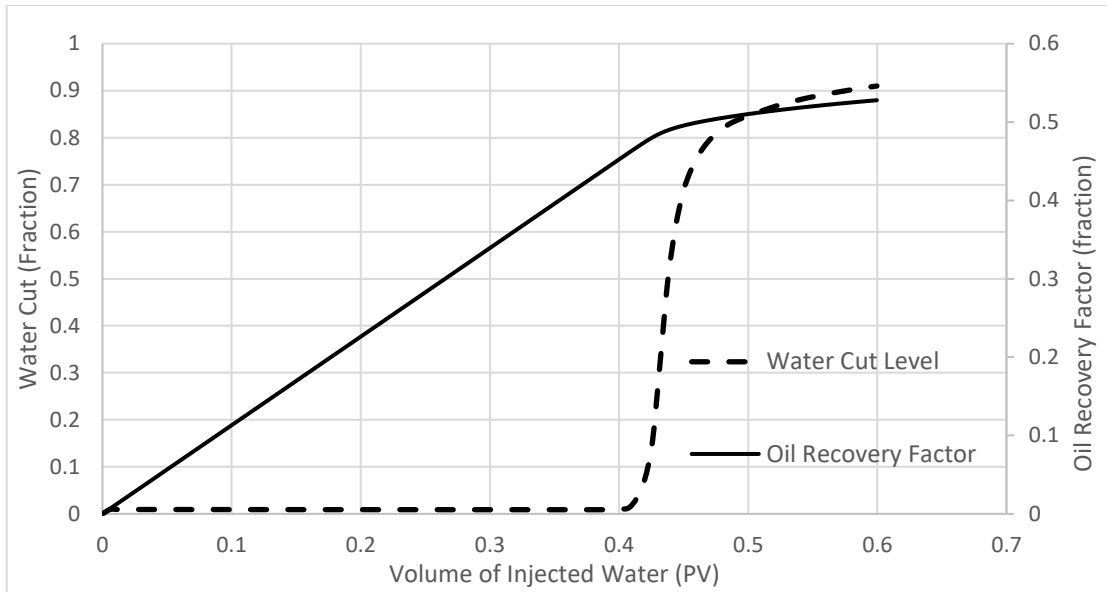
Fig. 4-2: Post water-flooding process for DDP model

After water flooding, the predicted water saturation was 0.585. Then, the injection process continued with gas injection from the top of the composite core, and oil was recovered at the bottom. The simulation data illustrated that, after 1 PV of injected gas, approximately 10.3% OOIP was recovered. After the next 10 PV of injected gas, an additional about 12% OOIP was recovered, and after over 2000 PV of injected gas, a total of around 38.5% OOIP was recovered by the gas injection process. These data fit quite well with the experimental results from Wang et al. and are presented in Fig. 4-4.
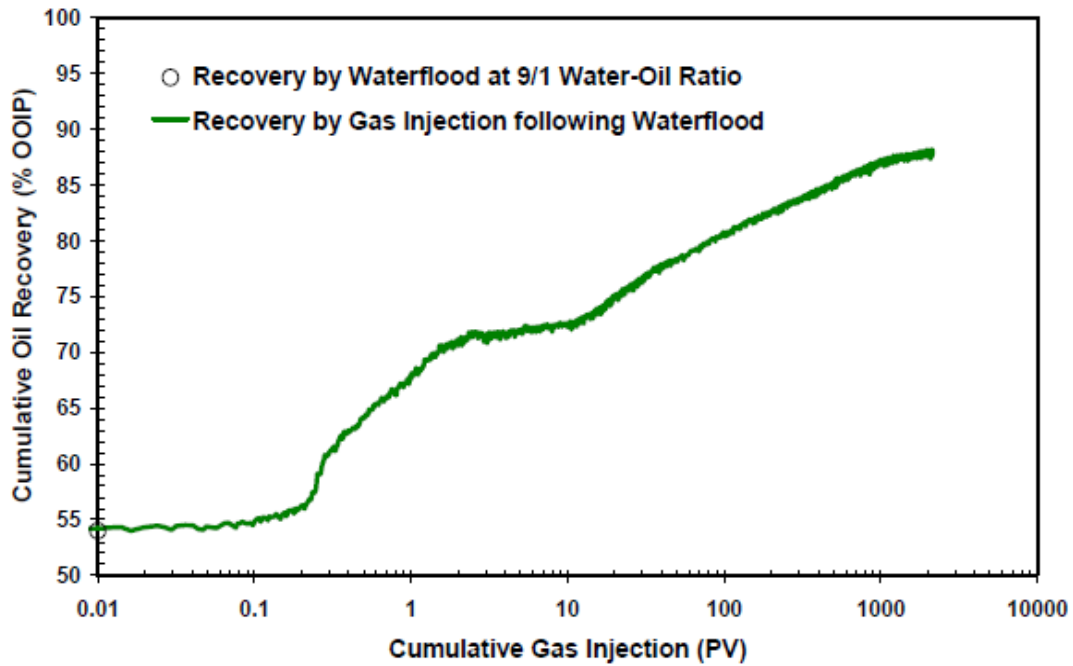
Fig. 4-3: The volume of cumulative oil recovery by gas injection of DDP experiment
[Wang et al.,2006]
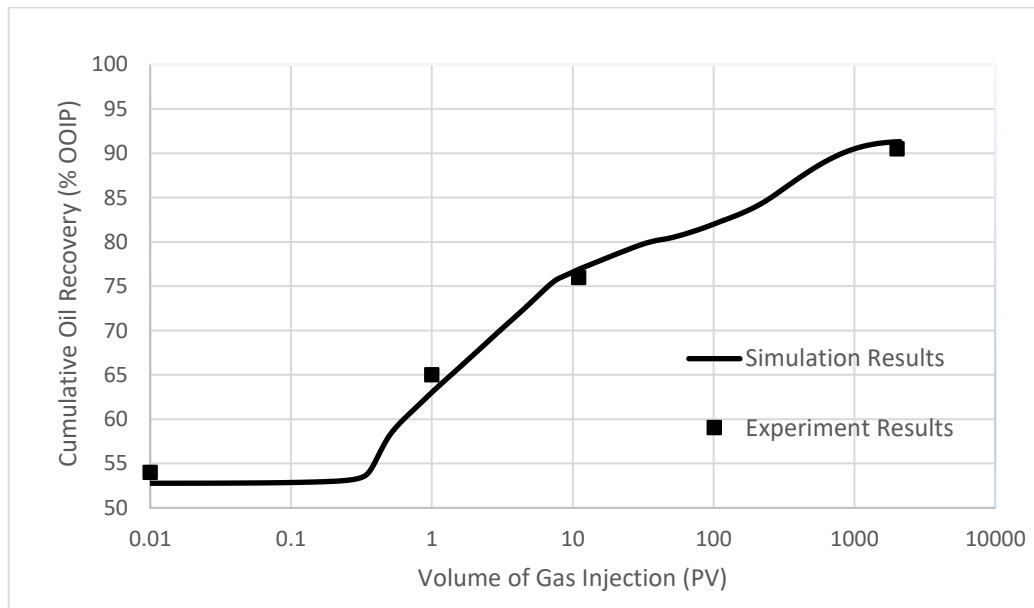
Fig. 4-4: Comparison between DDP simulation model and DDP experimental data after
2011 PV of injected gas

These comparison results validated that the properties of the composite core models are good

with an acceptable match to the experimental data as shown in Fig. 4-4. After injecting 1 PV

of gas, the simulation DDP model indicates the cumulative oil recovery is about 63%, compared with experimental data as below 65%. When injecting more 10 PV of gas, the cumulative oil recovery of DDP model is approximately 76.6%, while experimental data reported 76%. After a total of around 2011 PV of injected gas, simulation DDP model present the cumulative oil recovery as around 91%, while the experimental result was above 90%. The average errors over three observed points is equal to 1.7%, which is considered to be appropriate. Having confidence in the simulation results, the composite core simulation model is used to compare DDP to IWAG and to optimize the operating parameters of IWAG.

4.2 Comparison of DDP Simulation and IWAG Simulation

In order to compare the performance of gas injection from DDP model, IWAG simulated injection also operated after the post water-flooding when the water cut at the production points reached 90 %. In this case, a total of 1 PV of injected fluids of the IWAG process were used to compare with 1 PV of gas injection for DDP. The injected rate was the same as the condition for DDP-gas injection while other operational parameters were optimized by PSO as shown in Table 4-1.

Table 4-1: The optimum operational parameter of 1 PV of IWAG injection after post water-flooding

Operational Parameters	Optimum Value
A-Timing	0.122 (S_{wi})
B-Ratio	0.427
C-Flow Rate	4 cc/min
D-Slug Size	0.11
E-Sequence	Gas

As can be seen from the table, because of the large amount of water inside the composite core model from post water-flooding, the IWAG should start gas slug first instead of water slug, and the WAG ratio should be smaller than 1, which is more volume of gas for each cycle. Furthermore, the slug size should be small enough to better enhance oil recovery [Kim et al., 2015; Alkhazmi et al., 2017]. The simulation results indicated that a suitable operational condition of IWAG injection could improve approximately more than 3% OOIP cumulative oil recovery than an additional gas injection by DDP after 1 PV of injected fluids as Fig. 4-5.
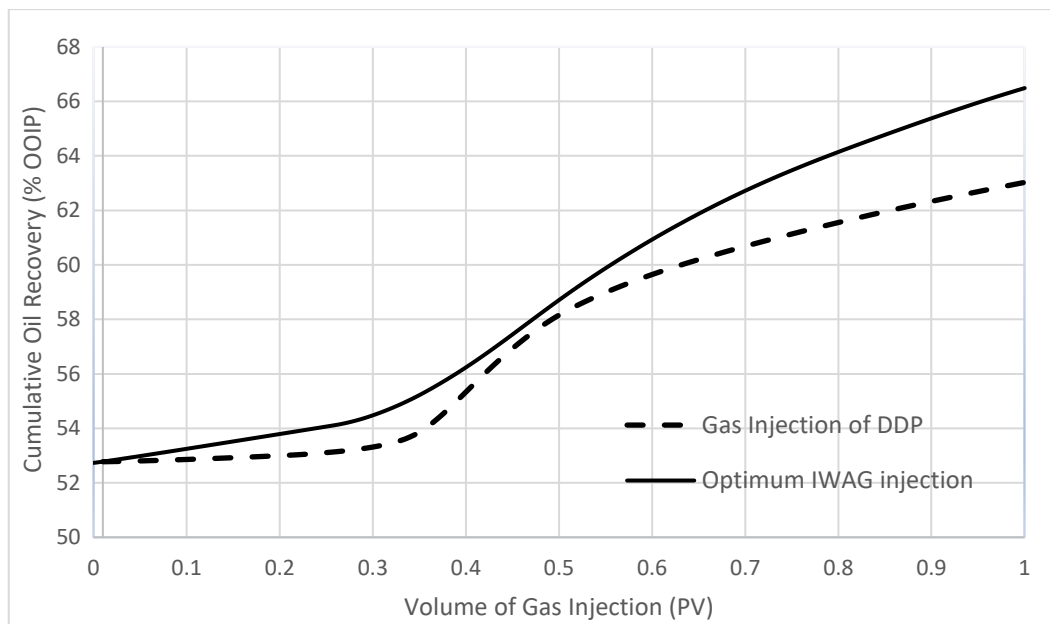
Fig. 4-5: Comparison between DDP simulation model and optimum IWAG injection after post water-flooding lead to water cut equal 90%

It can be concluded that the IWAG injection is more efficient than the double displacement process. For DDP, when starting the gas injection from the top, at first 0.3 PV injected fluid, not much oil was produced due to the large amount of water contained inside the pore system, the double displacement initially pushing water out. For the IWAG injection, the oil continued to produce steadily after post water-flooding due to its connectivity and the advantage of combining the macroscopic and microscopic sweep efficiency immiscible 3-phases injection.

4.3 Immiscible WAG Injection Optimization

4.3.1 Response Surface Methodology (RSM)

The method central composite design (CCD) was used to create the response surface for the objective function of the oil recovery volume (ORV) after 1 PV of IWAG injection at the initial condition of the composite core. The ANOVA table below presents the sensitivity results of the CCD-RSM application for this case.

ANOVA for 2FI model

Response 1: ORV

Source	Sum of Squares	df	Mean Square	F-value	p-value	
Model	0.3933	15	0.0262	622.40	< 0.0001	significant
A-Timing	0.3821	1	0.3821	9070.52	< 0.0001	
B-Ratio	0.0030	1	0.0030	71.84	< 0.0001	
C-Flow Rate	0.0003	1	0.0003	6.76	0.0138	
D-Slug Size	0.0020	1	0.0020	46.90	< 0.0001	
E-Sequence	0.0028	1	0.0028	66.18	< 0.0001	
AB	1.475E-06	1	1.475E-06	0.0350	0.8527	
AC	6.592E-06	1	6.592E-06	0.1565	0.6950	
AD	0.0000	1	0.0000	0.3769	0.5435	
AE	0.0003	1	0.0003	6.15	0.0184	
BC	0.0000	1	0.0000	0.7831	0.3826	
BD	1.823E-06	1	1.823E-06	0.0433	0.8365	
BE	0.0012	1	0.0012	28.96	< 0.0001	
CD	3.575E-06	1	3.575E-06	0.0849	0.7726	
CE	0.0005	1	0.0005	10.90	0.0023	
DE	0.0008	1	0.0008	18.59	0.0001	
Residual	0.0014	33	0.0000			
Cor Total	0.3947	48				

Fig. 4-6: ANOVA table for CCD-RSM application of IWAG injection model

As can be seen from the table, the full two-factor interaction (2FI) model was applied to present the response surface of the model objects. With the significant value (alpha) equal to 0.05, the full two-factor interaction model is generally significant with p-value < 0.0001. All the main operational parameters including timing (A), ratio (B), flow rate (C), slug size (D)

and sequence (E) are significant for the response surface because of their p-value all smaller than the alpha value. Timing is the most significant factor that makes the most impact on the optimum objective, its F-value equal to 9070.52 is the highest. The response model suggested that starting the IWAG injection at initial water saturation reached the highest volume of oil recovery combined with other parameters. Fig. 4-7 below illustrates all information about significant terms and insignificant terms for the predicted response surface model from the ANOVA table by comparing their p-value with alpha value.
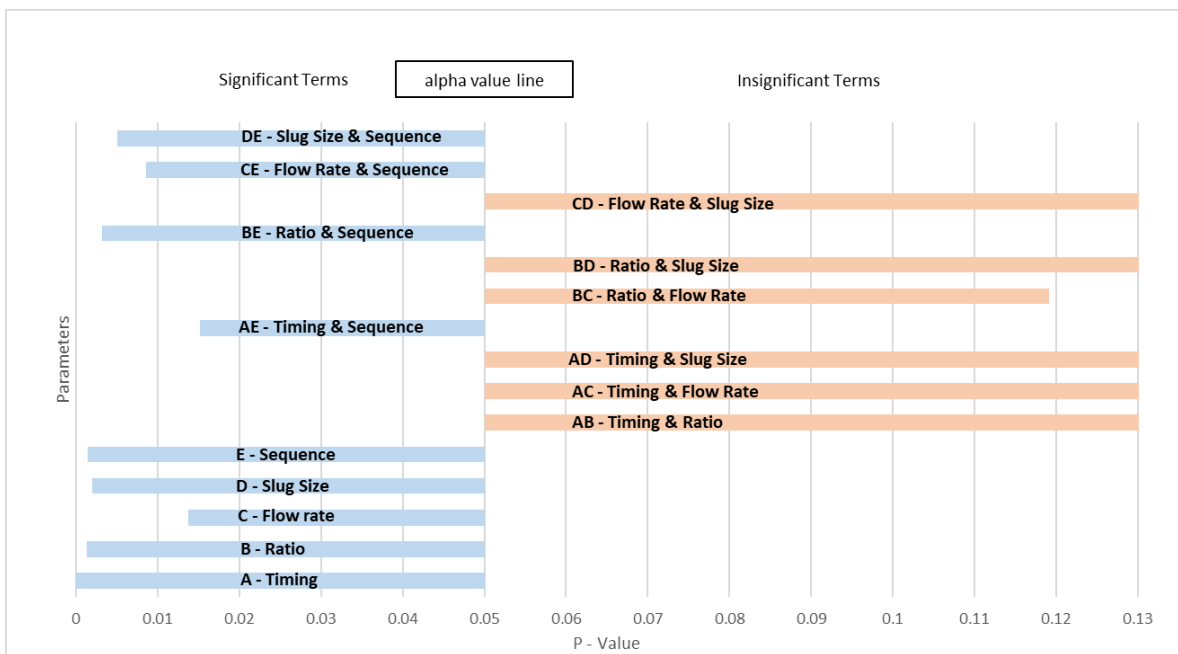
Fig. 4-7: The impact of operational parameters on oil recovery volume by RSM model from the ANOVA table

All interaction terms containing sequence factor (E) are significant when comparing their p-value with the alpha value, especially the interaction term of ratio and sequence (BE) with its p-value < 0.0001. In Fig. 4-7, when increasing the ratio value, changing from injecting water to gas first will improve the recovery performance.
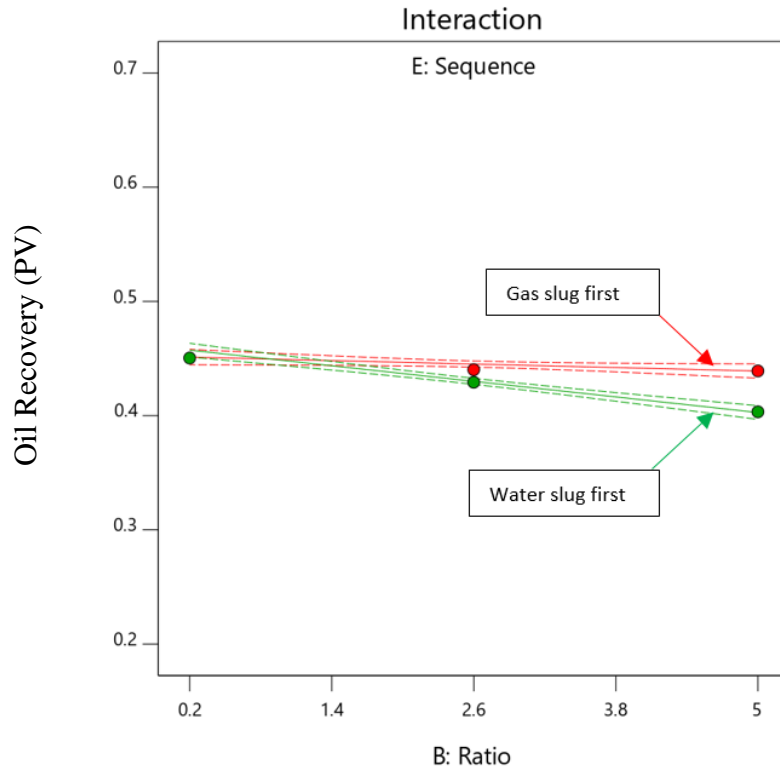
Fig. 4-8: The interaction between Ratio and Sequence

All terms that have the p-value larger than alpha value are insignificant for the model. By removing all the insignificant terms, it improves the R-square adjusted and predicted value as shown in Fig. 4-10. However, both the full two-factor interaction model and the reduced full two-factor interaction model present a significantly high value of R-square with the differences of adjusted and predicted values are small.

ANOVA for Reduced 2FI model

Response 1: ORV

Source	Sum of Squares	df	Mean Square	F-value	p-value	
Model	0.3932	9	0.0437	1173.15	< 0.0001	significant
A-Timing	0.3821	1	0.3821	10259.67	< 0.0001	
B-Ratio	0.0030	1	0.0030	81.26	< 0.0001	
C-Flow Rate	0.0003	1	0.0003	7.65	0.0086	
D-Slug Size	0.0020	1	0.0020	53.04	< 0.0001	
E-Sequence	0.0028	1	0.0028	74.85	< 0.0001	
AE	0.0003	1	0.0003	6.95	0.0120	
BE	0.0012	1	0.0012	32.76	< 0.0001	
CE	0.0005	1	0.0005	12.33	0.0011	
DE	0.0008	1	0.0008	21.03	< 0.0001	
Residual	0.0015	39	0.0000			
Cor Total	0.3947	48				

Fig. 4-9: Reduced ANOVA table with only significant terms

Fit Statistics

Std. Dev.	0.0065	R^2	0.9965
Mean	0.4373	Adjusted R^2	0.9949
C.V. %	1.48	Predicted R^2	0.9924
		Adeq Precision	100.3032

Fit Statistics

Std. Dev.	0.0061	R^2	0.9963
Mean	0.4373	Adjusted R^2	0.9955
C.V. %	1.40	Predicted R^2	0.9941
		Adeq Precision	134.9353

(a)   (b)

Fig. 4-10: Adjusted and predicted R-square value between (a) including insignificant interaction terms and (b) without insignificant interaction terms

In the analysis of variances, three main assumptions need to be satisfied to validate the results, including that the residual is normally distributed, constant variances and independence between runs. The following plots (Fig. 4-11) validate these assumptions above, namely Normal Distribution Plot of Residual, Residual vs. Predicted and Residual vs. Run.
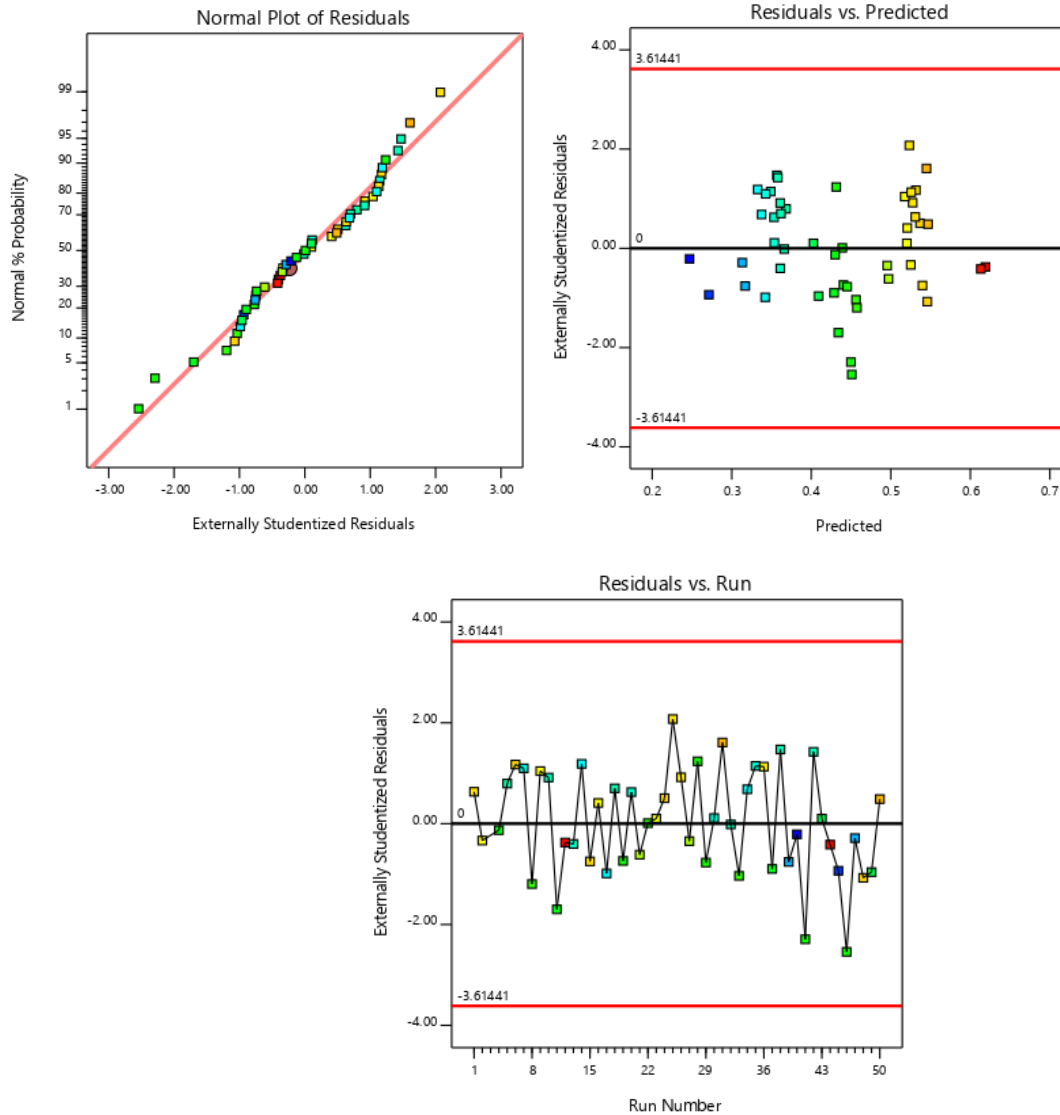
Fig. 4-11: ANOVA assumptions checking plots

The prediction response surface function in actual models are presented below, including all terms of the full two-factor interaction model.

For gas slug first: Oil Recovery (PV) = 0.642339 - 0.948356 × A - 0.000473 × B + 0.00797 × C − 0.0352 × D + 0.00934 × AB - 0.00109 × AC + 0.062168 × AD- 0.000188 × BC - 0.001624 × BD + 0.000606 × CD

(4.1)

For water slug first: Oil Recovery (PV)ORV = 0.692925 - 0.998576 × A − 0.009306 × B + 0.000423 × C − 0.101163 × D + 0.001934 × AB - 0.00109 × AC + 0.062168 × AD -0.000188 × BC - 0.001624 × BD + 0.000606 × CD

After removing all the insignificant terms, the prediction response surface function in actual models are presented as below

For gas slug first: Oil Recovery (PV) = 0.645181 - 0.939468 × A - 0.002539 × B + 0.001229 × C − 0.019394 × D

(4.2)

For water slug first: Oil Recovery (PV) = 0.695768 - 0.989689 × A − 0.011373 × B + 0.000146 × C − 0.085349 × D

To validate the predicted function, several confirmation runs were carried out. The Table 4-2 shows a set of trial runs for this predicted function. The responses place between the range of 95% confidence interval indicates that the model is good for prediction and optimization with a significant value equal to 5%.

Table 4-2: Results of confirmation runs for the predicted model

Run#	Timing	Ratio	Flow Rate	Slug Size	Sequence	Simulation oil recovery (PV)	95% Predicted Interval Low	95% Predicted Interval High
1	0.365	3.463	16.29	0.034	Water	0.287	0.275	0.304
2	0.077	3.344	7.60	0.452	Water	0.536	0.528	0.556
3	0.264	0.771	4.98	0.250	Gas	0.400	0.383	0.410
4	0.186	2.827	11.69	0.472	Gas	0.462	0.455	0.482
5	0.030	0.920	20.00	0.094	Water	0.644	0.629	0.659
6	0.036	0.601	1.33	0.015	Water	0.626	0.622	0.654

4.3.2 Particle Swarm Optimization (PSO)

PSO method was employed to maximize the optimization for IWAG injection. In this section, the results of the three cases of optimization IWAG processes are presented, including different total volumes of injected fluids as 0.8 PV, 1 PV, and 1.2 PV. In all cases, the PSO models reached good convergent results after 2000 runs, such as is shown in the following figures.
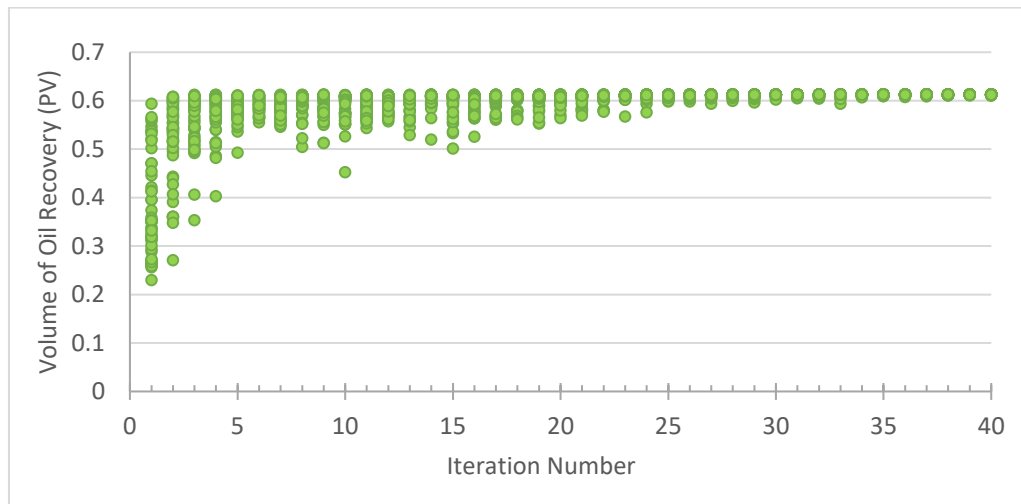
Fig. 4-12: Particle Swarm Optimization (PSO) for 0.8 PV of IWAG injection
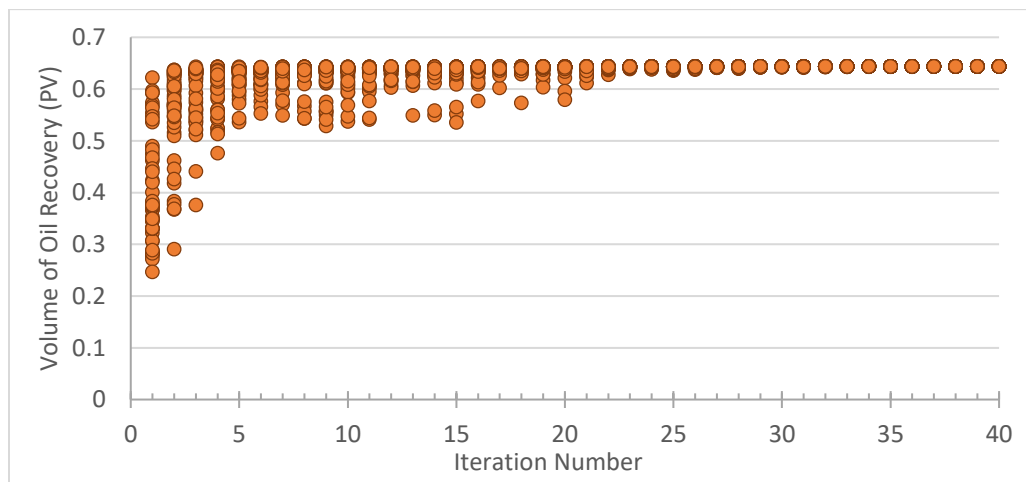
Fig. 4-13: Particle Swarm Optimization (PSO) for 1 PV of IWAG injection
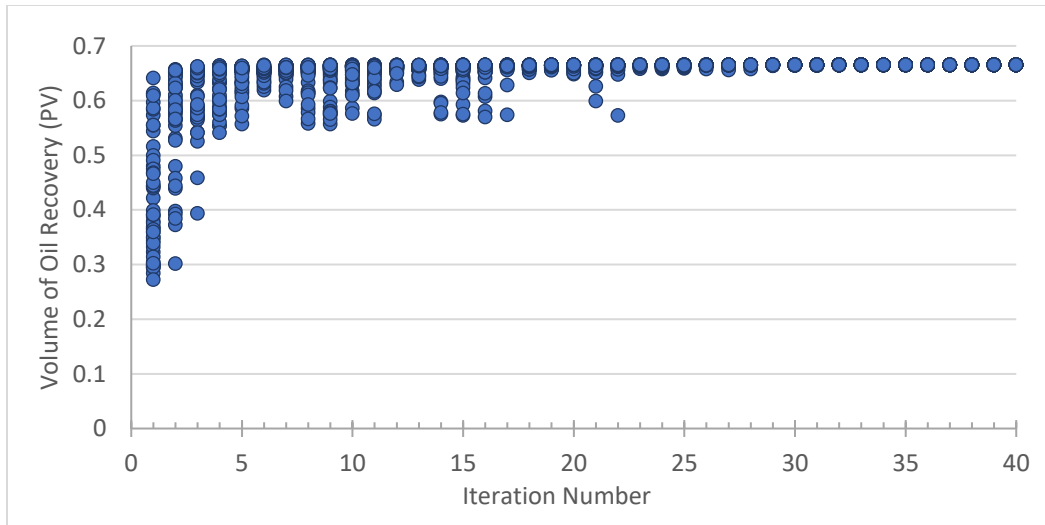
Fig. 4-14: Particle Swarm Optimization (PSO) for 1.2 PV of IWAG injection

Table 4-3: The optimum IWAG operational parameters by the PSO model

		PSO		
Total Injection (PV)		0.8	1.0	1.2
A – Timing (Sw)	0.03 – 0.4	0.03	0.03	0.03
B - Ratio	0.2 – 5	0.88	0.92	0.82
C - Flow Rate (ft/day)	0.14 – 1.41	1.41	1.41	1.41
D - Slug Size (PV)	0.01 – 0.5	0.200	0.094	0.091
F - Sequence	Gas or Water slug first	Water	Water	Water
Oil Recovery (PV)		0.613	0.650	0.666

As can be seen from Table 4-3, the process of IWAG should be started at the initial water

saturation (S_{wi}) of the composite core and combining with suitable other parameters to give

the best volume of oil recovery for different total volume of injected fluid. A suitable high

flow rate of the injection, starting at S_{wi} reached the highest oil recovery volume. The impact

of sequence was significant, which was validated by the RSM results. Starting IWAG

injection at S_{wi}, the first injected slug must be water to enhance the sweep efficiency at the

beginning stage of injection. The ratio and slug size of IWAG injection are various through

115

the different total volumes of injection. The optimum ratio is 0.88 for 0.8 PV of WAG injection, while this number for cases 1.0 PV and 1.2 PV injection is 0.92 and 0.82, respectively. The optimum slug size is 0.200 for 0.8 PV of WAG injection, while this number for cases 1.0 PV and 1.2 PV injection decreasing slightly from 0.094 to 0.091. The data points out the importance of optimizing suitable operational parameters for different operational scenarios. Fig. 4-14 below illustrates the oil recovery volume for three optimum cases with different volumes of injected fluids, as presented in Table 4-3. The optimized operational parameters will be variable for different total volumes of fluids injected for IWAG injection to get the highest oil recovery volume.
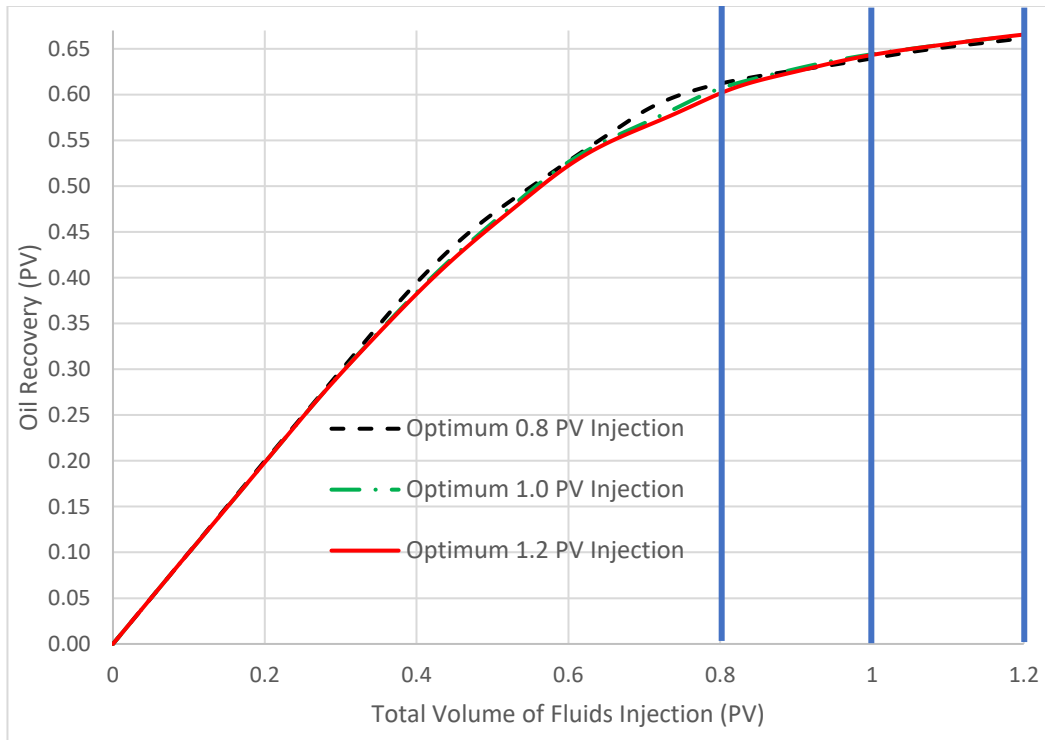
Fig. 4-15: Optimum IWAG injection for different volume of injected fluids

Table 4-4: Comparison of the optimal IWAG operational parameters using PSO and RSM models from initial water saturation (Swi)

	PSO	RSM	
Total Injection (PV)	1	1	
A – Timing (Sw)	0.030	0.036	Optimum Operational Parameters
B - Ratio	0.920	0.601	
C - Flow Rate (ft/day)	1.41	1.33	
D - Slug Size (PV)	0.094	0.015	
F - Sequence	Water	Water	
Predicted oil recovery (PV) using optimal operational parameters (above)	0.650	0.626	
Estimated oil recovery (PV) using RSM Equation (4.2)	0.646	0.650	
Absolute error (%)	0.62	3.83	

In Table 4-4, when applying the optimum combination of operational parameters of case 1 PV injection for RSM model as the function (4.2), the value of oil recovery volume is 0.646 PV, which is quite similar to the results of PSO model as 0.6 PV, with an absolute error around 0.6 %. The suggested optimum operational parameters from the RSM model predicted to get approximately 0.65 PV oil recovery volume. Compared with the simulation results, there is an absolute error of around 3.83% when the simulated oil recovery volume is approximately 0.626 PV. It can be concluded that the optimum result from the PSO model is more accurate for prediction than the RSM model due to the confidence level as 95 % of the response surface and a lower number of input data.

To investigate the impact of significant operational parameters acquired from the RSM model for the PSO model, a maximum oil recovery volume fixes at 0.65 PV based on the optimum operating parameters of the PSO model from Table 4-4. Then, each significant term is varied

to get the minimum oil recovery volume for each case. The average base value is the average value of all mean value between minimum oil recovery volume and maximum oil recovery volume for each significant parameter. All results are illustrated in Fig. 4-15 below.
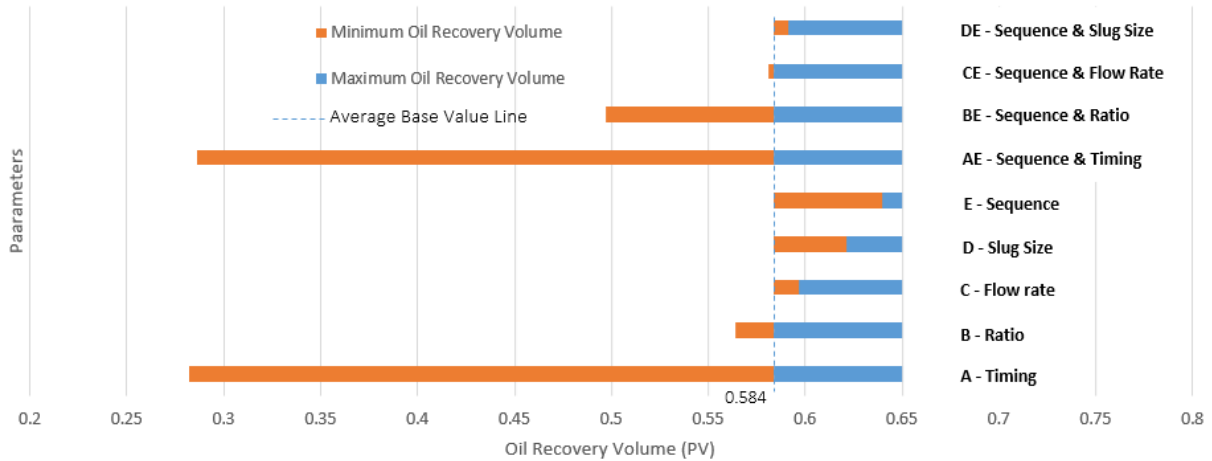
Fig. 4-16: Sensitivity analysis of IWAG operating parameters on oil recovery considering the PSO model

As can be seen from Fig. 4-15, timing has the most significant impact on oil recovery volume when the difference between the maximum and minimum oil recovery volume values is the largest. The impact order of other operational parameters decreases from ratio to sequence. All the interaction terms between sequence and other parameters significantly impact the oil recovery volume, which is similar to the result from the ANOVA table of the RSM model (Fig. 4-6). It can be concluded that sequence has a strong interaction with other parameters to impact the oil recovery volume. When starting IWAG injection at the early stage when the volume of water in the pore system is low, a water slug should be injected first to improve the sweep efficiency with suitable other operational parameters. However, when the pore system has more water, a gas slug should be injected first to push oil out of the larger pores to improve the connection of oil in the pores and improve the oil recovery performance.

4.4 Optimum IWAG Injection Oil Recovery Efficiency Comparison

Further tests were run to check the comparison between the performance of optimum IWAG injection with other oil recovery techniques including water-flooding, gas injection and water injection for a total of 1 PV of fluid injection starting at the initial composite core condition with the same operational condition from Table 4-3. The results presented in Fig. 4-16 below indicate that the optimum IWAG injection has the highest oil recovery factor, which is about 5% higher than water-flooding, quite similar to the double displacement process (DDP), and approximately 20% better than gas injection.

Fig. 4-17: Comparison of different oil recovery techniques

For field applications in the future, IWAG injection could be applied after post water-flooding when the water cut reaches 90%. A further simulation was tested on the composite core simulation model to determine the efficiency of optimum IWAG injection in comparison with continuing waterflooding after 90% water cut.

Starting at the initial water saturation $S_{wi} = 0.03$, the simulation result indicates that after 0.75

PV of water-flooding (Fig. 4-16) with the standard flow rate at 1 ft/day, the water cut value

will equal to 90%.
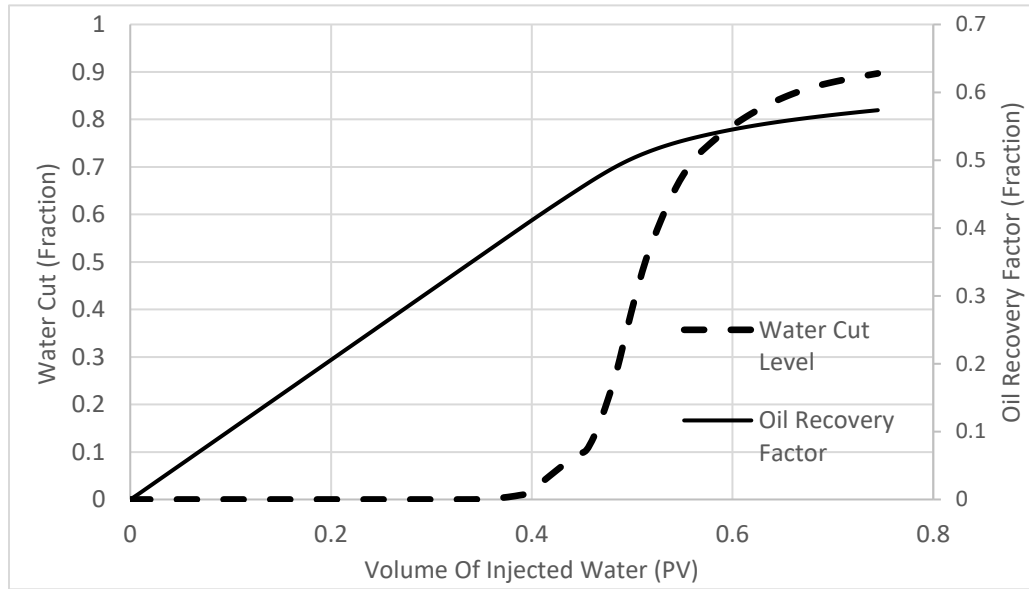
Fig. 4-18: Post water-flooding process as secondary recovery stage

After applying PSO technique to optimize IWAG injection for a total of 1 PV injected fluids,

the result of optimum operational parameters is presented in Table 4-5.

Table 4-5: Optimum operational parameters of IWAG injection after post water-flooding

Total Injection (PV)	1
A – Timing (Sw)	0.586
B - Ratio	0.2
C - Flow Rate (ft/day)	0.14
D - Slug Size (PV)	0.12
F - Sequence	Gas
Incremental Oil Recovery (PV)	0.123

As can be seen from Table 4-5, due to a significant amount of water volume inside the pore system, the volume of water used for WAG injection should be much lower than the volume of gas (WAG ratio = 0.2). The flow rate should be lower than the standard flow rate of post water-flooding (1 ft/ day) to let the gas slug contact with the oil left after the water-flood. The optimum slug size for this case is 0.12 PV and the volume of oil that can be recovered with 1 PV IWAG injection is 0.123 PV. Fig. 4-18 illustrates the efficiency comparison between optimized IWAG injection and continued waterflood. After 1 PV of IWAG injection, the total oil recovery factor is above 0.7. If the water injection continues with the same volume of injected fluid, the oil recovery factor is almost 10 % lower than IWAG injection. It can be concluded that, when the water cut of the production point gets to 90%, a suitable optimum IWAG injection can improve the further recovery stage than continue injecting.
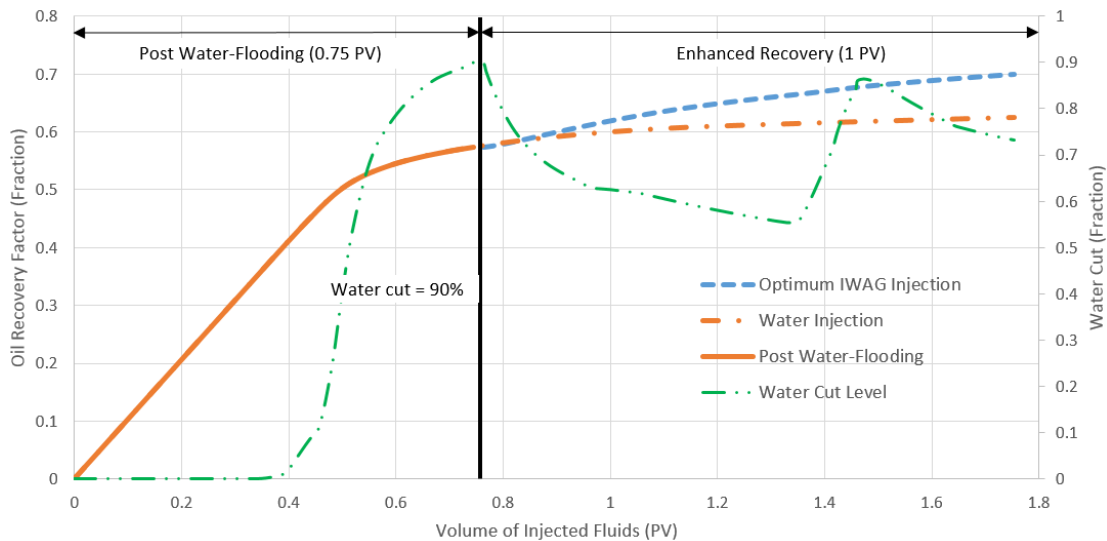
Fig. 4-19: Comparison between the efficiency of optimum IWAG injection and Water injection

121

CHAPTER 5. CONCLUSIONS AND RECOMMENDATIONS

5.1 Summary and Conclusions

A black oil model simulator, Schlumberger Eclipse E100, was employed to simulate the composite core flooding processes for three-phase immiscible injection. The composite core model was first validated by Double Displacement Process (DDP) experimental data by the comparison between the recovery performance of DDP simulation and experimental data. The results showed that good validation was made with good fitting in the curves of cumulative oil recovery data. Furthermore, an optimum Immiscible WAG (IWAG) injection was acquired with a similar operational condition as the DDP model to compare the performance of oil recovery between two the EOR techniques. The results indicated that the IWAG injection is more efficient than the double displacement process, improve approximately more than 3% OOIP cumulative oil recovery than an additional gas injection of DDP injection. The combination of the macroscopic and microscopic sweep efficiency of immiscible three-phase injection may improve more than the gravity segregation sweep efficiency from the gas injection of DDP.

Particle Swarm Optimization (PSO), was used to optimize the IWAG process for the initial composite core flooding model. A range of values for operational parameters including timing, ratio, flow rate, slug size, and sequence were determined from the literature review for use in optimizing IWAG injection. For the RSM method, Central Composite Design (CCD) was used because of its rotatability and its wide application. A total of 50 combinations of operational parameters were input to create the predicted response surface of oil recovery volume. The results indicated that the two-factor interaction (2FI) model was well represented for the response surface with a suitably adjusted and predicted R-square values, both higher

than 0.99. A set of validation of output figures (Fig. 4-10) verifies the appropriate model. The ANOVA table showed that all the main operational parameters including timing, ratio, flow rate, slug size, and sequence are significant for the response surface model because their p-values are all smaller than 0.05 (significant value). Timing is the most significant factor that makes the most impact on the optimum objective with the highest F-value (equal to 9070.52). All interaction terms containing the sequence factor are significant when comparing their p-values with the significant value, especially the interaction term of ratio and sequence, with its p-value < 0.0001. A set of a random combination of operational parameters was chosen to validate the predicted response surface function. The results of these were good with all the simulation calculated values in the range of 95% confidence interval. It can be concluded that the model is good for prediction and optimization with a confidence level equal to 95%.

A total of three cases of IWAG injection, dependent on their total of injected fluid, including 0.8 PV, 1PV, and 1.2 PV were optimized by the PSO technique. The results are clear that, after 2000 runs, PSO models reach good convergent results. The volume of oil recovery for each case was 0.613 PV, 0.65 PV, and 0.666 PV, respectively. In comparison with the RSM predicted response surface by the same combination of optimum operational parameters from the PSO model, the results were quite similar, 0.646 PV of oil recovery from RSM model and 0.65 of oil recovery from PSO models. A conclusion is made that the process of IWAG should be started at the initial water saturation (S_{wi}) of the composite core and combining with the suitable other parameters. A suitable high flow rate of the injection starting at S_{wi} reach to the highest oil recovery volume and the first injected slug must be water but gas due to its strong impact in interaction with other parameters. The ratio and slug size of IWAG injection are various through the different total volume of injection. Therefore, it is necessary to optimize

the suitable operational parameters for different operational scenarios by appropriate optimization tools such as RSM and PSO. The performance of optimum IWAG injection is significantly better than only water-flooding or gas injection, which is about 5% higher than water-flooding, quite similar to double displacement process (DDP), and approximately 20% better than gas injection for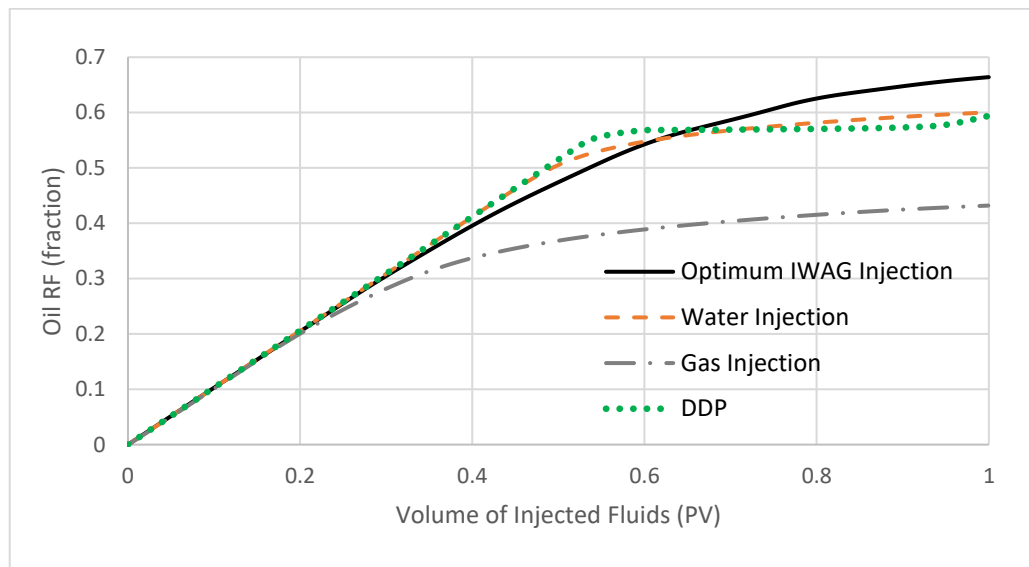 the same operational conditions. For field application in the future, IWAG injection could be applied after post water-flooding when the water cut value at the production well approaches 90%. The result from the simulation indicates that after 1 PV of IWAG injection, the total oil recovery factor is above 0.7 which is almost 10 % higher in comparison with only water-flooding.

5.2 Recommendations

RSM can be employed as an appropriate DOE method to reduce the number of runs to optimize the IWAG process for immiscible core-flooding experiments in the future. It could also be a good tool to present the impact of operational parameters for other WAG injection models, which should be applied for a further miscible core-scale flooding model. PSO is proven to be a great technique to determine the optimum combination of operational parameters for maximizing the oil recovery factors. It is suggested that this tool is be widely used in further numerical simulation models.

REFERENCES

Afzali, S., Rezaei, N., & Zendehboudi, S. (2018). A comprehensive review on enhanced oil recovery by water alternating gas (WAG) injection. Fuel, 227, 218-246.

Aarts, E. H. (1987). Simulated annealing: Theory and applications.

Abdassah, D., Mucharam, L., Soengkowo, I., Trikoranto, H., & Sumantri, R. (1996). Coupling Seismic Data with Simulated Annealing Method Improves Reservoir Characterization.

Abdelhalim, M. B., & Habib, S. E. D. (2009). Particle swarm optimization for HW/SW partitioning. Particle Swarm Optimization, 49-76.

Abidi, M. A., Gribok, A. V., & Paik, J. (2016). Optimization Techniques in Computer Vision: Ill-posed problems and regularization. Springer.

Afzali, S., Rezaei, N., & Zendehboudi, S. (2018). A comprehensive review on enhanced oil recovery by water alternating gas (WAG) injection. Fuel, 227, 218-246.

Ahmadi, Y., Eshraghi, S. E., Bahrami, P., Hasanbeygi, M., Kazemzadeh, Y., & Vahedian, A. (2015). Comprehensive Water–Alternating-Gas (WAG) injection study to evaluate the most effective method based on heavy oil recovery and asphaltene precipitation tests. Journal of Petroleum Science and Engineering, 133, 123-129.

Alkhazmi, B., Sohrabi, M., & Farzaneh, S. A. (2017, October). An Experimental Investigation of the Effect of Gas and Water Slug Size and Injection Order on the Performance of Immiscible WAG Injection in a Mixed-Wet System. In SPE Kuwait Oil & Gas Show and Conference. Society of Petroleum Engineers.

Al-Shuraiqi, H. S., Muggeridge, A. H., & Grattoni, C. A. (2003, January). Laboratory investigations of first contact miscible WAG displacement: the effects of WAG ratio

and flow rate. In SPE International Improved Oil Recovery Conference in Asia Pacific. Society of Petroleum Engineers.

Al-sumaiti, A. M., & Kazemi, H. (2012, January). Experimental and numerical modeling of double displacement oil recovery process in tight fractured carbonate reservoirs. In Abu Dhabi International Petroleum Conference and Exhibition. Society of Petroleum Engineers.

Amin, M. E., Zekri, A. Y., Almehaideb, R., & Al-Attar, H. (2012). Optimization of CO2 WAG processes in a selected carbonate reservoir: an experimental approach. In Proceedings of the Abu Dhabi International Petroleum Exhibition & Conference, Abu Dhabi, UAE (pp. 11-14).

Anderson, M. J., & Whitcomb, P. J. (2016). DOE simplified: practical tools for effective experimentation. Productivity press.

Aote, S. S., Raghuwanshi, M. M., & Malik, L. (2013). A brief review on particle swarm optimization: limitations & future directions. International Journal of Computer Science Engineering (IJCSE), 2(5), 196-200.

Assareh, E., Behrang, M. A., Assari, M. R., & Ghanbarzadeh, A. (2010). Application of PSO (particle swarm optimization) and GA (genetic algorithm) techniques on demand estimation of oil in Iran. Energy, 35(12), 5223-5229.

Aurand, K. (2017). Enhanced oil recovery using silica nanoparticles: An experimental evaluation of oil production, recovery mechanisms and nanofluid stability.

Averbuch, D., Gainville, M., Pierchon, A., & Dejean, J. P. (2005, May). Response surface models for hydrate prediction: deterministic and probabilistic applications. In 12th International Conference on Multiphase Production Technology. BHR Group.

Awan, A. R., Teigland, R., & Kleppe, J. (2008). A survey of North Sea enhanced-oil-recovery projects initiated during the years 1975 to 2005. SPE Reservoir Evaluation & Engineering, 11(03), 497-512.

Awotunde, A. A. (2012, January). Reservoir parameter estimation with improved particle swarm optimization. In SPE Annual Technical Conference and Exhibition. Society of Petroleum Engineers.

Bagrezaie, M. A., Pourafshary, P., & Gerami, S. (2014, March). Study of different water alternating carbon dioxide injection methods in various injection patterns in an Iranian non fractured carbonate reservoir. In Offshore Technology Conference-Asia. Offshore Technology Conference.

Bansal, J. C., Singh, P. K., Saraswat, M., Verma, A., Jadon, S. S., & Abraham, A. (2011, October). Inertia weight strategies in particle swarm optimization. In 2011 Third world congress on nature and biologically inspired computing (pp. 633-640). IEEE.

Barnawi, M. T. (2008). A simulation study to verify Stone's simultaneous water and gas injection performance in a 5-spot pattern (Doctoral dissertation, Texas A&M University).

Batruny, P., & Babadagli, T. (2015). Effect of waterflooding history on the efficiency of fully miscible tertiary solvent injection and optimal design of water-alternating-gas process. Journal of Petroleum Science and Engineering, 130, 114-122.

Bertsimas, D., & Tsitsiklis, J. (1993). Simulated annealing. Statistical science, 8(1), 10-15.

Box, G. E., & Wilson, K. B. (1951). On the experimental attainment of optimum conditions. Journal of the Royal Statistical Society: Series B (Methodological), 13(1), 1-38.

Brandimarte, P. (2014). Handbook in Monte Carlo simulation: applications in financial engineering, risk management, and economics. John Wiley & Sons.

Brooks, R., & Corey, T. (1964). HYDRAU uc properties of porous media. Hydrology Papers, Colorado State University, 24, 37.

Cai, X., Cui, Z., Zeng, J., & Tan, Y. (2009). Individual parameter selection strategy for particle swarm optimization. Particle swarm optimization, 978-953.

Carley, K. M., Kamneva, N. Y., & Reminga, J. (2004). Response surface methodology (No. CMU-ISRI-04-136). Carnegie-Mellon Univ Pittsburgh Pa School of Computer Science.

Carlson, L. O. (1988, January). Performance of Hawkins field unit under gas drive-pressure maintenance operations and development of an enhanced oil recovery project. In SPE Enhanced Oil Recovery Symposium. Society of Petroleum Engineers.

Carson, Y., & Maria, A. (1997, December). Simulation optimization: methods and applications. In Proceedings of the 29th conference on Winter simulation (pp. 118-126). IEEE Computer Society.

Caudle, B. H., & Dyes, A. B. (1958). Improving miscible displacement by gas-water injection.

Cavazzuti, M. (2012). Optimization methods: from theory to design scientific and technological aspects in mechanics. Springer Science & Business Media.

Cavazzuti, M. (2013). Design of experiments. In Optimization methods (pp. 13-42). Springer, Berlin, Heidelberg.

Chen, C. H., & Lee, L. H. (2011). Stochastic simulation optimization: an optimal computing budget allocation (Vol. 1). World scientific.

Chen, S., Li, H., Yang, D., & Tontiwachwuthikul, P. (2010). Optimal parametric design for water-alternating-gas (WAG) process in a CO2-miscible flooding reservoir. Journal of Canadian Petroleum Technology, 49(10), 75-82.

Chen, Y. P. (2006). Extending the Scalability of Linkage Learning Genetic Algorithms: Theory & Practice (Vol. 190). Springer Science & Business Media.

Choudhary, M. K., Parekh, B., Dezabala, E., Solis, H. A., Pujiyono, P., De Narvaez, Z., & Zambrano, J. (2011, January). Design, Implementation and Performance of a Down-Dip WAG Pilot. In International petroleum technology conference. International Petroleum Technology Conference.

Christensen, J. R., Stenby, E. H., & Skauge, A. (1998, January). Review of WAG field experience. In International petroleum conference and exhibition of Mexico. Society of Petroleum Engineers.

Christensen, J. R., Stenby, E. H., & Skauge, A. (2001, April 1). Review of WAG Field Experience. Society of Petroleum Engineers. doi:10.2118/71203-PA

Christian, L. D., Shirer, J. A., Kimbel, E. L., & Blackwell, R. J. (1981). Planning a tertiary oil-recovery project for Jay/LEC fields unit. Journal of Petroleum Technology, 33(08), 1-535.

Crogh, N. A., Eide, K., & Morterud, S. E. (2002, January). WAG injection at the statfjord field, a success story. In European Petroleum Conference. Society of Petroleum Engineers.

Dang, C. T., Nghiem, L. X., Chen, Z., Nguyen, N. T., & Nguyen, Q. P. (2014, April). CO2 low salinity water alternating gas: a new promising approach for enhanced oil recovery. In SPE Improved Oil Recovery Symposium. Society of Petroleum Engineers.

Dariu, H., Granger, P. Y., & Garotta, R. J. (2005). Shear-wave splitting analysis using simulated annealing. In SEG Technical Program Expanded Abstracts 2005 (pp. 881-884). Society of Exploration Geophysicists.

Darvishnezhad, M. J., Moradi, B., Zargar, G., Jannatrostami, A., & Montazeri, G. H. (2010, January). Study of various water alternating gas injection methods in 4-and 5-spot injection patterns in an Iranian fractured reservoir. In Trinidad and Tobago Energy Resources Conference. Society of Petroleum Engineers.

Deyhimi, F., Salamat-Ahangari, R., Arabieh, M., & Parvin, L. (2006). Application of response surface methodology for modelling the enzymatic assay of hydrogen peroxide by Emerson–Trinder reaction using 4-iodophenol. International Journal of Environmental and Analytical Chemistry, 86(15), 1151-1163.

Eberhart, R., & Kennedy, J. (1995, November). Particle swarm optimization. In Proceedings of the IEEE international conference on neural networks (Vol. 4, pp. 1942-1948).

Eberhart, R., & Kennedy, J. (1995, October). A new optimizer using particle swarm theory. In MHS'95. Proceedings of the Sixth International Symposium on Micro Machine and Human Science (pp. 39-43). Ieee.

Esmaiel, T. E., & Heeremans, J. C. (2006, January). Optimization of the WAG process under Uncertainty in a Smart Wells Environment: Utility Theory Approach. In Intelligent Energy Conference and Exhibition. Society of Petroleum Engineers.

Evensen, G. (1994). Sequential data assimilation with a nonlinear quasi-geostrophic model using Monte Carlo methods to forecast error statistics. Journal of Geophysical Research: Oceans, 99(C5), 10143-10162.

Evers, J. F., & Jennings, J. W. (1973, January). How to Use Monte Carlo Simulation in Profitability Analysis. In SPE Rocky Mountain Regional Meeting. Society of Petroleum Engineers.

Fanchi, J. (2010). Integrated reservoir asset management: principles and best practices. Gulf Professional Publishing.

Fassihi, M. R., & Gillham, T. H. (1993, January). The use of air injection to improve the double displacement processes. In SPE Annual Technical Conference and Exhibition. Society of Petroleum Engineers.

Fatemi, M., Shahrokhi, O., Sohrabi, M., Vieira, R., & Ahmed, K. (2015, November). Experimental investigation of oil recovery from carbonate reservoir rocks under oil-wet condition: waterflood, gas injection, SWAG and WAG injections. In Abu Dhabi International Petroleum Exhibition and Conference. Society of Petroleum Engineers.

Fatemi, S. M., Sohrabi, M., Jamiolahmady, M., Ireland, S., & Robertson, G. (2011, January). Experimental investigation of near-miscible water-alternating-gas (WAG) injection performance in water-wet and mixed-wet systems. In Offshore Europe. Society of Petroleum Engineers.

Fisher, R. A. (1958). Statistical methods for research workers, 356 pp. Oliver and Boyd, Edinburgh.

Fortini, C., Maggi, D., Lipari, V., & Ferla, M. (2013). Particle swarm optimization for seismic velocity analysis. In SEG Technical Program Expanded Abstracts 2013 (pp. 4864-4868). Society of Exploration Geophysicists.

Gary, W. O. (2010). A first course in design and analysis of experiments. University of Minnesota, Minnesota, United States of America.

Ghaderi, S. M., Clarkson, C. R., & Chen, Y. (2012, January). Optimization of WAG process for coupled CO2 EOR-storage in tight oil formations: an experimental design approach. In SPE Canadian Unconventional Resources Conference. Society of Petroleum Engineers.

Ghafoori, A., Shahbazi, K., Darabi, A., Soleymanzadeh, A., & Abedini, A. (2012). The experimental investigation of nitrogen and carbon dioxide water-alternating-gas injection in a carbonate reservoir. Petroleum Science and Technology, 30(11), 1071-1081.

Gilman, J. R., Brickey, R. T., & Red, M. M. (1998, January). Monte Carlo techniques for evaluating producing properties. In SPE Rocky Mountain Regional/Low-Permeability Reservoirs Symposium. Society of Petroleum Engineers.

Goldberg, D. E. Genetic algorithms in search, optimization, and machine learning. Reading, MA: Addison-Wesley; 1989.

Green, D. W., & Willhite, G. P. (1998). Enhanced oil recovery (Vol. 6, pp. 143-154). Richardson, TX: Henry L. Doherty Memorial Fund of AIME, Society of Petroleum Engineers.

Güler, O. (2010). Foundations of optimization (Vol. 258). Springer Science & Business Media.

Hamzei, A., Zargar, G., Arabjamaloei, R., Ekramzadeh, M. A., & Azad, M. (2011). Comparative Study of Hysteresis Models in Immiscible Water Alternating Gas (WAG) Process. Petroleum Science and Technology, 29(12), 1214-1226.

Han, L., & Gu, Y. (2015, September). Miscible CO 2 Water-Alternating-Gas (CO 2-WAG) Injection in a Tight Oil Formation. In SPE Annual Technical Conference and Exhibition. Society of Petroleum Engineers.

Harding, T. J., Radcliffe, N. J., & King, P. R. (1998). Hydrocarbon production scheduling with genetic algorithms. SPE Journal, 3(02), 99-107.

Hassan, A., Elkatatny, S., Mahmoud, M., Abdulraheem, A., & Hossain, E. (2018, August). New Technique to Estimate Temperature Distribution During Thermal EOR Operations. In SPE Kingdom of Saudi Arabia Annual Technical Symposium and Exhibition. Society of Petroleum Engineers.

Haupt, R. L., & Ellen Haupt, S. (2004). Practical genetic algorithms.

Holland, J. (1975). Adaptation in natural and artificial systems: an introductory analysis with application to biology. Control and artificial intelligence.

Holtz, M. H. (2016, April). Immiscible Water Alternating Gas (IWAG) EOR: Current State of the Art. In SPE Improved Oil Recovery Conference. Society of Petroleum Engineers.

Hood, S. J., & Welch, P. D. (1993, December). Response surface methodology and its application in simulation. In Proceedings of 1993 Winter Simulation Conference-(WSC'93) (pp. 115-122). IEEE.

https://www.glossary.oilfield.slb.com/en/Terms/a/areal_sweep_efficiency.aspx

Huang, K. Y., & Chou, Y. L. (2008). Simulated annealing for hierarchical seismic pattern detection. In SEG Technical Program Expanded Abstracts 2008 (pp. 869-873). Society of Exploration Geophysicists.

Huang, K. Y., & Hsieh, Y. H. (2011). Seismic pattern detection using very fast simulated annealing. In SEG Technical Program Expanded Abstracts 2011 (pp. 1181-1186). Society of Exploration Geophysicists.

Instefjord, R., & Todnem, A. C. (2002, January). 10 years of WAG injection in Lower Brent at the Gullfaks Field. In European Petroleum Conference. Society of Petroleum Engineers.

Itriago, Y. C., Araujo, M., & Molinaris, J. (2018, April). Best Practices for Laboratory Evaluation of Immiscible WAG. In SPE Improved Oil Recovery Conference. Society of Petroleum Engineers.

Jackson, D. D., Andrews, G. L., & Claridge, E. L. (1985, January). Optimum WAG ratio vs. Rock wettability in CO2 flooding. In SPE Annual Technical Conference and Exhibition. Society of Petroleum Engineers.

Jamiolahmady, M., Alajmi, E., Nasriani, H. R., Ghahri, P., & Pichestapong, K. (2014, October). A thorough investigation of clean-up efficiency of hydraulic fractured wells using statistical approaches. In SPE Annual Technical Conference and Exhibition. Society of Petroleum Engineers.

Janssen, M. T., Azimi, F., & Zitha, P. L. (2018, April). Immiscible Nitrogen Flooding in Bentheimer Sandstones: Comparing Gas Injection Schemes for Enhanced Oil Recovery. In SPE Improved Oil Recovery Conference. Society of Petroleum Engineers.

Jesmani, M., Bellout, M. C., Hanea, R., & Foss, B. (2015, September). Particle swarm optimization algorithm for optimum well placement subject to realistic field development constraints. In SPE Reservoir Characterisation and Simulation Conference and Exhibition. Society of Petroleum Engineers.

Jiang, H., Nuryaningsih, L., & Adidharma, H. (2010, January). The effect of salinity of injection brine on water alternating gas performance in tertiary miscible carbon dioxide flooding: experimental study. In SPE Western Regional Meeting. Society of Petroleum Engineers.

Juanes, R., & Blunt, M. J. (2006, January). Impact of viscous fingering on the prediction of optimum WAG ratio. In SPE/DOE Symposium on Improved Oil Recovery. Society of Petroleum Engineers.

Kalos, M. H., & Whitlock, P. A. (2009). Monte carlo methods. John Wiley & Sons.

Kantzas, A., Bryan, J., & Taheri, S. (2012). Fundamentals of fluid flow in porous media. Pore size distribution.

Kennedy, J., & Eberhart, R. C. (1997, October). A discrete binary version of the particle swarm algorithm. In 1997 IEEE International conference on systems, man, and cybernetics. Computational cybernetics and simulation (Vol. 5, pp. 4104-4108). IEEE.

Khanifar, A., Raub, M. R. A., Tewari, R. D., Zain, Z. M., & Sedaralit, M. F. (2015, December). Designing of Successful Immiscible Water Alternating Gas (IWAG) Coreflood Experiment. In International Petroleum Technology Conference. International Petroleum Technology Conference.

Khezrnejad, A., James, L. A., & Johansen, T. E. (2014, October). Water enhancement using nanoparticles in water alternating gas (WAG) micromodel experiments. In SPE Annual Technical Conference and Exhibition. Society of Petroleum Engineers.

Khosravi, M., Fatemi, S., & Rostami, B. (2011, January). Assessing Structured Uncertainty in a Mature Fractured Reservoir, Using Combination of Response Surface Method and

Reservoir Simulation. In SPE Reservoir Characterisation and Simulation Conference and Exhibition. Society of Petroleum Engineers.

Kiefer, J., & Wolfowitz, J. (1959). Optimum designs in regression problems. The Annals of Mathematical Statistics, 30(2), 271-294.

Kim, G., Jang, H., Cho, M., & Lee, J. (2015, July). Optimizing the Design Parameters for Performance Evaluation of the CO 2-WAG Process in a Heterogeneous Reservoir. In the Twenty-fifth International Ocean and Polar Engineering Conference. International Society of Offshore and Polar Engineers.

Kiranyaz, S., Ince, T., & Gabbouj, M. (2014). Multidimensional particle swarm optimization for machine learning and pattern recognition (pp. 1-80). Berlin: Springer.

Kirkpatrick, S., Gelatt, C. D., & Vecchi, M. P. (1983). Optimization by simulated annealing. science, 220(4598), 671-680.

Komlosi, Z. P., & Komlosi, J. (2009, January). Application of the Monte Carlo Simulation in Calculating HC-Reserves. In EUROPEC/EAGE Conference and Exhibition. Society of Petroleum Engineers.

Kossack, C. A. (2000, January). Comparison of reservoir simulation hysteresis options. In SPE Annual Technical Conference and Exhibition. Society of Petroleum Engineers.

Kulkarni, M. M., & Rao, D. N. (2005). Experimental investigation of miscible and immiscible Water-Alternating-Gas (WAG) process performance. Journal of Petroleum Science and Engineering, 48(1-2), 1-20.

Kulkarni, M. M., & Rao, D. N. (2006, January). Characterization of operative mechanisms in gravity drainage field projects through dimensional analysis. In SPE Annual Technical Conference and Exhibition. Society of Petroleum Engineers.

Kumar, J., Agrawal, P., & Draoui, E. (2017). A Case Study on Miscible and Immiscible Gas-Injection Pilots in a Middle East Carbonate Reservoir in an Offshore Environment. SPE Reservoir Evaluation & Engineering, 20(01), 19-29.

Lake, L. W. (1989). Enhanced oil recovery.

Langenberg, M. A., Henry, D. M., & Chlebana, M. R. (1995). Performance and expansion plans for the Double displacement process in the Hawkins field unit. SPE Reservoir Engineering, 10(04), 301-308.

Larsen, J. A., & Skauge, A. (1999, January). Simulation of the immiscible WAG process using cycle-dependent three-phase relative permeabilities. In SPE Annual Technical Conference and Exhibition. Society of Petroleum Engineers.

Lawrence, J. J., Sahoo, H., Teletzke, G. F., Banfield, J., Long, J. M., Maccallum, N., ... & James, L. A. (2013, July). Optimisation of Gas Utilisation to Improve Recovery at Hibernia. In SPE Enhanced Oil Recovery Conference. Society of Petroleum Engineers.

Le Van, S., & Chon, B. H. (2017). Effects of salinity and slug size in miscible CO2 water-alternating-gas core flooding experiments. Journal of industrial and engineering chemistry, 52, 99-107.

Li, B., & Firedmann, F. (2005, January). A Novel Response Surface Methodology Based on" Amplitude Factor" Analysis for Modeling Nonlinear Responses Caused by Both Reservoir and Controllable Factors. In SPE Annual Technical Conference and Exhibition. Society of Petroleum Engineers.

Lien, S. C., Lie, S. E., Fjellbirkeland, H., & Larsen, S. V. (1998, January). Brage Field, lessons learned after 5 years of production. In European Petroleum Conference. Society of Petroleum Engineers.

Lyklema, J. (2005). Fundamentals of interface and colloid science: soft colloids (Vol. 5). Elsevier.

Lyons, W. C., & Plisga, G. J. (2011). Standard handbook of petroleum and natural gas engineering. Elsevier.

Ma, T. D., Rugen, J. A., Stoisits, R. F., & Voungren, G. K. (1995, January). Simultaneous water and gas injection pilot at the Kuparuk River Field, reservoir impact. In SPE annual technical conference and exhibition. Society of Petroleum Engineers.

Maloney, D. R., & Milligan, B. E. HIBERNIA THREE-PHASE RELATIVE PERMEABILITY MEASUREMENTS AT RESERVOIR CONDITIONS.Chicago

McPhee, C., Reed, J., & Zubizarreta, I. (2015). Core analysis: A best practice guide (Vol. 64). Elsevier.

Merchant, D. H. (2010, January). Life Beyond 80: A look at conventional WAG recovery beyond 80% HCPV injected in CO2 tertiary floods. In SPE International Conference on CO2 Capture, Storage, and Utilization. Society of Petroleum Engineers.

Minssieux, L. (1994, January). Wag flow mechanisms in presence of residual oil. In SPE Annual Technical Conference and Exhibition. Society of Petroleum Engineers.

Mitchell, M. (1998). An introduction to genetic algorithms. MIT press.

Mohagheghian, E. (2016). An application of evolutionary algorithms for WAG optimisation in the Norne Field (Master dissertation, Memorial University of Newfoundland).

Moldoveanu, S. C., & David, V. (2016). Selection of the HPLC method in chemical analysis. Elsevier.

Mollaei, A., & Delshad, M. (2011, January). A Novel Forecasting Tool for Water Alternating Gas (WAG) Floods. In SPE Eastern Regional Meeting. Society of Petroleum Engineers.

Montgomery, D. C. (2017). Design and analysis of experiments. John wiley & sons.

Mun, J. (2006). Modeling risk: Applying Monte Carlo simulation, real options analysis, forecasting, and optimization techniques (Vol. 347). John Wiley & Sons.

Murtha, J. (2006). Some challenges for monte carlo simulation. The Way Ahead, 2(02), 13-18.

Murtha, J. A. (1994). Incorporating historical data into Monte Carlo simulation. SPE Computer Applications, 6(02), 11-17.

Murtha, J. A. (1997). Monte Carlo simulation: its status and future. Journal of Petroleum Technology, 49(04), 361-373.

Nadeason, G., Zain, Z., Sayegh, S., & Girard, M. (2001). Assessment of Dulang field immiscible water-alternating-gas (WAG) injection through composite core displacement studies. Paper No. SPE 72140. In SPE Asia Pacific Improved Oil Recovery Conference, Kuala Lumpur, Malaysia, October (pp. 8-9).

Namani, M., & Kleppe, J. (2011, January). Investigation of the effect of some parameters in miscible WAG process using black-oil and compositional simulators. In SPE Enhanced Oil Recovery Conference. Society of Petroleum Engineers.

Narayanan, K., White, C. D., Lake, L. W., & Willis, B. J. (1999, January). Response surface methods for upscaling heterogeneous geologic models. In SPE Reservoir Simulation Symposium. Society of Petroleum Engineers.

Neddermeijer, H. G., Van Oortmarssen, G. J., Piersma, N., & Dekker, R. (2000, December). A framework for response surface methodology for simulation optimization. In Proceedings of the 32nd conference on Winter simulation (pp. 129-136). Society for Computer Simulation International.

Nuryaningsih, L., Jiang, H., & Adidharma, H. (2010, January). Experimental study on optimum half-cycle slug size of water alternating gas under tertiary miscible carbon dioxide flooding. In SPE International Conference on CO2 Capture, Storage, and Utilization. Society of Petroleum Engineers.

Onwunalu, J. E., & Durlofsky, L. J. (2010). Application of a particle swarm optimization algorithm for determining optimum well location and type. Computational Geosciences, 14(1), 183-198.

Oren, P. E., & Pinczewski, W. V. (1994). The effect of wettability and spreading coefficients on the recovery of waterflood residual oil by miscible gasflooding. SPE Formation Evaluation, 9(02), 149-156.

Oren, P. E., Billiotte, J., & Pinczewski, W. V. (1992). Mobilization of waterflood residual oil by gas injection for water-wet conditions. SPE Formation Evaluation, 7(01), 70-78. Chicago

Pampara, G., Franken, N., & Engelbrecht, A. P. (2005, September). Combining particle swarm optimisation with angle modulation to solve binary problems. In 2005 IEEE congress on evolutionary computation (Vol. 1, pp. 89-96). IEEE.

Panda, M., Ambrose, J. G., Beuhler, G., & McGguire, P. L. (2009). Optimized eor design for the Eileen west end area, Greater Prudhoe bay. SPE Reservoir Evaluation & Engineering, 12(01), 25-32.

Panda, M., Nottingham, D. W., & Lenig, D. C. (2010, January). Systematic surveillance techniques for a large miscible WAG flood. In SPE Oil and Gas India Conference and Exhibition. Society of Petroleum Engineers.

Pedersen, J. M., Vestergaard, P. D., & Zimmerman, T. (1991, January 1). Simulated Annealing-Based Seismic Inversion. Society of Exploration Geophysicists.

Ramanathan, R., Shehata, A. M., & Nasr-El-Din, H. A. (2015, October). Water Alternating CO_2 Injection Process-Does Modifying the Salinity of Injected Brine Improve Oil Recovery? In OTC Brasil. Offshore Technology Conference.

Rao, S. S. (2009). Engineering optimization: theory and practice. John Wiley & Sons.

Raychaudhuri, S. (2008, December). Introduction to monte carlo simulation. In 2008, Winter simulation conference (pp. 91-100). IEEE.

Ren, W., Bentsen, R., & Cunha, L. B. (2004). Pore-level observation of gravity-assisted tertiary gas-injection processes. SPE Reservoir Evaluation & Engineering, 7(03), 194-201.

Richards, F. W., Vrolijk, P. J., Gordon, J. D., & Miller, B. R. (2010). Reservoir connectivity analysis of a complex combination trap: Terra Nova Field, Jeanne d'Arc Basin, Newfoundland, Canada. Geological Society, London, Special Publications, 347(1), 333-355.

Righi, E. F., Royo, J., Gentil, P., Castelo, R., Del Monte, A., & Bosco, S. (2004, January). Experimental study of tertiary immiscible WAG injection. In SPE/DOE Symposium on Improved Oil Recovery. Society of Petroleum Engineers.

Romero, C. E., Carter, J. N., Gringarten, A. C., & Zimmerman, R. W. (2000, January). A modified genetic algorithm for reservoir characterisation. In International oil and gas conference and exhibition in China. Society of Petroleum Engineers.

Salehi, M. M., Safarzadeh, M. A., Sahraei, E., & Nejad, S. A. T. (2014). Comparison of oil removal in surfactant alternating gas with water alternating gas, water flooding and gas

flooding in secondary oil recovery process. Journal of Petroleum Science and Engineering, 120, 86-93.

Sarich, M. D. (2001, January). Using genetic algorithms to improve investment decision making. In SPE Asia Pacific Oil and Gas Conference and Exhibition. Society of Petroleum Engineers.

Satitkanitkul, W., & Athichanagorn, S. (2013). Evaluation and Optimization of Double Displacement Process (Doctoral dissertation, Chulalongkorn University).

Satter, A., & Iqbal, G. M. (2015). Reservoir Engineering: The fundamentals, simulation, and management of conventional and unconventional recoveries. Gulf Professional Publishing.

Shahrokhi, O., Fatemi, M., Sohrabi, M., Ireland, S., & Ahmed, K. (2014, April). Assessment of three phase relative permeability and hysteresis models for simulation of water-alternating-gas (WAG) injection in water-wet and mixed-wet systems. In SPE Improved Oil Recovery Symposium. Society of Petroleum Engineers.

Sheng, J. (2010). Modern chemical enhanced oil recovery: theory and practice. Gulf Professional Publishing.

Shetty, S., Hughes, R. G., & Afonja, G. (2014, March). Experimental Evaluation of Simultaneous Water and Gas Injection Using Carbon Dioxide. In SPE EOR Conference at Oil and Gas West Asia. Society of Petroleum Engineers.

Shi, Y., & Eberhart, R. (1998, May). A modified particle swarm optimizer. In 1998 IEEE international conference on evolutionary computation proceedings. IEEE world congress on computational intelligence (Cat. No. 98TH8360) (pp. 69-73). IEEE.

Skauge, A., & Sorbie, K. (2014, March). Status of fluid flow mechanisms for miscible and immiscible WAG. In SPE EOR Conference at Oil and Gas West Asia. Society of Petroleum Engineers.

Sohrabi, M. T. D. H., Tehrani, D. H., Danesh, A., & Henderson, G. (2001, January). Visualisation of oil recovery by water alternating gas (WAG) injection using high pressure micromodels-oil-wet & mixed-wet systems. In SPE Annual Technical Conference and Exhibition. Society of Petroleum Engineers.

Soleng, H. H. (1999, July). Oil reservoir production forecasting with uncertainty estimation using genetic algorithms. In Proceedings of the 1999 Congress on Evolutionary Computation-CEC99 (Cat. No. 99TH8406) (Vol. 2, pp. 1217-1223). IEEE.

Srivastava, J. P., & Mahli, L. (2012). Water alternating gas (WAG) injection a novel EOR technique for mature light oil fields a laboratory investigation for GS-5C sand of gandhar field. In A paper presented in biennial international conference and exposition in petroleum geophysics, Hyderabad.

Stern, D. (1991, January). Mechanisms of miscible oil recovery: effects of pore-level fluid distribution. In SPE Annual Technical Conference and Exhibition. Society of Petroleum Engineers.

Suicmez, V. S., Piri, M., & Blunt, M. J. (2006, January). Pore-scale modeling of three-phase WAG injection: Prediction of relative permeabilities and trapping for different displacement cycles. In SPE/DOE Symposium on Improved Oil Recovery. Society of Petroleum Engineers.

Taguchi, G. (1986). Introduction to quality engineering: designing quality into products and processes (No. 658.562 T3).

Taguchi, G. (1987). System of experimental design; engineering methods to optimize quality and minimize cost (No. 04; QA279, T3.).

Taguchi, G., Chowdhury, S., & Taguchi, S. (2000). Robust engineering (Vol. 224). New York: McGraw-Hill.

Tanner, C. S., Baxley, P. T., Crump III, J. G., & Miller, W. C. (1992, January). Production performance of the Wasson Denver Unit CO2 flood. In SPE/DOE Enhanced Oil Recovery Symposium. Society of Petroleum Engineers.

Teigland, R., & Kleppe, J. (2006, January). EOR survey in the North Sea. In SPE/DOE Symposium on Improved Oil Recovery. Society of Petroleum Engineers.

Torabi, F., Jamaloei, B. Y., Zarivnyy, O., Paquin, B. A., & Rumpel, N. J. (2012). The evaluation of variable-injection rate waterflooding, immiscible CO2 flooding, and water-alternating-CO2 injection for heavy oil recovery. Petroleum Science and Technology, 30(16), 1656-1669.

Tunio, S. Q., Tunio, A. H., Ghirano, N. A., & El Adawy, Z. M. (2011). Comparison of different enhanced oil recovery techniques for better oil productivity. International Journal of Applied Science and Technology, 1(5).

Van Goldfracht, T., Perrotti, G., & Gorini, G. (1966, January). The Optimization of Gas Reservoirs. In Fall Meeting of the Society of Petroleum Engineers of AIME. Society of Petroleum Engineers.

Wang, F. H. L., Honarpour, M. M., Djabbarah, N. F., & Haynes, F. M. (2006, September). Characterization of multiphase flow properties for tertiary immiscible displacement processes in an oil-wet reservoir. In Society of Core Analysis Conference Paper SCA2006-33 (pp. 1-15).

Wang, F. H. L., Honarpour, M. M., Djabbarah, N. F., & Haynes, F. M. (2006, September). Characterization of multiphase flow properties for tertiary immiscible displacement processes in an oil-wet reservoir. In Society of Core Analysis Conference Paper SCA2006-33 (pp. 1-15).

Wang, P., Litvak, M., & Aziz, K. (2002). Optimization of Production Operations in Petroleum Fields. Paper SPE 77658. In SPE Annual Technical Conference and Exhibition, San Antonio, TX.

Wang, X., & Qiu, X. (2013). Application of particle swarm optimization for enhanced cyclic steam stimulation in an offshore heavy oil reservoir. arXiv preprint arXiv:1306.4092.

Weihs, C., Luebke, K., & Czogiel, I. (2006). Response surface methodology for optimizing hyper parameters (No. 2006, 09). Technical Report/Universität Dortmund, SFB 475 Komplexitätsreduktion in Multivariaten Datenstrukturen.

Wu, X., Ogbe, D. O., Zhu, T., & Khataniar, S. (2004, January). Critical design factors and evaluation of recovery performance of miscible displacement and WAG process. In Canadian International Petroleum Conference. Petroleum Society of Canada.

Xu, S., Zhang, M., Zeng, F., & Chan, C. (2015). Application of genetic algorithm (GA) in history matching of the vapour extraction (VAPEX) heavy oil recovery process. Natural Resources Research, 24(2), 221-237.

Yang, D., Zhang, Q., & Gu, Y. (2003). Integrated optimization and control of the production-injection operation systems for hydrocarbon reservoirs. Journal of petroleum science and Engineering, 37(1-2), 69-81.

Yang, D., Zhang, Q., Cui, H., Feng, H., & Li, L. (2000, January). Optimization of multivariate production-injection system for water-alternating-gas miscible flooding in Pubei oil field. In SPE/AAPG Western Regional Meeting. Society of Petroleum Engineers.

Zekri, A. Y., & Natuh, A. A. (1992, January). Laboratory study of the effects of miscible WAG process on tertiary oil recovery. In Abu Dhabi Petroleum Conference. Society of Petroleum Engineers.

Zekri, A. Y., Nasr, M. S., & AlShobakyh, A. (2011, January). Evaluation of Oil Recovery by Water Alternating Gas (WAG) Injection-Oil-Wet & Water-Wet Systems. In SPE enhanced oil recovery conference. Society of Petroleum Engineers.

Zendehboudi, S., Ahmadi, M. A., James, L., & Chatzis, I. (2012). Prediction of condensate-to-gas ratio for retrograde gas condensate reservoirs using artificial neural network with particle swarm optimization. Energy & Fuels, 26(6), 3432-3447.

Zhang, Y. P., Sayegh, S., & Huang, S. (2006, January). Enhanced heavy oil recovery by immiscible WAG injection. In Canadian International Petroleum Conference. Petroleum Society of Canada.

Zolfaghari, H., Zebarjadi, A., Shahrokhi, O., & Ghazanfari, M. H. (2013). An experimental study of CO2-low salinity water alternating gas injection in sandstone heavy oil reservoirs. Iranian Journal of Oil & Gas Science and Technology, 2(3), 37-47.

APPENDIX

A. ECLIPSE Data File of Double Displacement Process (DDP) Model

-- DDP CORE-FLOODING MODEL

RUNSPEC

TITLE

'DDP-COREFLOODING'

LAB

OIL

WATER

GAS

DISGAS

FULLIMP

SATOPTS

HYSTER/

DIMENS

2   2   120   /

TABDIMS

2 1 200 50 3 8* 1 /

WELLDIMS

20 50 20 4 /

MESSAGES

2* 10 6* 10000 /

START

19 MAY 2019 /

UNIFIN

UNIFOUT

GRID

```
TOPS

4*1 4*1.02 4*1.04 /

DX

480*1.673 /

DY

480*1.673 /

DZ

480*0.26 /

EQUALS

   PERMX  1919     1  2    1  2    1   20/

   PERMX  1919     1  2    1  2    20  40/

   PERMX  1919     1  2    1  2    40  60/

   PERMX  1919     1  2    1  2    60  80/

    PERMX  1919      1  2    1  2    80  100/

    PERMX  1919      1  2    1  2    100 120/

   PORO  0.1789   1  2   1  2     1   20/

    PORO  0.1789   1  2   1  2     20  40/

    PORO  0.1789   1  2   1  2     40  60/

    PORO  0.1789   1  2   1  2     60  80/

    PORO  0.1789   1  2   1  2     80  100/

    PORO  0.1789   1  2   1  2     100 120/

/

COPY

   PERMX  PERMY /

   PERMX  PERMZ /

/

INIT

PROPS
```

ROCK

272.2 1.5E-06 /

DENSITY

0.7686 1.0753 0.00100179 /

PVTW

306.2 1.02769 0.39395E-04 0.411   0.90953E-04 /

PVTO

  73.8   145   1.23449   1.047

          195   1.22453   1.137

          245   1.21581   1.226

          295   1.20809   1.316

          305   1.20658   1.335

          345   1.20119   1.406

          395   1.19497   1.495 /

 101.7   195   1.30233   0.888

          245   1.29091   0.957

          295   1.28090   1.026

          305   1.27895   1.041

          345   1.27204   1.096

          395   1.26411   1.165 /

 132.0   245   1.37456   0.743

          295   1.36165   0.795

          305   1.35915   0.806

          345   1.35034   0.848

          395   1.34030   0.902 /

 166.4   295   1.45615   0.585

          305   1.45292   0.592

          345   1.44159   0.617

```
          395   1.42881      0.649  /

   174.5   305   1.47556      0.558

          345   1.46358      0.582

          395   1.45008      0.611  /

   207.2   345   1.55356      0.474

          395   1.53700      0.498  /

/

PVDG

   145     0.00740    0.0187

   195     0.00555    0.0226

   245     0.00458    0.0291

   295     0.00410    0.0417

   305     0.00405    0.0459

   345     0.00400    0.0665

   395     0.00365    0.0957

/

SWFN

0.03    0      0

0.141   0.0038   -0.0172

0.2404   0.0195   -0.0293

0.3134   0.0417   -0.0315

0.4138   0.0908   -0.0339

0.4941   0.1478   -0.0364

0.5523   0.2001   -0.0391

0.6071   0.2585   -0.0421

0.7123   0.3971   -0.0952

0.772    0.4924   -0.256

0.8014   0.5440   -0.5524
```

0.8249   0.5875 -0.9952

0.8531   0.6425 -1.7422

0.8598   0.656 -2.006

/

0.03   0   0

0.141   0.0038 -0.0172

0.2404   0.0195 -0.0293

0.3134   0.0417 -0.0315

0.4138   0.0908 -0.0339

0.4941   0.1478 -0.0364

0.5523   0.2001 -0.0391

0.6071   0.2585 -0.0421

0.7123   0.3971 -0.0952

0.772   0.4924 -0.256

0.8014   0.5440 -0.5524

0.8249   0.5875 -0.9952

0.8531   0.6425 -1.7422

0.8598   0.656 -2.006

/

SGFN

0   0   0

0.2857   0.0153   0.0136

0.3394   0.0273   0.017

0.4031   0.0488   0.0204

0.4865   0.0922   0.0238

0.6467   0.2451   0.0272

0.8007   0.4967   0.136

0.8694   0.656   1.224

0.8944   0.722   6.936

/

0   0   0

0.2857   0.0153   0.0136

0.3394   0.0273   0.017

0.4031   0.0488   0.0204

0.4865   0.0922   0.0238

0.6467   0.2451   0.0272

0.8007   0.4967   0.136

0.8694   0.656   1.224

0.8944   0.722   6.936

/

SOF3

0.0759   0   0

0.1696   0   0.002

0.1751   0   0.0075

0.1986   0   0.0102

0.228   0.0002   0.0125

0.2877   0.0014   0.0206

0.3206   0.0016   0.0284

0.3929   0.0109   0.0526

0.4477   0.023   0.0852

0.4838   0.032   0.1146

0.5059   0.0444   0.1346

0.5672   0.078   0.1905

0.5862   0.0944   0.2125

0.6309   0.1332   0.2657

0.6846   0.1985   0.3419

0.6866   0.2041   0.3426

0.7596   0.3287   0.4845

0.859   0.5786   0.7074

0.97   1   1

/

0.0759   0   0

0.1696   0   0.002

0.1751   0   0.0075

0.1986   0   0.0102

0.228   0.0002   0.0125

0.2877   0.0014   0.0206

0.3206   0.0016   0.0284

0.3929   0.0109   0.0526

0.4477   0.023   0.0852

0.4838   0.032   0.1146

0.5059   0.0444   0.1346

0.5672   0.078   0.1905

0.5862   0.0944   0.2125

0.6309   0.1332   0.2657

0.6846   0.1985   0.3419

0.6866   0.2041   0.3426

0.7596   0.3287   0.4845

0.859   0.5786   0.7074

0.97   1   1

/

EHYSTR

0.1 2 1.0 /

REGIONS

SATNUM

480*1 /

IMBNUM

480*2 /

SOLUTION

PRESSURE

480*306.2/

SGAS

480*0/

SWAT

480*0.122/

RPTRST

basic=2 NORST=1 VGAS VOIL SOIL SGAS KRO KRG /

RS

480*174.5

/

EXTRAPMS

3 /

SUMMARY

RPTONLY

FOPT

FWPT

FGPT

FOSAT

FWSAT

FGSAT

FOIP

FWIP

FWCT

FGIP

FRPV

FOPV

FWPV

FGPV

WBHP

/

FOE

RUNSUM

EXCEL

SCHEDULE

WELSPECS

PROD1 G1 1 1 1* OIL /

PROD2 G1 1 2 1* OIL /

PROD3 G1 2 1 1* OIL /

PROD4 G1 2 2 1* OIL /

PROD5 G3 1 1 1* OIL /

PROD6 G3 1 2 1* OIL /

PROD7 G3 2 1 1* OIL /

PROD8 G3 2 2 1* OIL /

INJ1 G2 1 1 1* WATER /

INJ2 G2 1 2 1* WATER /

INJ3 G2 2 1 1* WATER /

INJ4 G2 2 2 1* WATER /

INJ5 G4 1 1 1* GAS /

INJ6 G4 1 2 1* GAS /

INJ7 G4 2 1 1* GAS /

INJ8 G4 2 2 1* GAS /

/

COMPDAT

PROD1 1 1 1 1 O 1* 7500/

PROD2 1 2 1 1 O 1* 7500/

PROD3 2 1 1 1 O 1* 7500/

PROD4 2 2 1 1 O 1* 7500/

PROD5 1 1 120 120 O 1* 7500/

PROD6 1 2 120 120 O 1* 7500/

PROD7 2 1 120 120 O 1* 7500/

PROD8 2 2 120 120 O 1* 7500/

INJ1 1 1 120 120 O 1* 7500/

INJ2 1 2 120 120 O 1* 7500/

INJ3 2 1 120 120 O 1* 7500/

INJ4 2 2 120 120 O 1* 7500/

INJ5 1 1 1 1 O 1* 7500/

INJ6 1 2 1 1 O 1* 7500/

INJ7 2 1 1 1 O 1* 7500/

INJ8 2 2 1 1 O 1* 7500/

/

WCONINJE

INJ1 WATER OPEN RESV 1* 60/

INJ2 WATER OPEN RESV 1* 60/

INJ3 WATER OPEN RESV 1* 60/

INJ4 WATER OPEN RESV 1* 60/

INJ5 GAS SHUT RESV 1* 60/

INJ6 GAS SHUT RESV 1* 60/

INJ7 GAS SHUT RESV 1* 60/

INJ8 GAS SHUT RESV 1* 60/

/

WCONPROD

PROD1 OPEN BHP 5* 306.2/

PROD2 OPEN BHP 5* 306.2/

PROD3 OPEN BHP 5* 306.2/

PROD4 OPEN BHP 5* 306.2/

PROD5 SHUT BHP 5* 306.2/

PROD6 SHUT BHP 5* 306.2/

PROD7 SHUT BHP 5* 306.2/

PROD8 SHUT BHP 5* 306.2/

/

TSTEP

100*0.00156/

/

WCONINJE

INJ1 WATER SHUT RESV 1* 60/

INJ2 WATER SHUT RESV 1* 60/

INJ3 WATER SHUT RESV 1* 60/

INJ4 WATER SHUT RESV 1* 60/

INJ5 GAS OPEN RESV 1* 60/

INJ6 GAS OPEN RESV 1* 60/

INJ7 GAS OPEN RESV 1* 60/

INJ8 GAS OPEN RESV 1* 60/

/

WCONPROD

PROD1 SHUT BHP 5* 306.2/

PROD2 SHUT BHP 5* 306.2/

PROD3 SHUT BHP 5* 306.2/

PROD4 SHUT BHP 5* 306.2/

PROD5 OPEN BHP 5* 306.2/

PROD6 OPEN BHP 5* 306.2/

PROD7 OPEN BHP 5* 306.2/

PROD8 OPEN BHP 5* 306.2/

/

TSTEP

100*0.0040/

/

END

B. ECLIPSE Data File of Immiscible Water Alternating Gas (IWAG) Injection Model

-- IWAG CORE-FLOODING MODEL

RUNSPEC

TITLE

'IWAG-COREFLOODING'

LAB

OIL

WATER

GAS

DISGAS

FULLIMP

SATOPTS

HYSTER/

DIMENS

2   2   120   /

TABDIMS

2 1 200 50 3 8* 1 /

WELLDIMS

20 50 20 4 /

MESSAGES

2* 10 6* 10000 /

START

19 MAY 2019 /

UNIFIN

UNIFOUT

GRID

TOPS

4*1 4*1.02 4*1.04 /

DX

480*1.673 /

DY

480*1.673 /

DZ

480*0.26 /

EQUALS

  PERMX 1919   1 2   1 2   1 20/

  PERMX 1919   1 2   1 2   20 40/

  PERMX 1919   1 2   1 2   40 60/

  PERMX 1919   1 2   1 2   60 80/

   PERMX 1919   1 2   1 2   80 100/

   PERMX 1919   1 2   1 2   100 120/

  PORO 0.1789   1 2 1 2   1 20/

   PORO 0.1789   1 2 1 2   20 40/

  PORO 0.1789   1 2 1 2   40 60/

  PORO 0.1789   1 2 1 2   60 80/

  PORO 0.1789   1 2 1 2   80 100/

  PORO 0.1789   1 2 1 2   100 120/

/

COPY

  PERMX PERMY /

  PERMX PERMZ /

/

INIT

PROPS

ROCK

272.2 1.5E-06 /

DENSITY

0.7686 1.0753 0.00100179 /

PVTW

306.2 1.02769 0.39395E-04 0.411 0.90953E-04 /

PVTO

```
 73.8    145   1.23449    1.047
         195   1.22453    1.137
         245   1.21581    1.226
         295   1.20809    1.316
         305   1.20658    1.335
         345   1.20119    1.406
         395   1.19497    1.495 /
101.7    195   1.30233    0.888
         245   1.29091    0.957
         295   1.28090    1.026
         305   1.27895    1.041
         345   1.27204    1.096
         395   1.26411    1.165 /
132.0    245   1.37456    0.743
         295   1.36165    0.795
         305   1.35915    0.806
         345   1.35034    0.848
         395   1.34030    0.902 /
166.4    295   1.45615    0.585
         305   1.45292    0.592
         345   1.44159    0.617
         395   1.42881    0.649 /
174.5    305   1.47556    0.558
```

```
              345    1.46358     0.582

              395    1.45008     0.611  /

  207.2    345    1.55356    0.474

              395    1.53700    0.498  /

/

PVDG

   145     0.00740    0.0187

   195     0.00555    0.0226

   245     0.00458    0.0291

   295     0.00410    0.0417

   305     0.00405    0.0459

   345     0.00400    0.0665

   395     0.00365    0.0957

/

SWFN

0.03    0      0

0.141    0.0038  -0.0172

0.2404   0.0195  -0.0293

0.3134   0.0417  -0.0315

0.4138   0.0908  -0.0339

0.4941   0.1478  -0.0364

0.5523   0.2001  -0.0391

0.6071   0.2585  -0.0421

0.7123   0.3971  -0.0952

0.772    0.4924  -0.256

0.8014   0.5440  -0.5524

0.8249   0.5875  -0.9952

0.8531   0.6425  -1.7422
```

0.8598   0.656   -2.006

/

0.03   0   0

0.141   0.0038   -0.0172

0.2404   0.0195   -0.0293

0.3134   0.0417   -0.0315

0.4138   0.0908   -0.0339

0.4941   0.1478   -0.0364

0.5523   0.2001   -0.0391

0.6071   0.2585   -0.0421

0.7123   0.3971   -0.0952

0.772   0.4924   -0.256

0.8014   0.5440   -0.5524

0.8249   0.5875   -0.9952

0.8531   0.6425   -1.7422

0.8598   0.656   -2.006

/

SGFN

0   0   0

0.2857   0.0153   0.0136

0.3394   0.0273   0.017

0.4031   0.0488   0.0204

0.4865   0.0922   0.0238

0.6467   0.2451   0.0272

0.8007   0.4967   0.136

0.8694   0.656   1.224

0.8944   0.722   6.936

/

```
0      0      0

0.2857   0.0153   0.0136

0.3394   0.0273   0.017

0.4031   0.0488   0.0204

0.4865   0.0922   0.0238

0.6467   0.2451   0.0272

0.8007   0.4967   0.136

0.8694   0.656    1.224

0.8944   0.722    6.936

/

SOF3

0.0759   0      0

0.1696   0      0.002

0.1751   0      0.0075

0.1986   0      0.0102

0.228    0.0002   0.0125

0.2877   0.0014   0.0206

0.3206   0.0016   0.0284

0.3929   0.0109   0.0526

0.4477   0.023    0.0852

0.4838   0.032    0.1146

0.5059   0.0444   0.1346

0.5672   0.078    0.1905

0.5862   0.0944   0.2125

0.6309   0.1332   0.2657

0.6846   0.1985   0.3419

0.6866   0.2041   0.3426

0.7596   0.3287   0.4845
```

0.859   0.5786   0.7074

0.97   1   1

/

0.0759   0   0

0.1696   0   0.002

0.1751   0   0.0075

0.1986   0   0.0102

0.228   0.0002   0.0125

0.2877   0.0014   0.0206

0.3206   0.0016   0.0284

0.3929   0.0109   0.0526

0.4477   0.023   0.0852

0.4838   0.032   0.1146

0.5059   0.0444   0.1346

0.5672   0.078   0.1905

0.5862   0.0944   0.2125

0.6309   0.1332   0.2657

0.6846   0.1985   0.3419

0.6866   0.2041   0.3426

0.7596   0.3287   0.4845

0.859   0.5786   0.7074

0.97   1   1

/

EHYSTR

0.1 2 1.0 /

REGIONS

SATNUM

480*1 /

IMBNUM

480*2 /

SOLUTION

PRESSURE

480*306.2/

SGAS

480*0/

SWAT

480*0.122/

RPTRST

basic=2 NORST=1 VGAS VOIL SOIL SGAS KRO KRG /

RS

480*174.5

/

EXTRAPMS

3 /

SUMMARY

RPTONLY

FOPT

FWPT

FGPT

FOSAT

FWSAT

FGSAT

FOIP

FWIP

FWCT

FGIP

FRPV

FOPV

FWPV

FGPV

WBHP

/

FOE

RUNSUM

EXCEL

SCHEDULE

WELSPECS

PROD G1 1 1 1* OIL /

PROD1 G1 1 2 1* OIL /

PROD2 G1 2 1 1* OIL /

PROD3 G1 2 2 1* OIL /

INJ   G2 1 1 1* GAS /

INJ1 G2 1 2 1* GAS /

INJ2 G2 2 1 1* GAS /

INJ3 G2 2 2 1* GAS /

/

COMPDAT

PROD 1 1 1 1 O 1* 7500/

PROD1 1 2 1 1 O 1* 7500/

PROD2 2 1 1 1 O 1* 7500/

PROD3 2 2 1 1 O 1* 7500/

INJ 1 1 120 120 O 1* 7500/

INJ1 1 2 120 120 O 1* 7500/

INJ2 2 1 120 120 O 1* 7500/

INJ3 2 2 120 120 O 1* 7500/

/

WCONINJE

INJ WATER OPEN RESV 1* 60.000000/

INJ1 WATER OPEN RESV 1* 60.000000/

INJ2 WATER OPEN RESV 1* 60.000000/

INJ3 WATER OPEN RESV 1* 60.000000/

/

WCONPROD

PROD OPEN BHP 5* 306.2/

PROD1 OPEN BHP 5* 306.2/

PROD2 OPEN BHP 5* 306.2/

PROD3 OPEN BHP 5* 306.2/

/

TSTEP

100*0.00156/

/

WCONINJE

INJ GAS OPEN RESV 1* 60.000000/

INJ1 GAS OPEN RESV 1* 60.000000/

INJ2 GAS OPEN RESV 1* 60.000000/

INJ3 GAS OPEN RESV 1* 60.000000/

/

WCONPROD

PROD OPEN BHP 5* 306.2/

PROD1 OPEN BHP 5* 306.2/

PROD2 OPEN BHP 5* 306.2/

PROD3 OPEN BHP 5* 306.2/

/

TSTEP

100*0.000069/

/

WCONINJE

INJ WATER OPEN RESV 1* 60.000000/

INJ1 WATER OPEN RESV 1* 60.000000/

INJ2 WATER OPEN RESV 1* 60.000000/

INJ3 WATER OPEN RESV 1* 60.000000/

/

WCONPROD

PROD OPEN BHP 5* 306.2/

PROD1 OPEN BHP 5* 306.2/

PROD2 OPEN BHP 5* 306.2/

PROD3 OPEN BHP 5* 306.2/

/

TSTEP

100*0.000029/

/

WCONINJE

INJ GAS OPEN RESV 1* 60.000000/

INJ1 GAS OPEN RESV 1* 60.000000/

INJ2 GAS OPEN RESV 1* 60.000000/

INJ3 GAS OPEN RESV 1* 60.000000/

/

WCONPROD

PROD OPEN BHP 5* 306.2/

PROD1 OPEN BHP 5* 306.2/

PROD2 OPEN BHP 5* 306.2/

PROD3 OPEN BHP 5* 306.2/

/

TSTEP

100*0.000069/

/

WCONINJE

INJ WATER OPEN RESV 1* 60.000000/

INJ1 WATER OPEN RESV 1* 60.000000/

INJ2 WATER OPEN RESV 1* 60.000000/

INJ3 WATER OPEN RESV 1* 60.000000/

/

WCONPROD

PROD OPEN BHP 5* 306.2/

PROD1 OPEN BHP 5* 306.2/

PROD2 OPEN BHP 5* 306.2/

PROD3 OPEN BHP 5* 306.2/

/

TSTEP

100*0.000029/

/

END

C. Input Data for Central Composite Design (CCD) Model

Run#	Timing	Ratio	Flow Rate	Slug Size	Sequence	Oil RF (PV)
1	0.1225	3.8	15.5	0.3775	Gas	0.534007
2	0.1225	1.4	6.5	0.3775	Gas	0.523468
3	0.215	0.2	11	0.255	Gas	0.346194
4	0.215	2.6	11	0.255	Water	0.429216
5	0.3075	1.4	15.5	0.1325	Gas	0.372266
6	0.1225	1.4	6.5	0.1325	Gas	0.537304
7	0.3075	1.4	15.5	0.3775	Water	0.348185
8	0.215	0.2	11	0.255	Water	0.450462
9	0.1225	3.8	15.5	0.1325	Water	0.522835
10	0.3075	1.4	15.5	0.1325	Water	0.365645
11	0.215	2.6	2	0.255	Gas	0.424564
12	0.03	2.6	11	0.255	Gas	0.616779
13	0.3075	3.8	15.5	0.1325	Gas	0.359008
14	0.3075	3.8	15.5	0.1325	Water	0.338548
15	0.1225	1.4	15.5	0.3775	Gas	0.536075
16	0.1225	3.8	6.5	0.1325	Water	0.522779
17	0.3075	1.4	6.5	0.3775	Water	0.337192
18	0.3075	1.4	6.5	0.1325	Water	0.365437
19	0.215	2.6	11	0.5	Gas	0.436121
20	0.3075	1.4	6.5	0.3775	Gas	0.35638
21	0.1225	3.8	6.5	0.3775	Water	0.494079

22	0.215	5	11	0.255	Gas	0.439133
23	0.1225	3.8	6.5	0.3775	Gas	0.520698
24	0.1225	3.8	15.5	0.1325	Gas	0.539334
25	0.1225	1.4	6.5	0.3775	Water	0.533376
26	0.1225	3.8	6.5	0.1325	Gas	0.532136
27	0.1225	3.8	15.5	0.3775	Water	0.493671
28	0.215	2.6	2	0.255	Water	0.43845
29	0.215	2.6	11	0.255	Gas	0.440233
30	0.3075	3.8	6.5	0.1325	Gas	0.35419
31	0.1225	1.4	15.5	0.1325	Gas	0.552647
32	0.3075	1.4	15.5	0.3775	Gas	0.366015
33	0.215	2.6	20	0.255	Gas	0.450256
34	0.3075	3.8	6.5	0.1325	Water	0.340991
35	0.3075	3.8	6.5	0.3775	Gas	0.354877
36	0.1225	1.4	15.5	0.3775	Water	0.531364
37	0.215	2.6	20	0.255	Water	0.423532
38	0.3075	1.4	6.5	0.1325	Gas	0.363963
39	0.3075	3.8	6.5	0.3775	Water	0.313012
40	0.4	2.6	11	0.255	Water	0.245712
41	0.215	2.6	11	0.01	Gas	0.437461
42	0.3075	3.8	15.5	0.3775	Gas	0.36499
43	0.215	5	11	0.255	Water	0.403345
44	0.03	2.6	11	0.255	Water	0.61071

45	0.4	2.6	11	0.255	Gas	0.265959
46	0.215	2.6	11	0.01	Water	0.437343
47	0.3075	3.8	15.5	0.3775	Water	0.311811
48	0.1225	1.4	6.5	0.1325	Water	0.540487
49	0.215	2.6	11	0.5	Water	0.403568
50	0.1225	1.4	15.5	0.1325	Water	0.549344